
# POLITECNICO DI MILANO

**Facoltà di Ingegneria Civile, Ambientale e Territoriale**

**Corso di Laurea Specialistica in Ingegneria Civile - Oritentamento Strutture**

## FIRE SAFETY IN TUNNEL

## NUMERICAL MODELING OF SMALL SCALE TESTS

**Relatore:**

**Prof. Ing. Roberto Felicetti**

**Tesi di Laurea di:**

**Wan Yannan - 780269**

Anno Accademico 2012-2013

# Index

# Acknowledgements

I would like to thank my supervisor: Prof. Roberto Felicetti, for his guidance throughout the days that I have worked on this project. He told me right from the beginning that there will be peaks and valleys along the way. He reminded me that I was only at one of those valleys every time I had felt that my research was going nowhere.

Thanks and sincere appreciations also go to Mahmoud Mohamed Kamal Ahmed, a student in school of engineering, Politecnico Di Milano, he did the small scale tunnel fire experiment in the year 2012, the test results will used for comparing with the numerical analysis result in my research.

Finally, I would like to thank my family for their support and encouragement.

# Abstract

Tunnels are considered as important critical lifeline where people died along many years due to lack of safety. This is a serious problem; it has the potential to become much worse in the future as more and longer tunnels are constructed as traffic densities increase. Firstly, there has been research under the aegis of various programs. Secondly, there have been more very serious fires in both road and rail tunnels. Tunnel construction worldwide has continued at a fast pace in recent years, in both urban and non-urban settings. Rapid changes, both in the technology and methods directly associated with tunnels and in society in general, mean that research and learning from the experience of others becomes more important. In addition, every tunnel is unique, and there is no 'one size fits all' solution. Alongside this there is a concern within society about tunnel safety and fire safety in particular.

There is no doubt that the consequences of a fire in a tunnel can be more serious than the consequences of a fire in the open air. Although a lot of researches have already been done trying to develop new parameters and produce results to help civil community and engineers, new plans and researches are still required to mitigate the risk in tunnels.

Common testing methods for using real scale tunnels in fire tests have many problems not only regarding the huge budget required to perform the tests but also for the negative safety effects that could occur as a result of performing tests in real existing tunnels. One of the efficient test methods is to use scaled test that can help a lot to perform tests repetitively with low cost and high efficiency but it still needs to be more developed.

Within this context, it is hoped that this research will provide a bridge between tunnel fire research and those who need to know the basic results, techniques and current thinking in relation to tunnel fire safety. It is also a vehicle for the transmission of experience gained from real tunnels.

# 1. Introduction

## 1.1 Background

Over the past 10 years, fire accidents in tunnels denoted the serious consequences in such evens .For example, in 1999, a fire accident involving multiple heavy goods vehicles (HGVs) and passenger cars in the Mont Blanc tunnel. The estimated peak HRR of this fire was between 300 and 380 MW. This fire cost the deaths of over forty people and caused significant damage to the tunnel. Two years later, another catastrophic fire occurred in the St. Gotthard (Switzerland) tunnel which resulted in 11 fatalities. As in these cases, most of the fires resulted in multiple fatalities. In additional, in most cases the fires affected the tunnel facilities which cause an interruption of regular tunnel operations for fire investigations and repair. The closure of tunnels introduced disturbances to nearby traffic and additional financial damage to the economy due to bad road transportation conditions.The increasing frequency of such fires has cause greater efforts to identify and reduce potential fire risks in tunnels.

Technology of tunnels construction is developed continuously which allows longer tunnels with bigger space volume to be constructed. Assuring the safety and risk mitigation for these tunnels is a high priority requirement meanwhile being complicated. Tunnels are closed volumes that need extra parameters to ensure safety for risk mitigation having a big chance of disasters in comparison to normal roads because of being dosed volume with no air exchange and difficulty to get external support. Thus engineers are requested to produce new studied, plans, parameters and new strategies to reduce the risk making it safer for passengers.

Fire risk is a serious problem causing death for many people during past decades. Due to the lack of safety in these tunnels, many fire tests were performed in past 40 years. Each fire test led to finding new parameters and results which enhance the researchers and designers to produce safer tunnels and decision makers to attain better emergency plans.

## 1.2 Aim of the research

The aim of this study is to describe the behavior and distribution of temperature resulting from fires in a scaled tunnel model (concrete tube) under the effect of ventilation and non-ventilation conditions. It is important to monitor and study the behavior of fire in scaled models.

Due to the high costs on real scale fire tests in tunnels, researchers have started recently to use scaling and modeling analysis by numerical methods. In this research, the work will include the scaling concept, monitoring the temperature distribution along the concrete tube under fire. As discussed before that fire scaling played a very important role in reducing cost and at the same time gives reliable results that can be used in design of emergency plans of tunnels.

There has been also a lack of information regarding the temperature behavior in scaled tunnels and if it behaves as the full scale or some differences occur. Therefore, the most important scopes of this research is to identify the results coming from the experimental test of concrete tube by numerical modeling by using MATLAB (Multi-Zone concept), then doing the evaluation of consistence between achieved experimental and numerical results and compare themselves. After checking and verifying results, this will enable the research program to perform a parametric study by varying input data and check the results related for this change.

Fig 1-1 Scaled tunnel (concrete tube) with thermocouples to measure the temperature

## 1.3 The outline of the thesis

There are 9 chapters in the work. Some chapters are concerned with the literature review about the main elements related to fire dynamics and fire safety in fire tunnels while the other chapters are related to experimental and numerical modeling researches. Following chart shows an outline of the chapters.

Table 1-2 Outline of the thesis

| Chapter | Name | Description |
|---|---|---|
| Chapter 1 | Introduction | Shows the aim of the research and the main outlines of the thesis |
| Chapter 2 | Fire in tunnels | Brief introduction about the history of tunnel fires and its significant aspects |
| Chapter 3 | Fire dynamics | Describes the issues related to fire dynamics such as the main topics of fire rise and evolution with its main related definitions |
| Chapter 4 | Fire safety | Deals with the basic background about fire safety and its main concepts of fire protection and prevention |
| Chapter 5 | Fire tests in tunnels | Shows the history of tunnel fire tests over the world and the relative results |
| Chapter 6 | Small scale experiment | Describes the small scale tunnel fire experiment |
| Chapter 7 | Numerical modeling | Numerical modeling of small scale tunnel fire by using the Multi-Zone concept with MATLAB script |
| Chapter 8 | Results of the analyses | Collecting all main results followed by a comparison between experimental and numerical model |
| Chapter 9 | Conclusions | Describe the most important scope of this research, analyze the advantages and disadvantages of the numerical model |

# 2. Fire in tunnels

## 2.1 Introduction

Accidents seem to occur less frequently in road tunnels than in the open road. This is possibly because tunnels are more controlled environment in road than the open road; there are generally no complications caused by weather, drivers are more attentive when driving in tunnels. However, there is no doubt that the fire in a tunnel can be far more serious than the consequences of a fire in the open air. According to the French statistics, there will only be one or two car fires (per kilometer of tunnel) for every hundred million cars pass through the tunnel. Similarly, out of every hundred million heavy goods vehicles passing through a tunnel, there will be about eight fires (per kilometer of tunnel), only one of which will be serious enough to cause any damage to the tunnel itself. On the basis of the statistics, there will be between one and three very serious fires out of every thousand million HGVs (per kilometer of tunnel). The chance of a serious accidental fire may sound vanishingly small from these statistics, but when considers that many road tunnels have very high traffic densities, there are over 15000 operational road, rail and underground railway tunnels in Europe alone, and that some of these tunnels are kilometers long, the chance of a serious fire incident in a tunnel may be greater than is commonly thought. Indeed, significant and fatal accidental fires in tunnels seem to occur on an annual basis.

*[Main reference: Handbook of Tunnel Fire Safety, 2nd edition, Richard Carvel, Guy Marlair, Chapter 1]*

## 2.2 Example studies in road tunnel fires

A HGV travelling through the Mont Blanc Tunnel from France to Italy caught fire on 24 March 1999, possibly due to the engine overheating. This HGV stopped 6 km into the tunnel, when the driver aware of the fire; he was unable to put the fire out. Within minutes the tunnel operators aware of the fire, and prevented more vehicles from entering the tunnel. However, 18 HGVs, nine cars, a van and a motorcycle had already entered the tunnel from France after the first HGV and before the tunnel was closed. In these 29 vehicles, four HGVs managed to pass the burning HGV and travel on towards Italy in safety, but the other 25 vehicles became trapped in the smoke and eventually involved in the fire. Nobody travelling in any of these vehicles

survived. Due to the prevailing wind direction (south) and the different ventilation regimes at end of the tunnel (all ventilation ducts at the Italian end were set to supply fresh air, whereas at the French end some ducts were set to supply and some were set to exhaust), virtually all the smoke from the fire was carried towards France. As the airflow velocity was higher than 1 m/s, the smoke didn't remain stratified, and within minutes there was no fresh air in the tunnel downstream of the fire. The fire grew to involve 25 vehicles behind the first HGV, eight HGVs (which had been abandoned by their drivers, the nearest one being 290 m from the initial HGV fire), and the first fire-fighting vehicle which entered the tunnel from the French side.

At the height of the fire, the blaze was estimated about 190 MW in size, with temperatures in the tunnel exceeding 1000 °C. The fire took 53 hours to extinguish, and hot spots were still being dealt after 5 days. 38 tunnel users and 1 firefighter died as a result of the fire, 27 in their vehicles, 2 in an emergency shelter and the rest on the roadway trying to reach the French portal. This was the greatest ever loss of life in any road-tunnel fire.

*[Main reference: Handbook of Tunnel Fire Safety, 2nd edition, Richard Carvel, Guy Marlair, Chapter 1]*

## 2.3 Example studies in rail tunnel fires

The majority of mass-transit systems used for public transport is railway systems, which consist of trains, each with the capacity for carrying several hundred passengers. These systems clearly have a higher potential for a large number of casualties in the event of a fire, compared with fires in road tunnels. Two incidents in recent years have highlighted the horrendous scale of possible consequences of fires in mass-transit (metro) systems: In 2003, nearly 200 people died following an arson attack on an underground railway/metro train in South Korea; In 1995, over 200 people died following an electrical fire on an underground railway/metro train in Azerbaijan.

Fire disasters have also occurred on conventional and funicular railways. On 11 November 2000, a fire started on a railway carrying skiers up to the Kitzsteinhorn glacier, near Kaprun in Austria. The train been travelling up the side of the mountain rather than through a tunnel, it is unlikely that the fire would have made the news outside of Austria, but due to the confines of the tunnel fire was directly responsible for the deaths of 151 people on the train, The survivors were those who fled down the tunnel; those trying to escape the fire by going up the tunnel were all killed by smoke.

*[Main reference: Handbook of Tunnel Fire Safety, 2nd edition, Richard Carvel, Guy Marlair, Chapter 1]*

## 2.4 Historic overview and analysis of tunnel-fire incidents

### 2.4.1 Road tunnels

| Year | Tunnel length | Location country | Vehicle where fire occurred | Most possible cause of fire | Duration of fire | People | Damaged vehicles | structures and installations |
|---|---|---|---|---|---|---|---|---|
| 1949 | HOLLAND 2550m | New York USA | Lorry with 11 tons of carbondisulfid | load lorry explosion | 4h | 66 injured smoke inhalation | 10 lorries 13 cars | serious damage over 200m |
| 1974 | MONTBLANC 11600m | France-Italy | Lorry | motor | 15min | 1 injured | | |
| 1978 | VELSEN 770m | Velsen Nederland | 4 lorries 2 cars | front-rear collision | 1h20 | 5 dead 5 injured | 4 lorries 2 cars | serious damage over 30m |
| 1979 | NIHONZAKA 2045 m | Shitzuoka Japan | 4 lorries 2 cars | front-rear collision | 159h | 7 dead 1 injured | 127 lorries 46 cars | serious damage over 1100m |
| 1982 | CALDECOTT 1028m | Oakland USA | 1 car 1 coach 1 lorry of petrol | front-rear collision | 2h40 | 7 dead 2 injured | 3 lorries 4 cars 1 coach | serious damage over 580m |
| 1983 | PECORILA 662m | A10 Italy | Lorry with fish | front-rear collision | | 9 dead 22 injured | 10 cars | little damage |
| 1986 | L'MRME 1105m | Nice France | Lorry with trailer | braking after high speed | | 3 dead 5 injured | 1 lorries 4 cars | some damage |
| 1990 | MONTBLANC 11600m | France-Italy | Lorry with 20 tons of cotton | motor | | 2 injured | 1 lorries | some damage |
| 1993 | SERRARIPOLI 442m | A1 Italy | 1 car + lorry of paper | collision | 2h30 | 4 dead 4 injured | 5 lorries 11 cars | little damage |
| 1994 | HUGUENOT 3914m | South Africa | Bus with 45 passengers | electrical fault | 1h | 1 dead 28 injured | 1 coach | serious damage |
| 1995 10Apr | PFANDER 6719m | Austria | lorry with trailer | collision | 1h | 3 dead 4 injured | 1 lorry 1 car 1 van | serious damage |
| 1996 18Mar | ISOLA DELLE FEMMINE 148m | Palermo Italy | 1tanker with liquid gas + 1 little bus | front-rear collision | | 5 dead 20 injured | 1 tanker 1 bus 18 cars | serious damage Tunnel closed 25days |
| 1999 24Mar | MONTBLANC 11600m | France-Italy | lorry with flour and margarine | oil leakage motor | | 39 dead | 23 lorries 10 cars 1 motor 2 fireengines | serious damage Tunnel reopens 22.12.2001 |

| | | | | | | | | |
|---|---|---|---|---|---|---|---|---|
| 1999 29May | TAUERN 6401m | A10 Austria | lorry with paint | front-rear collision | | 12 dead 49 injured | 14 lorries 26 cars | serious damage |
| 2001 28May | PRAPONTIN 4409m | A32 Italy | truck loaded with beets | mechanical problem | | 19 injured by smoke | | closed till 6.June |
| 2001 6Aug | GLEINALM 8320m | A9 Austria | car | collision lorry-car | | 5 dead 4 injured | 1 lorries 1 cars | |
| 2001 24Oct | SLCOTTLAND 16918m | A2 Switzerland | lorry | collision 2 lorries | 2days | 11 dead | 13 lorries 16 cars 4 vans | serious damage closed 2 months |
| 2005 4June | FREJUS 12895m | T2 France-Italy | 1.load: tyers 2.load: cheese 3.load: scrap 4.load: glue | diesel leakage in lorry loaded with tyres | 6hours | 2 dead 21 treated for smoke inhalation | 4 lorries 3 fire fighting vehicles | serious damage Tunnel closed |

Table 2-1 Historic overview of road tunnel fires

It seems that human behavior is a major factor contributing to fatalities in road tunnel fires. The fires in the Nihonzaka and Caldecott Tunnels are both started as a result of collision, whereas many of the people who died in the Mont Blanc incident may have survived if they had evacuated their vehicles quickly and run away from the smoke. The condition in the Mont Blanc Tunnel may also have been less severe if the operators in the control centers had adopted a different ventilation strategy; during the fire incident, ventilation duct was set to supply air at a number of locations, including the fire location; if it had been set to extract smoke, there would have been less oxygen to feed the fire. Approximately 1/3 of all road tunnel fires started as the result of human behavior, while just over fifty percent of the incidents started due to mechanical or electrical failure. One of the primary lessons to be learned from these incidents is that tunnel users need to be appropriately informed in case of an emergency, and this is particularly true in long tunnels. It is also incumbent upon tunnel designers and operators to take account of human behavior in the tunnel situations.

*[Main reference: Lönnermark A "On the characteristics of Fires in Tunnels" Lund University, Sweden. 2005]*

### 2.4.2 Rail tunnels

| Year | Tunnel length | Location | Vehicle where fire occurred | Most possible cause of fire | Duration of fire | People | Damaged vehicles | structure |
|---|---|---|---|---|---|---|---|---|
| 1903 10Aug | Couronnes underground | Paris France | | electrical fault | | >84 dead | | |
| 1921 21Oct | Batignolles L=1000m | Paris France | | collision | | >28 dead | | |
| 1958 28July | London underground Holland park | UK | Train | spark over in electro technical equipment | | 1 dead 51 injured | | |
| 1971 14Feb | Wranduk L=1500m | Yugoslavia | | fire in engine | | 34 dead 120 injured | | |
| 1972 6Nov | Hokoriku | Japan | restaurant car | | | 30 dead 690 injured | 2 carriages | |
| 1979 17Jan | San-Francisco underground | USA | underneath a metro car | short circuit | | 1 dead 58 injured | | |
| 1987 18Nov | Kings Cross station | London UK | escalator 4 (wooden) | | 6h | 31 dead | | |
| 1990 28Dec | New York underground | USA | cable in tunnel | | | 2 dead 200 injured | | |
| 1991 1June | Moscow underground | Russia | under a train | electrical fire | | 7 dead >10 injured | | |
| 1995 28Oct | Baku underground | Azerbaijan | at the rear of the 4th car | electrical fault | | 289 dead 265 injured | 2 rail cars completely damaged | cables |
| 1996 18Nov | Channel Tunnel L=50000m | England-France | 1 HGV | suspected arson | 2.5h | 30 injured by smoke | 10 HGVs | severe damage |
| 1998 10July | Gueizhou L=800m | China | Train | explosion in gas canisters | | >80 dead | | |
| 1999 23May | Salemo L=9000m | Italy | Train | smoke bomb | | 4 dead 9 injured | | |
| 2000 11Nov | Kitzsteinhorn funicular tunnel | Austria | the rear driver's cab | hydraulic oil leakage into the heater | 3h | 155 dead | Train completely burnt out | |

Table 2-2 Historic overview of rail tunnel fires

The lack of a safety management system is partly responsible for the number of deaths. In Kaprun incident, the possibility that the passengers could be carrying flammable materials, at least in the form of clothing, also appears to have never been considered.

The lack of communication led to fatalities. Some 15 minutes after the fire started, the emergency ventilation system was switched on, and this directed the smoke towards the majority of the passengers – the lack of communication meant that those in the control room did not have idea what was going on at the fire.

Aside from these incidents, large scale fires rarely happen on passenger trains, as there is comparatively little fuel to burn, and many people are able to extinguish the fire while it is still small. This is not the case for goods trains. Possibly the most severe train fire in a tunnel also resulted in no fatalities.

The majority of the fires in rail tunnels appear started as the result of electrical or mechanical failure, only with a small percentage starting as a direct result of human behavior. An important fire safety issue concerning existing railway tunnels has been raised. While a significant number of safety measures have been implemented in tunnels constructed in last few decades, there are a vast number of older tunnels, particularly in Europe, many of which are hundred years old. It has been questioned whether fire safety requirements can ever be met in these tunnels, and indeed, if it is even safe for fire fighters to fight fires or mount rescue attempts in such tunnels. In many cases, there is not even a local water supply for fire fighters to use.

*[Main reference: Lönnermark A "On the characteristics of Fires in Tunnels" Lund University, Sweden. 2005]*

# 3. Fire dynamics

## 3.1 Introduction

The occurrence of some catastrophic fires has put the focus on fire dynamics in tunnels. In particular there has a need for a better understanding of the influence of ventilation on the HRR (heat release rate), and how fire and the smoke spread in a tunnel.

The principal phenomena of tunnel fires and fire dynamics are discussed here. Descriptions are given of the development of fires in tunnels and building compartments, and the influence of ventilation on a fire (fuel control and ventilation control). In addition, information are given for the gas temperatures, the stratification of smoke, flame lengths, the incident radiation, and the spread of fire between vehicles.

## 3.2 Tunnel fires and open fires

*[Main reference: Handbook of Tunnel Fire Safety, 2nd edition, Haukur Ingason, Chapter 13]*

Tunnel fires different from open fires in at least two important ways. 1. The feedback of heat to burning vehicles in a tunnel tends to be more effective than that in an open-air environment, because of the confined space. This effective heat feedback often causes vehicles that do not burn intensely in an open fire to burn vigorously in a tunnel fire. 2. As a fire develops in a tunnel, it interacts with the ventilation airflow and generates aerodynamic disturbance in the tunnel. This interaction and disturbance may lead to changes in the ventilation flow pattern, such as throttling of airflow (buoyancy effects).

## 3.3 Tunnel fires and compartment fires

*[Main reference: Handbook of Tunnel Fire Safety, 2nd edition, Haukur Ingason, Chapter 13]*

Tunnel fires different from building compartment fires in at least three important ways. 1. The maximum heat-release rate in compartment fires is usually dictated by the natural ventilation, in tunnels, however, the fire size, tunnel slope, cross-sectional area, length, type of tunnel and meteorological conditions at the entrance all govern the natural ventilation. Tunnels are also

often equipped with mechanical ventilation, such as exhaust fans and/or jet fans in the ceiling. 2. Compartment fires can easily grow to 'flashover' within a few minutes. Flashover can hardly take place outside of a 'compartment'. Tunnel fires are, therefore, not likely to grow to conventional 'flashover', due to the large heat loss from the fire to the surrounding walls and the lack of containment of hot gases. 3. The formation of the stratified smoke layer. In the early stages of compartment fires, an upper quiescent buoyant smoke layer is formed, with a cold smoke-free layer below. A similar smoke layer may be created in tunnels during the early stage in a fire when there is essentially no longitudinal ventilation. The smoke layer will gradually move further away from the fire. If the tunnel is very long, the smoke layer may move to the tunnel surface. The distance from the fire that may occur depends on the fire size, the tunnel type, the perimeter and height of the tunnel cross-section. When the longitudinal ventilation is gradually increased, this stratified layer gradually dissolves. A back-layering of smoke is happened on the upstream side of the fire, and the degree of stratification of the smoke downstream from the fire is governed by the heat loss to the surrounded walls and by the turbulent mixing between the buoyant smoke layer and the cold layer moving to the opposite direction.

### 3.3.1 Fire development

The fire in a compartment is usually divided into two separate stages: the pre-flashover stage and post-flashover stage. Three distinct time periods of fire development are usually given within the pre and post flashover stages. The first is the growth period, the second is the fully developed fire, and the last stage is the decay period (Fig 3-1). The development of a fire in a tunnel can be described in the same way.

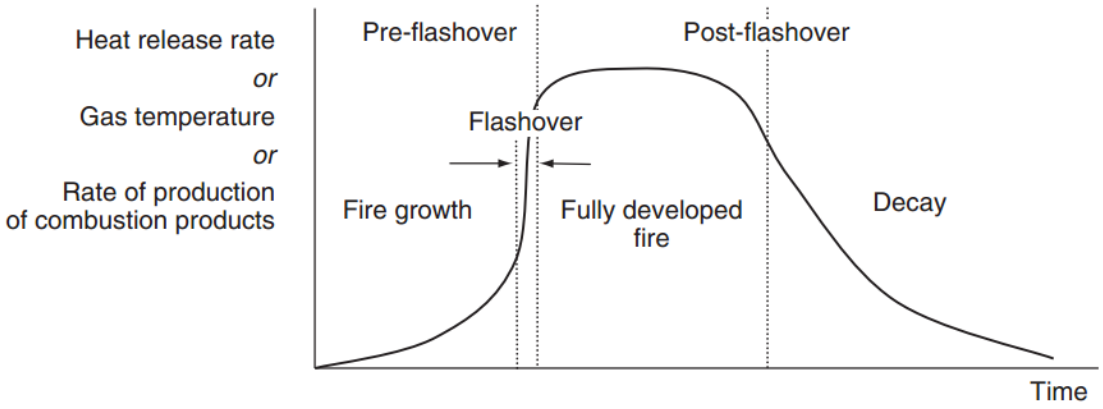


Fig 3-1 Different phases of a typical compartment fire

*[Handbook of Tunnel Fire Safety, 2nd edition, Haukur Ingason, Chapter 13]*

In the growth period in compartment fires, when there is sufficient oxygen available for combustion and the growth of the fire depends entirely on the flammability of the fuel and the geometry. During the fire growth period, the fire will either continue to develop to beyond a point at which interaction with the compartment boundaries becomes significant (flashover), or it will start to decay. The fire will either start to decay because lack of fuel, whereby the fire size is dictated by the inflow of fresh air towards the base of the fire source.

### 3.3.2 Fuel control and ventilation control

Compartment fires are usually defined as either fuel-controlled or ventilation-controlled. A fuel-controlled fire may also be described as well-ventilated, over ventilated, oxygen rich or fuel lean. A ventilation-controlled fire may be described as fuel rich, oxygen starved or under ventilated. A compartment fire is generally fuel-controlled during the pre-flashover stage, and even in the decay period, in rare cases, the post-flashover period. The fire is generally ventilation controlled in the post-flashover stage and in rare cases even in the pre-flashover stage. The difference between these two combustion modes are: For compartment fires, the transition period between these two physical conditions is usually defined as the 'flashover'. In tunnels, fires are usually fuel-controlled, but in severe fires where multiple vehicles are involved, the fires are ventilation controlled.

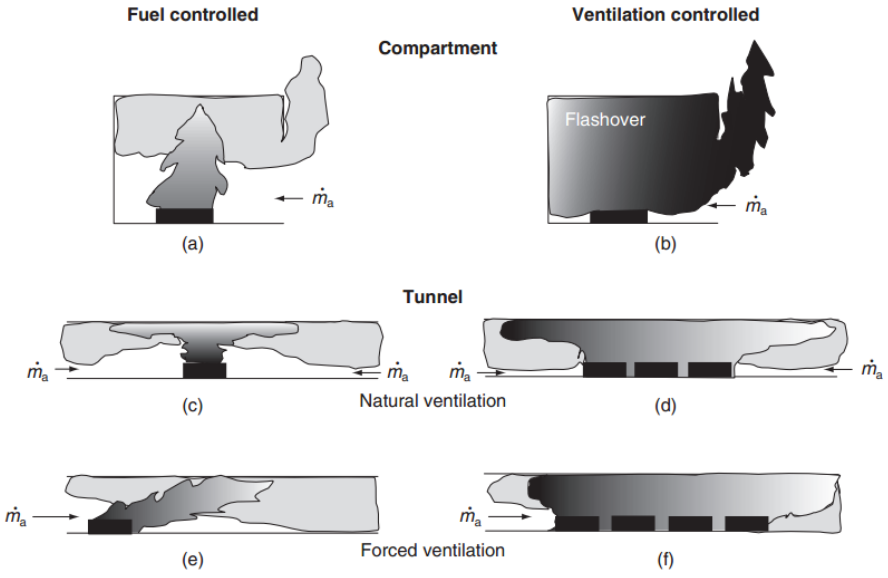


Fig 3-2 Principal sketch of fuel-controlled and ventilation-controlled fire

*[Handbook of Tunnel Fire Safety, 2nd edition, Haukur Ingason, Chapter 13]*

For the theoretical view of the two different conditions:

When the fire is fuel controlled, if the air/fuel mass ratio is greater than or equal to the stoichiometric value r, (i.e. $\dot{m}_a / \dot{m}_f \geq r$) or $\phi \geq 1$, the fire is assumed to be fuel controlled, and the heat-release rate is directly proportional to the rate of loss of fuel mass $\dot{m}_f$. Then consider the case where the oxygen concentration in the gases flowing out of the compartment or the tunnel exit is greater than zero. The heat-release rate Q (kW), which is directly proportional to the rate of loss of fuel mass loss $\dot{m}_f$ (kg/s), can then be calculated using the equation:

$$Q = \dot{m}_f \chi H_T \tag{3-1}$$

*[Handbook of Tunnel Fire Safety, 2nd edition, Haukur Ingason, Chapter 13]*

$H_T$ is the heat of complete combustion (kJ/kg), $\chi$ is the ratio of the effective heat of combustion to the net heat of complete combustion.

When the fire is ventilation controlled, if the air/fuel mass ratio is less than the stoichiometric value, $\dot{m}_a / \dot{m}_f < r$ or $\phi < 1$, the fire is defined as ventilation controlled and the HRR- Q is directly proportional to the mass flow rate of air $\dot{m}_a$ (i.e. it is proportional to the oxygen supply) available for combustion. Sometimes, but not always, we can simplify this by denoting that the oxygen concentration in the gases flowing out of the compartment or the tunnel exit is essentially zero. One notable exception is that ventilation-controlled fires in large compartments with small openings. There are numerous options available for calculating the heat release rate for these conditions. The simplest is the following equation, which assumes complete combustion and that all the air $\dot{m}_a$ is consumed:

$$Q = \dot{m}_a \frac{H_T}{r} \tag{3-2}$$

*[Handbook of Tunnel Fire Safety, 2nd edition, Haukur Ingason, Chapter 13]*

The ratio $H_T / r$ is assumed to be about 3000 kJ/kg of air consumed for most carbon-based materials.

It has been argued that, for incomplete combustion, there are counter-acting effects, which means that equation (3-2) is approximately valid in this case also, as well as for the case of complete combustion. If all the oxygen were consumed in the fire, the energy developed would correspond to $13 \times 10^3$ kJ/kg of oxygen consumed (i.e. 3000/0.231, assuming that 23.1% (mass) of the air is oxygen). This number is well known from calorimeter measurements made in fire laboratories, which use the average value of $13.1 \times 10^3$ kJ/kg.

### 3.3.3 Flashover

The parameters that govern whether a fire will spread dramatically include the fire load, the dimensions of the compartment and the ventilation openings, and the thermal properties of the surrounded walls. Flashover in a compartment has been explained as thermal instability caused by the rate of energy generation increasing faster with temperature than the rate of aggregated energy losses. This phenomenon usually occurs over a short period, and results in a rapid increase in the heat-release rate, gas temperatures and production of combustion products. After flashover occurred in a compartment, the rate of heat release will develop to produce temperatures of $900-1000^{\circ}C$. As mentioned above, the period after flashover is called the 'post-flashover stage' or the 'fully developed fire period' (Fig 3-1). During this period the HRR is dictated by the oxygen flow through the openings, and the fire is said to be 'ventilation controlled' (Fig 3-2). The amount of heat released depends on the relative quantities of air in the compartment. The mass flow rate of air through the opening $\dot{m}_a$ can be expressed in follows:

$$\dot{m}_a = \rho_a \delta \sqrt{g} A_0 \sqrt{h_0} \tag{3-3}$$

*[Handbook of Tunnel Fire Safety, 2nd edition, Haukur Ingason, Chapter 13]*

Where $\delta$ is a proportionality constant, which is a weak function of temperature, $A_0$ is the area of the opening ($m^2$) and $h_0$ is the height of the opening (m). The value of $\delta$ has been estimated to be 0.08 for pre-flashover fires and 0.13 for post-flashover fires.

## 3.4 Stratification of smoke in tunnels

*[Main reference: Handbook of Tunnel Fire Safety, 2nd edition, Haukur Ingason, Chapter 13]*

The stratification of smoke has important implications for those who escape from the tunnel. The characteristics of the smoke spread are highly dependent on the air velocity inside the tunnel. In order to illustrate that, we identified three typical ranges (groups) of air velocity:

### 3.4.1 Low or no forced air velocity (0–1 m/s)

For the low forced air velocity range, the stratification of the smoke is usually high in the vicinity of the fire source. This group normally includes tunnels with natural ventilation. The back layering distance of the smoke is relatively long, and in some cases the smoke travels nearly uniformly in both directions (Fig 3-3a). When the velocity increases and is close to about 1 m/s, back-layering of the smoke occurs upstream of the fire source, at a distance which can be of the order of 17 times the height of the tunnel (Fig 3-3b).

### 3.4.2 Moderate forced air velocity (1–3 m/s)

In the moderate forced air velocity group, the stratification in the vicinity of the fire is strongly affected by the air velocity, particularly at the higher velocities. This group normally includes tunnels with natural ventilation or forced ventilation. The back-layering distance can vary between 0 up to 17 times the tunnel height (Fig 3-3c).

### 3.4.3 High forced air velocity (>3 m/s)

In the high forced air velocity group, there is usually low stratification of the smoke downstream of the fire, and usually no back-layering (Fig 3-3d). This group normally includes tunnels with forced ventilation. The actual velocity, which is required to prevent any back-layering, is sometimes called the 'critical velocity'.

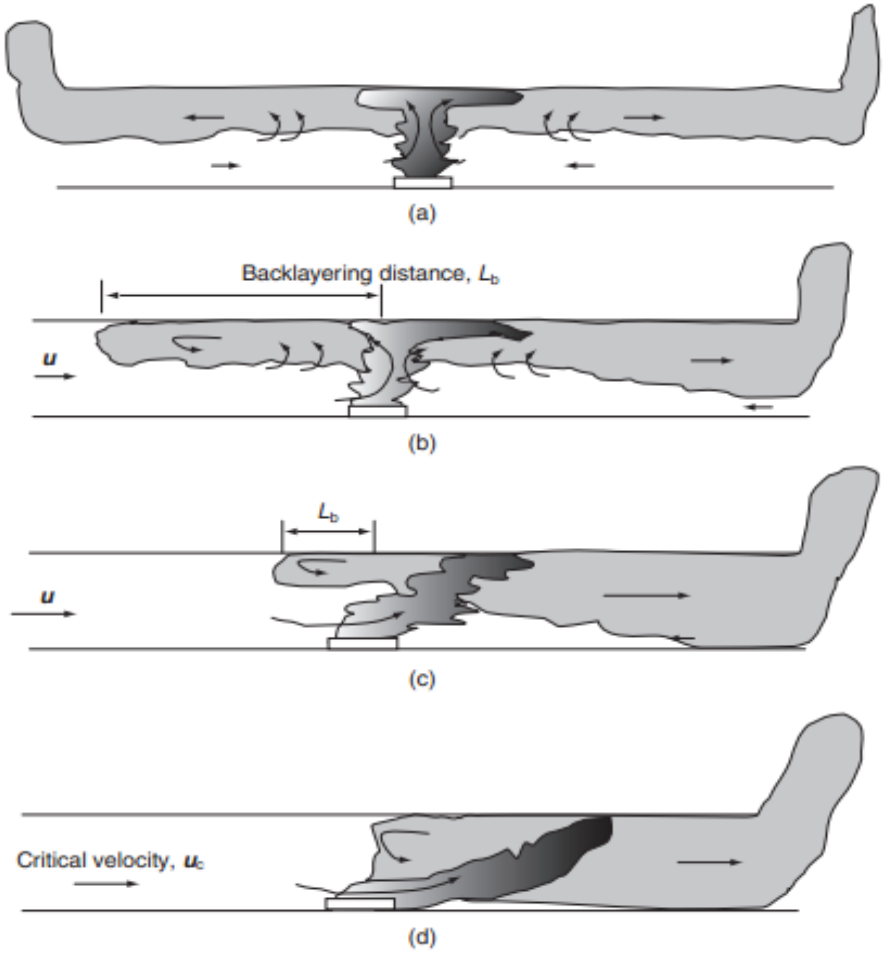


Fig 3-3 Schematic sketches showing the smoke stratification in tunnels having different forced air velocities

*[Handbook of Tunnel Fire Safety, 2nd edition, Haukur Ingason, Chapter 13]*

## 3.5 Nominal temperature-time curves

*[Main reference: Eurocode 1: Actions on structures- Part 1-2: General actions- Actions on structures exposed to fire]*

The time-temperature curve is used in fire-resistance tests, many countries around the world rely on full size fire-resistance tests to assess the fire performance of building materials and structural elements. Full scale tests are preferred to small-scale tests because they allow the method of construction to be assessed, including the effects of thermal expansion and deformation under load.

### 3.5.1 Standard temperature-time curve

(1) The standard temperature-time curve is given by:

$$\Theta_g = 20 + 345\log_{10}(8t+1);[^{\circ}C] \quad (3\text{-}4)$$

Where $\Theta_g[^{\circ}C]$ is the gas temperature in the fire compartment, t [min] is the time

(2) The coefficient of heat transfer by convection is:

$$\alpha_c = 25[W/m^2K]$$

### 3.5.2 External fire curve

(1) The external fire curve is given by

$$\Theta_g = 660(1-0.687e^{-0.32t}-0.313e^{-3.8t})+20;[^{\circ}C] \quad (3\text{-}5)$$

Where $\Theta_g[^{\circ}C]$ is the gas temperature in the fire compartment, t [min] is the time

(2) The coefficient of heat transfer by convection is:

$$\alpha_c = 25[W/m^2K]$$

### 3.5.3 Hydrocarbon curve

(1) The hydrocarbon temperature-time curve is given by:

$$\Theta_g = 1080(1-0.325e^{-0.167t}-0.675e^{-2.5t})+20;[^{\circ}C] \quad (3\text{-}6)$$

Where $\Theta_g[^{\circ}C]$ is the gas temperature in the fire compartment, t [min] is the time

(2) The coefficient of heat transfer by convection is:

$$\alpha_c = 50[W/m^2K]$$

## 3.6 Heat transfer

*[Main reference: Drysdale D., "An Introduction to Fire Dynamics", John Wiley & Sons, 2nd Edition, chapter 2]*

There are three basic mechanisms of heat transfer, conduction, convection and radiation. While it is probable that all three contribute in every fire, it is often found that one predominates at a given stage, or in a given location. So conduction determines the rate of heat flow in and through solids. It is important in problems relating to ignition and spread of flame over combustible solids, for fire resistance, where knowledge of heat transfer through compartment boundaries and into elements of structure is required. Convective heat transfer is associated with the exchange of heat between a gas or liquid and a solid, and involves movement of the fluid medium. It occurs at all stages in a fire but is particularly important early on then thermal radiation levels are low. For natural fires, the movement of gases associated with this transfer of heat is determined by buoyancy which also influences the shape and behavior of diffusion flames.

Unlike conduction and convection, radiation heat transfer requires no intervening medium between the heat source and receiver. It is the transfer of energy by electro-magnetic waves, of which visible light is the example with which we have most familiar. Radiation in all parts of the electromagnetic spectrum can be absorbed, transmitted or reflected at a surface, and any object placed in the way will cast a shadow, it becomes the dominant mode of heat transfer in fires as the fuel bed diameter increases beyond about 30cm, and determines the growth and spread of fires in compartments, it is the mechanism by which objects at a distance from the fire are heated to the fire point condition, and is responsible for the spread of fire through open fuel beds(e.g. forests) and between buildings. Amount of heat released in flames is transmitted by radiation to the surroundings. Most of this radiation is emitted by solid particles of soot which are formed in almost all diffusion flames: this is the source of their characteristic yellow luminosity. The effect of thermal radiation from flames, or indeed from any heated object, on nearby surfaces can be ascertained by carrying out a detailed heat transfer analysis. Such analysis are required to establish how rapidly combustible materials which are exposed to the thermal radiation will reach a state in which they can be ignited and will burn.

For this reason it is necessary to introduce the basic equations of the basic equations of heat transfer, as it is impossible to examine any one of the mechanisms in depth in isolation from the others.

### 3.6.1 Conduction

Conduction is the mode of heat transfer associated with solids. Although it also occurs in fluids, it is normally masked by convective motion in which heat is dissipated by a mixing process driven by buoyancy. It is a common experience that heat will flow from a region of high temperature to one of low temperature; this flow can be expressed as a heat flux, which is one direction is given by:

$$q = \lambda A(t_1 - t_2)/L \quad \text{or} \quad q = -\lambda A \partial t / \partial x \tag{3-7}$$

$q$ : thermal flux (W)

$\lambda$ : thermal conductivity( $W/m^{\circ}C$ )

Typical values of $\lambda$

Concrete: 0.8-1.4

Steel: 10-70

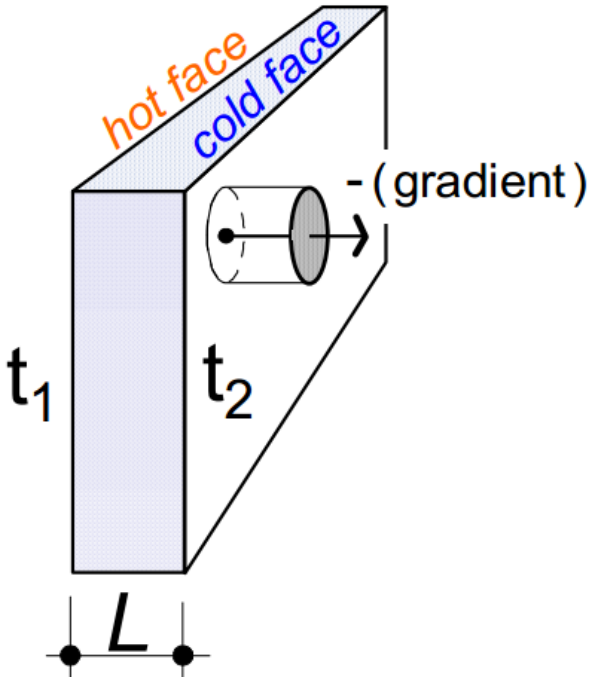


Fig 3-4 Heat transfer by conduction

### 3.6.2 Convection

Convection is that mode of heat transfer to or from a solid involving movement of a surrounding fluid, either gases or liquids. Convective heat transfer is an important factor in flame spread and in upward transport of smoke and hot gases to the ceiling or out the window from a room fire. Convective heat transfer calculations usually involve heat transfer between the surface of the solid and a surrounding fluid which heats or cools the solid material. The rate of heating or cooling depends on several factors especially the velocity of the fluid in surface. The empirical relationship shows below:

$$q = \alpha_c A(t_{surface} - t_{fluid}) \tag{3-8}$$

$q$ : thermal flux (W) $\alpha_c$ : thermal convection coefficient ( $W/m^{2\circ}C$ )

Typical values of $\alpha_c$ ($W/m^{2^\circ}C$):

Air-natural convection: 1-20 (forced: 40-250); Water-natural convection: 250-750 (forced: 1000-12000); Still air (sides not exposed to fire): 4; Including radiation in linearized form: 9 Air in turbulent regime (sides exposed to fire) ISO 834 and external nominal fires: 25; Hydrocarbon nominal fire: 50; Parametric fire and zone models: 35

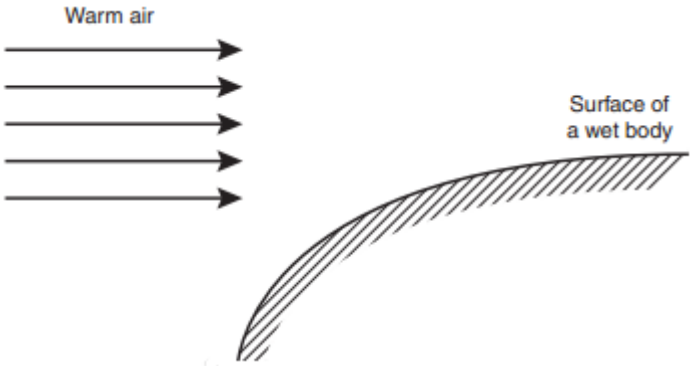


Fig 3-5 Heat transfer by convection

### 3.6.3 Radiation

Radiation is the transfer of energy by electromagnetic waves which can travel through the vacuum, transparent solid or liquid. It is very important in fires because it is the main mechanism for heat transfer from flames to fuel surfaces, from hot smoke to building objects and from the burning building to adjacent ones. According to the Stefan-Boltzmann equations, the total energy emitted by a body is proportional to $T^4$, where $T^4$ is the temperature in Kelvin, the total emissive power:

$$E = \varepsilon\sigma T^4 (W/m^2) \tag{3-9}$$

Where $\sigma$ is the Stefan-Boltzmann constant ($5.67\times10^{-8} W/m^2K^4$) and $\varepsilon$ is a measure of the efficiency of the surface as a radiator (emissivity). The perfect emitter: the 'black body' has an emissivity of unity. The intensity of radiant energy q falling on a surface remote from the emitter found by using the appropriate 'configuration factor' $\phi$ which takes into account the geometrical relationship between the emitter and the receiver:

$$q = \phi\varepsilon\sigma T^4 (W/m^2) \tag{3-10}$$

## 3.7 Fire plumes

*[Main reference: SFPE Handbook of Fire Protection Engineering, 3rd Edition, Gunnar Heskestad. Section 2 Chapter1]*

All fires go through an important initial stage; buoyant gas stream rises above a localized volume undergoing combustion into surrounding space of essentially uncontaminated air. This stage begins at ignition, then continues through a possible smoldering interval, into a flaming interval, and may be said to end prior to flashover. The buoyant gas stream is usually turbulent, except when the fire source is very small. The buoyant flow, including any flames, is referred to as a fire plume.

Combustion may be the result of pyrolysis of solid materials or evaporation of liquids because feedback of heat from the combustion volume, or of pressurized release of flammable gas. Other combustion situations may involve discharge of liquid sprays and aerosols. In the case of high-pressure release, the momentum of the release may be important. Flames in these situations are usually referred to as diffusion flames; being the result of combustible vapor or gas mixing or diffusing into air, as opposed to being premixed with an oxidant. The properties of fire plumes are important in dealing with problems related to fire detection, fire heating of building structures, smoke filling rates, fire venting. They can also be important in fire suppression system design.

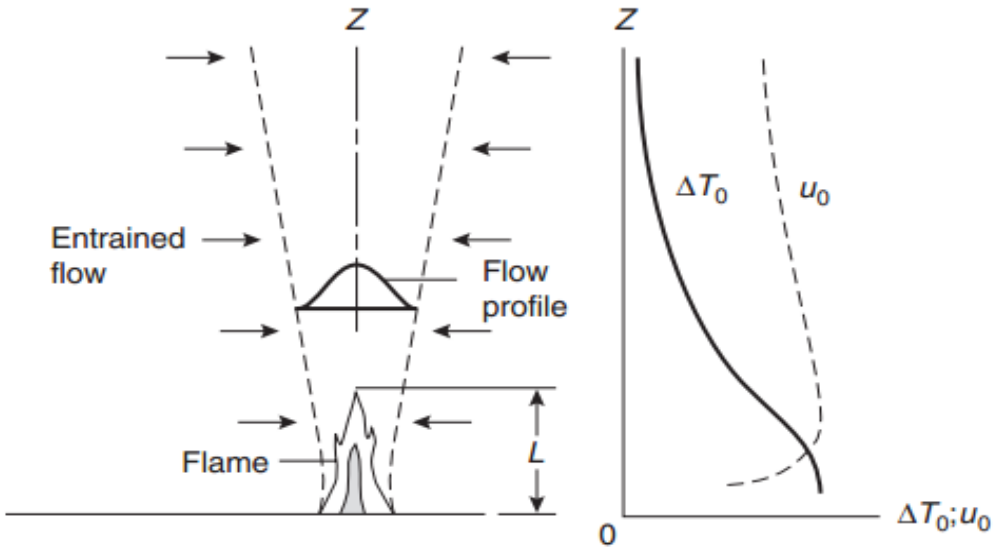


Fig 3-6 Features of a turbulent fire plume, including axial variations on the centerline of mean excess temperature, and mean velocity

*["SFPE Handbook of Fire Protection Engineering".3rd Edition, Gunnar Heskestad. Section 2 Chapter1]*

Fig 3-6 shows a schematic representation of a turbulent fire plume originating at a flaming source, which may be solid or liquid. Volatiles driven off from the combustible, by fed back of heat from the fire mix with the surrounding air and form a diffusion flame. Laboratory simulations often employ controlled release of flammable gas through a horizontal, porous surface. The mean height of the flame is surrounding the flame and extending up-ward is a boundary (broken lines) that confines the entire buoyant flow of combustion products and entrained air. The air is entrained across the boundary, which is very sharp, highly convoluted, and easily discernible in smoky fires. The flow profile could be the time-averaged temperature rise above the ambient temperature, or the concentration of a gas generated by the fire, or the axial velocity in the fire plume.

Fig 3-6 also suggests qualitatively, based on experimental observations, how the temperature rise on the centerline, $\Delta T_0$, and the velocity on the centerline, $u_0$, may behave along the plume axis. In this example of a relatively tall flame, the temperatures are nearly constant in the lower portion of the flame. Temperatures begin decay in the intermittent, upper portion of the flame as the combustion reactions trail off and air entrained from the surroundings cools the flow. The centerline velocities, $u_0$, tend to have the maxima slightly below the mean flame height and decay toward higher elevations. If the combustible is porous and supports internal combustion, there may not be as pronounced a falloff in the gas velocity toward the top of the combustible, just as suggested in the Figure.

The total heat release rate Q, often assumed to be equal to the theoretical heat release rate, which is based on complete combustion of the burning material. The theoretical heat release rate in KW is computed as the mass burning rate in kg/s multiplied by the heat of complete combustion in kJ/kg. The ratio of the total heat release rate to the theoretical heat release rate, which is the combustion efficiency, close to unity for some fire sources (e.g., methanol and heptane pools), but may deviate significantly from unity for others (e.g., a poly- styrene fire, the combustion efficiency is about 45 percent, and a fully involved stack of wood pallets, for which the combustion efficiency is 63 percent).

## 3.8 Flows

### 3.8.1 Ceiling jet flows

*[Main reference: "SFPE Handbook of Fire Protection Engineering".3rd Edition, Ronald L. Alpert Section 2 Chapter2]*

Much of the hardware associated with detection and suppression of fire, in commercial, manufacturing, storage, and modern residential buildings located near the ceiling surfaces. In the case of fire, hot gases in the fire plume rise directly above the burning fuel and impinge on the ceiling. The ceiling surface causes the flow to turn and move horizontally under the ceiling to other areas of the building remote from the position of fire. The response of smoke detectors, heat detectors, and sprinklers in-stalled below the ceiling so as to be submerged in this hot flow of combustion products from a fire provides the basis for building fire protection.

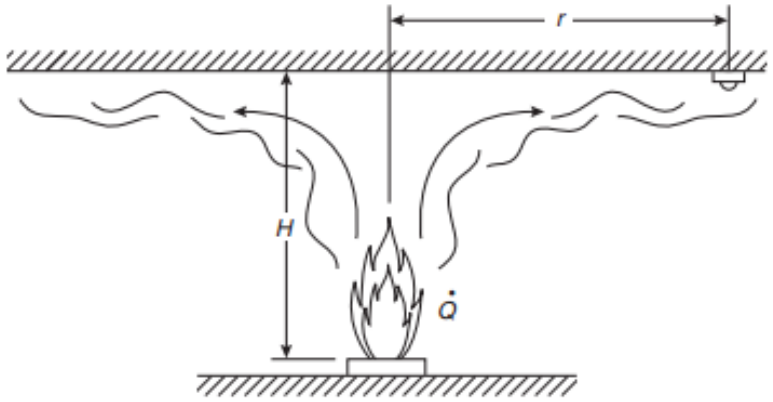


Fig 3-7 Ceiling jet flow beneath an unconfined ceiling

Fig 3-7 shows an idealization of an axisymmetric ceiling jet flow at varying radial positions r, beneath an unconfined ceiling. In actual fires in buildings, the simple conditions pictured a hot, rapidly moving gas layer sandwiched between the ceiling surface and tranquil, ambient temperature air; exist only at the beginning of fire, when the quantity of combustion gas produced is not sufficient to accumulate into a stagnant, heated gas layer in the upper portion of the compartment.

As shown in Fig 3-7, the ceiling jet flow emerges from the region of plume impingement on the ceiling, flowing radially away from the fire. The layer grows thicker by entraining room air at the lower boundary. This entrained air cools the gases in the jet and reduces its velocity. As the hot gas move out across the ceiling, heat transfer cools the portion adjacent to the ceiling surface.

### 3.8.2 Vent flows

*[Main reference: "SFPE Handbook of Fire Protection Engineering".3rd Edition, Howard W. Emmons Section 2 Chapter3]*

Fire releases a great amount of heat which causes the heated gas to expand. The expansion produced by fire in a room drives some of the gas out of the room. Any opening through which gas can flow out of the fire room called a vent.

The most obvious vents in a fire room are open doors and open or broken windows. Ventilation ducts also provide important routes for the release of gas. A room in a building may have all of its doors and windows closed and if ventilation ducts are also closed, the gas will leak around normal closed doors and windows and through any holes made for pipes or wires. These holes will act also as vents.

Gas will move only if it is pushed. The only forces acting on the gas are the pressure and gravity. Since gravity acts vertically, it seems that gas could only flow through a hole in the floor or ceiling. Gravity, however, can produce horizontal pressure changes, which will be explained in details below. A gas flow that is caused directly or indirectly by gravity is called a buoyant flow.

When a pressure difference exists in a vent, fluid (liquid or gas) will be pushed through. Precise calculation of such flows from the basic laws of nature could only be performed today by the largest computers. For fire purposes, and engineering purposes, calculations are carried out with sufficient precision using the methods of hydraulics. But these formulas are only approximate, they are made sufficiently accurate by a flow coefficient. These coefficients are determined by experimental tests. If a pressure drop, $\Delta P = P_1 - P_2$, exists across a vent of area A, with a fluid density $\rho$, the flow through the vent has (see Fig 3-8):

Velocity:

$$u = \sqrt{2\Delta P / \rho} \qquad (3\text{-}11)$$

Volume flow:

$$Q = CA\sqrt{2\Delta P / \rho} \qquad (3\text{-}12)$$

Mass flow:

$$\dot{m} = CA\sqrt{2\rho\Delta P} \qquad (3\text{-}13)$$

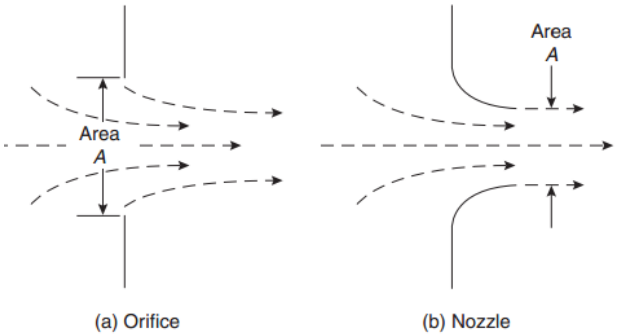


Fig 3-8 Vent flow

# 4. Fire safety

## 4.1 Introduction

A number of different kinds of safety system are installed in road, rail and underground railway/ metro tunnels, including fire detection, ventilation, suppression systems and alarm systems. While these systems are very diverse, all of them have the same basic aims, (i.e. to reduce the risk of injury or fatality for tunnel users and to reduce the risk of damage to the tunnel structure or operation). Central to the understanding of the expediency of these systems is an understanding of risk, and the related concepts of prevention and protection. With the terms 'hazard' and 'risk', there is often lack of clarity in the use of the terms prevention and protection. A measure that one person refers to as 'prevention' may be referred to by another person as 'protection'. There is no absolute answer in which these terms may be understood. However, these concepts may be seen in a straightforward manner in relation to the concept of a crucial event. Measures relating to prevention may regarded as those that reduce the probability of a crucial event occurring, while measures relating to protection may be seen as those aimed at reducing the consequences after a crucial event. ('protection' here may be regarded as including 'total protection' (i.e. no harm occurs), or 'mitigation' (i.e. 'partial protection'), in which some harm would come.) .

Fire safety management may be seen in terms of the two key concepts of prevention and protection, where protection is assumed includes mitigation. This is a special case of the management of risk in general. Measures aimed at reducing the probability of ignition may be regarded as preventive, and measures aimed at eliminating or reducing harm after ignition may be regarded as protective. As a part of overall fire safety management, it is essential to have a coherent fire safety management system. To be as effective as possible, it is essential that both prevention and protection can be considered at the start of the design stage. Categories of measures that fall within the ambit of fire safety management are summarized in Fig 4-1. Sometimes a measure may be regarded as both preventive and protective.

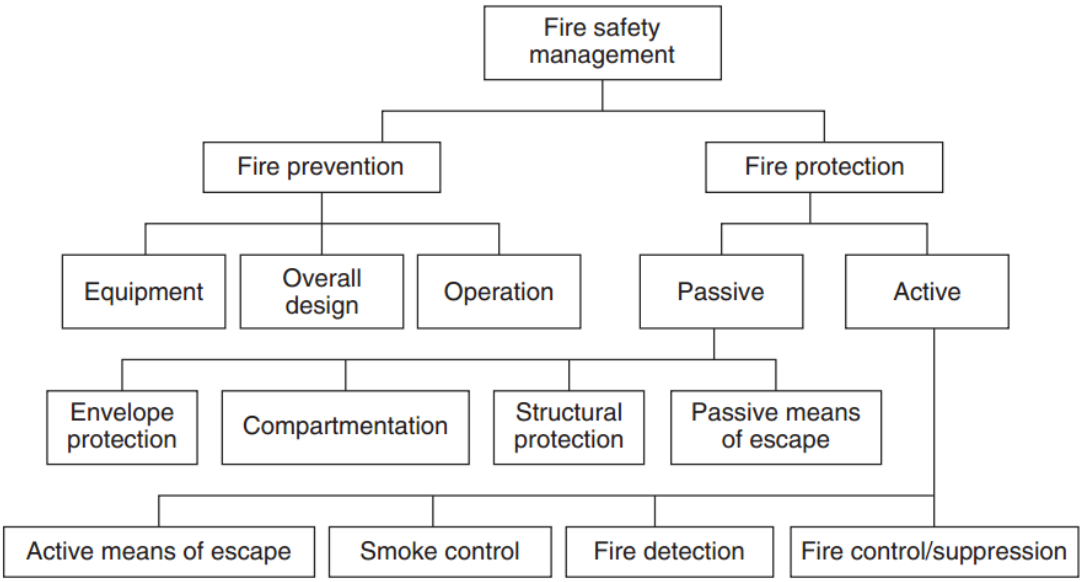


Fig 4-1 Categories of fire safety management

*[Handbook of Tunnel Fire Safety,2nd edition. Alan Beard. Paul Scott. Chapter 5]*

## 4.2 Fire prevention

*[Main reference: Handbook of Tunnel Fire Safety,2nd edition. Alan Beard. Paul Scott. Chapter 5]*

In general, fire prevention is to try to ensure that ignition does not take place. In the tunnel context, four general methods for achieving this are:

Category 1: eliminate or reduce the number of ignition sources and hot surfaces.

Category 2: have materials or items of 'low ignitability' wherever possible (e.g. fire retarded).

Category 3: keep ignition sources and potential fuels well separated.

Category 4: eliminate or reduce the chance of spontaneous ignition.

Two strategic methods are: prevent an ignited item moving into a tunnel; and prevent ignition of an item inside a tunnel. The word 'item' here is used for simplicity; it could just as easily be a fuel, such as a combustible liquid pool.

### 4.2.1 Prevention: some specific topics

A few specific topics are discussed below as examples of the kinds of practical measures might be taken to try to reduce the probability of a fire occurring in tunnel.

**Detection of overheated vehicles:**

An inspection facility at the entrance to a tunnel may be put in place, as in the Mont Blanc Tunnel. If a vehicle (especially a HGV) were found to be overheated, then it would not be allowed to enter the tunnel until it had cooled sufficiently. This may be regarded as category 1 above.

**Use of white surfaces:**

Increasing the illumination level in a tunnel may help to reduce the chance of an accident. Measurement that can contribute to this is to use a white or light-colored road and/or wall surface. This measure may be regarded as belonging to category 3 above, i.e. keeping potential fuels and ignition sources well separated by reducing the chance of a collision. It also be regarded as protective to some extent, in that a white or light-colored road surface may possibly assist escape.

**Speed control:**

Controlling the speed of vehicles in tunnels is extremely important. This may be regarded as risk category 3 above, i.e. reducing the chance of a collision.

**Spacing between vehicles:**

Maintaining sufficient space between vehicles is also very important. This measure may also be regarded as part of fire protection. As part of fire prevention, it may be seen as in category 3 above.

**Shuttle transport and road-ferries:**

The approach has also been proposed for use on congested bridges, where it has been called a ‘road-ferry’. It has been estimated that the system proposed would considerably increase, not decrease, the carrying capacity of the bridge. When relating to tunnels, it would provide one possible way of controlling the passage of HGVs and other vehicles through a tunnel. Such a measure may be regarded as in being in category 1 above.

**Fire-resistant materials and fire retardants:**

Using fire-resistant materials in vehicles may help to reduce combustibility, and this measure would come under category 2 above. In the sense that fire-resistant materials may not stop ignition but may impede fire growth, they may also be regarded as part of protection.

**Vehicle design:**

Changing vehicle design may have a significant effect on the chance of a fire starting or spreading in a tunnel. Changes may have the effect of increasing or decreasing the chance of harmful effects. For example, increasing the fuel tank size in HGVs is an undesirable change. This issue illustrates how tunnel safety results from the action of the broader system, not just the immediate tunnel system itself.

## 4.3 Fire protection

*[Main reference: Handbook of Tunnel Fire Safety,2nd edition. Alan Beard. Paul Scott. Chapter 5]*

As indicated in Fig 4-1, fire protection consists of active fire protection and passive fire protection.

### 4.3.1 Passive fire protection in concrete tunnels

Passive measures of fire protection are those related to the features of the tunnel structure itself, its subdivisions and the envelope of the structure. They are properties of the tunnel's construction that serve to limit the spread of smoke and fire, should a fire occur. Essentially, they are there for the lifetime of the tunnel. Passive fire-protection measures generally take one of three forms: a secondary layer of a concrete or cementations material applied to the inner surface of the tunnel. Cladding – Panels of protective materials, fixed in the tunnel walls and ceiling. Addition of certain fibers, etc., to the main concrete mix, to make the concrete more 'fireproof'. These measures are illustrated in Fig 4-2

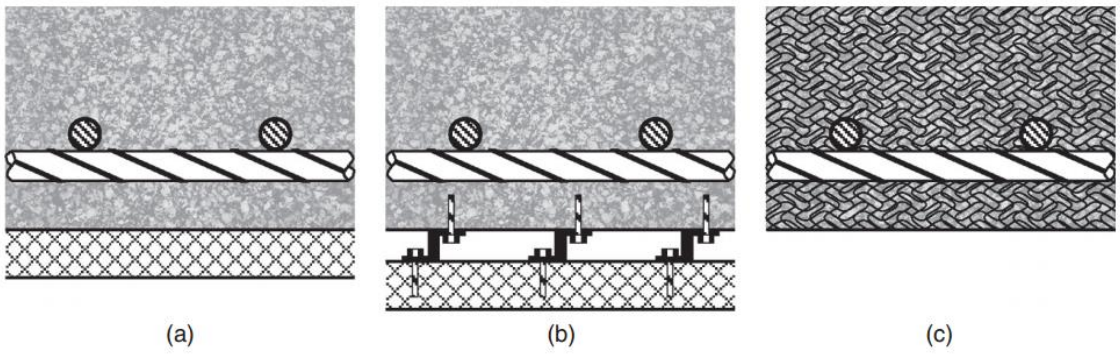


Fig 4-2 Types of passive fire protection (the bars in the concrete represent steel reinforcement rods). (a) A secondary layer of insulating material applied directly to the tunnel lining; (b) A panel cladding system. Certain types of cladding may be bolted directly to the tunnel lining, not separated by an air gap as shown. (c) T addition of fibers to the concrete mixture

#### 4.3.1.1 Secondary tunnel lining systems

The simplest and cheapest form of tunnel-lining system is the application of a layer of insulating material to the interior surfaces of the primary tunnel lining. These are generally known as ‘passive thermal barriers’, and are often of the form of vermiculite cements, which can be sprayed on the tunnel lining to the desired thickness. Vermiculite cements are inorganic materials that cannot burn, produce smoke or release toxic gases under high temperature conditions.

The passive thermal barriers should be designed in such a way that additional equipment (ventilators, traffic lights, etc.) can be safely suspended from ceilings and walls. It has occasionally been observed that the anchors used in suspension systems for additional equipment provided a pathway for heat leakage into the concrete, resulting in unexpected spalling (Fig 4-3).

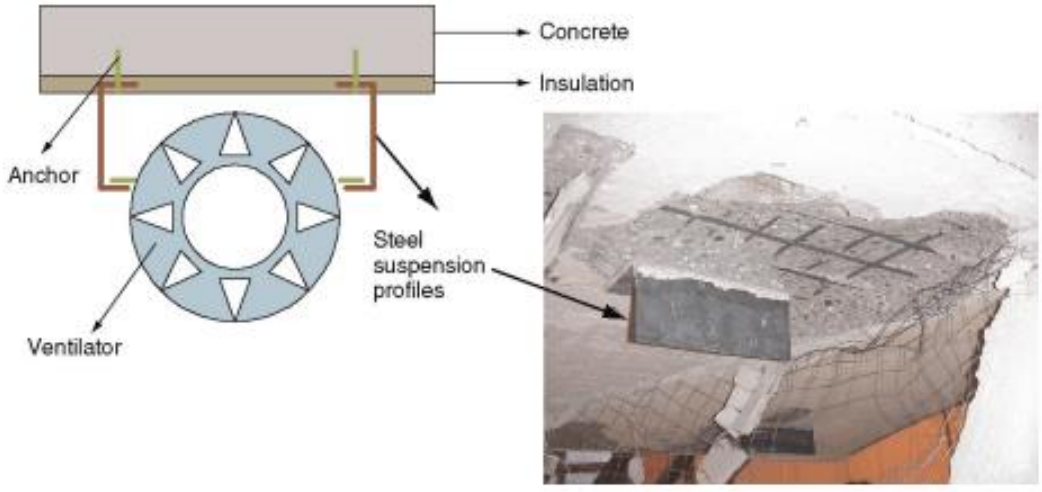


Fig 4-3 Example of spalling due to poorly designed equipment fixings

#### 4.3.1.2 Tunnel cladding and paneling systems

Many tunnel systems, particularly road tunnels, have a secondary lining composed of panels. These were originally employed for mainly cosmetic purposes, but recently these cladding systems have been developed to provide structural fire protection as well.

Tunnel claddings may consist of monolithic panels of materials such as calcium silicates, vermiculite cement, fiber cement or mineral wool, or may composite panels with rigid outer surfaces and an insulating core of a material such as mineral or glass wool. These products are said to be easy to install, and have the advantage of being prefabricated rather than having to be

constructed on site. However, the disadvantage of these systems is their installation can be time consuming and more expensive compared with some coating systems.

#### 4.3.1.3 Concrete additives

Another method of protecting the structural concrete of a tunnel is to make the concrete itself more fire resisting. The spalling failure mechanism is occur due to a buildup of vapor pressure within the concrete. If a concrete mix is used that contains materials which can release the pressure more effectively, the concrete will be able to withstand fire conditions for longer time before failure. Recent researches have focused on two different (combinations of) additives in the mix: polypropylene fibers and steel fibers

The main problem for reinforced concrete due to fire is the spalling of concrete cover which protects steel. Spalling happens due to generating vapor pressure inside concrete due to rise of temperature. The solution for this problem is adding some additives polypropylene and steel fibers which help to delay spalling so the concrete can resist a longer time. The main scientific idea of polypropylene fibers is to give more space for water pressure during fire so it will not spalling. Regarding the fibers, the main idea is to increase the ductility of concrete then it will resist internal pressure.

Fig 4-5 shows the results of a simulation using a finite-element model, the micro-crack development in heated concrete. The model includes aggregates and cement paste, as well as the interface zone between aggregates and paste

Fig 4-5 Computer simulation of micro-cracks between aggregates

#### 4.3.1.4 Other passive fire protection systems

In addition to the three main methods of passive fire protection described above, a number of other methods of fire protection have been demonstrated. Which include: A method of

prefabricating structural tunnel-lining elements with composite layers of fire protection built. Fiber-reinforced composites(to protect cabling, etc., rather than structural members). The use of organic coatings, including: intumescent products, which foam up on heating to form a thick layer; ablative products, which use large quantities of heat as they erode under a high temperature conditions; and subliming products, which also absorb heat when vaporize.

### 4.3.2 Active fire protection

Active measures of fire protection include: measures that operate in the event of a fire; and measures that exist all the time, and are aimed at protection should a fire occur in the tunnel. Measures in the first of these categories require some form of communication or activation to occur, by informing people or equipment of the presence of the fire, thus enabling action to be taken to contain the spread of the fire or to initiate escape. Some methods exist for fire detection, and it has been recommended that the fire-detection system incorporate redundancy by consisting of several different systems using different technologies. As a general rule, very rapid action is required to extinguish or substantially control a tunnel fire, especially fires that involve HGVs. So very rapid detection is needed, and detection systems are required that can do this reliably in an operational setting. Rapid action by operational staff is also a necessary part of the system.

Many active measures of containment are concerned with the control of smoke spread rather than the control of the spread of the fire. Measures of fire or smoke control generally depend on detection of the fire triggering some kind of countermeasure, which may be manual or automatic. Fire brigade action is also a effectively part of active fire protection. In recent years, much consideration has been given to fixed fire-suppression systems, and the World Road Association now recognizes that such systems may be efficient, even if it does not actually recommend these systems in all new tunnels.

## 4.4 Fire detection systems

*[Main reference: Handbook of Tunnel Fire Safety,2nd edition. Alan Beard. Paul Scott. Chapter 5]*

The development of fires mostly depends on the goods which are burned, although ventilation has a major effect. Common commuter cars (typical heat-release rate (HRR) in tunnels 3–5 MW) are the cause most tunnel fires. However, when heavy goods vehicles (HGVs) are involved the HRR may be considerably greater: 20–30 MW or possibly much more; about 200 MW has been found experimentally. Tanker fires may be even larger. In fact, very large amount

of smoke, often very toxic, is released, and fill the entire tunnel. Smoke and gases from burnt vehicles in tunnels are very poisonous for tunnel users, and most casualties in recent major tunnel fires have resulted from inhaled smoke.

The first signs of a fire are smoke or heat. Not all car or HGV fires start with a flaming fire (which occurs after an accident where liquid fuel spills out). Fires start usually with a smoldering phase, and tunnel users are able to extinguish the smoldering fire without further consequences (Fig 4-6).

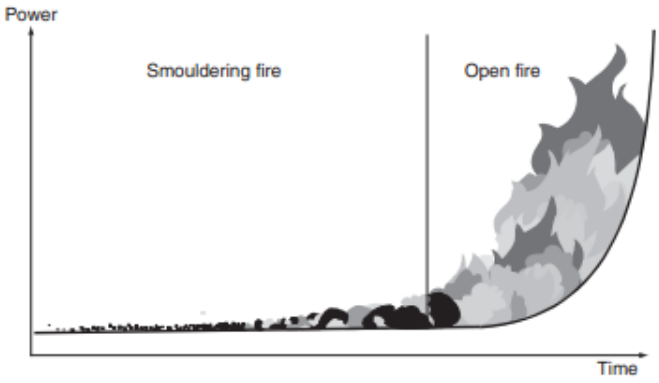


Fig 4-6 The usual fire development

The phenomena of smoke, heat and flame radiation in a fire are suitable for early detection of fire. The different detector types suited to each specific fire phenomenon under normal ambient conditions are described (Fig 4-7).

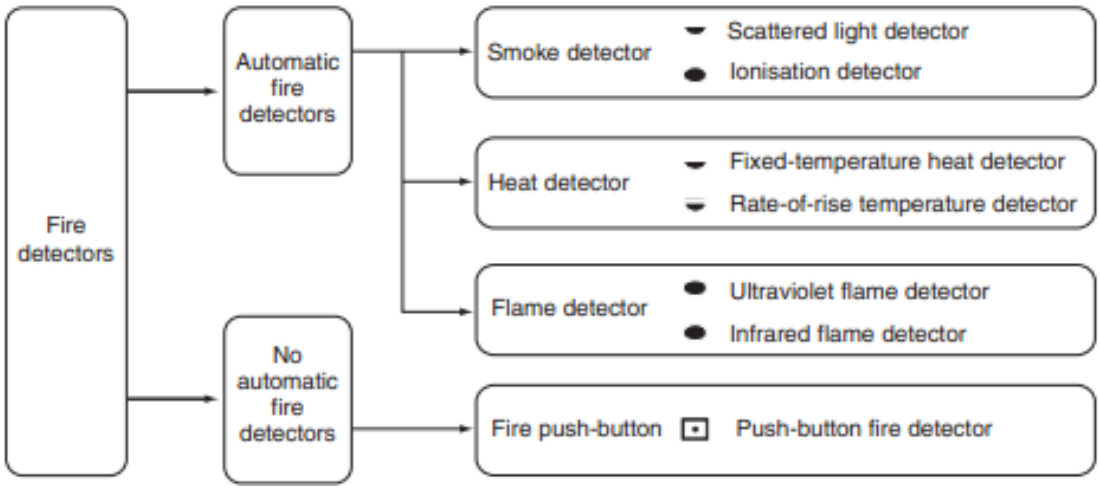


Fig 4-7 Fire detector types

### 4.4.1 Smoke detectors

*[Main reference: Handbook of Tunnel Fire Safety,2nd edition. Alan Beard. Paul Scott. Chapter 5]*

As a consequence of the disastrous fires mentioned above, some countries, such as Germany

and Switzerland, visibility monitors or special tunnel smoke detectors installed at intervals of 100–300 m are used for early fire detection in road tunnels. Basically, these systems use light emitters and light receivers to measure scattered light (Fig 4-8) or light absorption. The well-known devices are optical smoke detectors, which based on the reflection principle. In recent years, a new generation of tunnel smoke detectors has been developed, which based on visibility monitors.

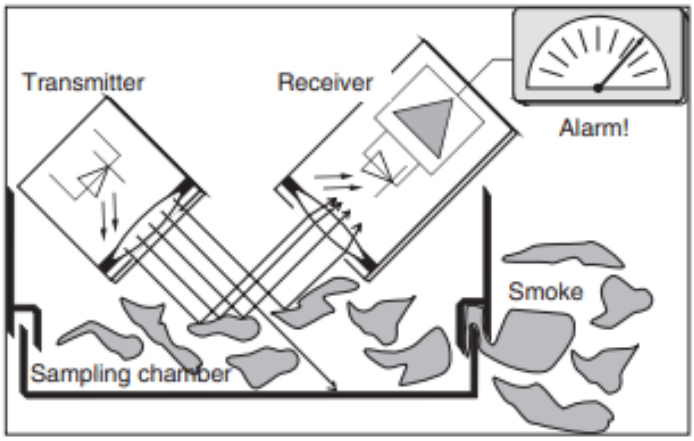


Fig 4-8 The principle of operation of smoke detectors

Another well-known system is the light barrier, or beam detector, based on the measurement of light absorption. A light emitter sends, over a distance of several meters, the light beam, which is received by a light-sensitive device. Depending on the loss of light intensity due to absorption by the smoke within the measurement length, the system activates an alarm (Fig 4-9).

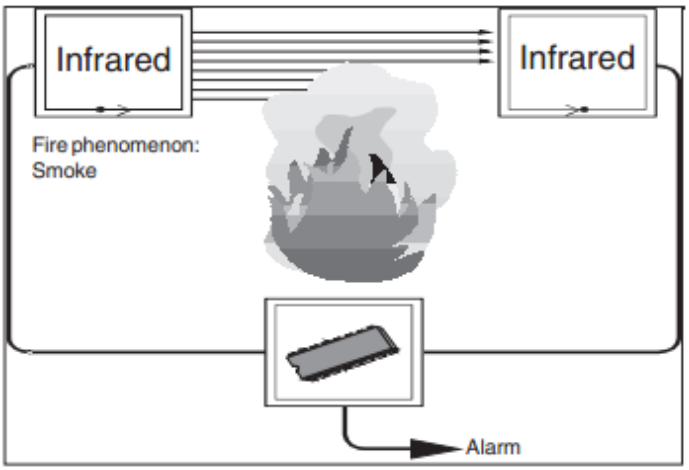


Fig 4-9 The principle of operation of beam detectors

Smoke can also be detected using video-image-processing software. These systems generally detect smoke and fire with a high reliability, but they still show too much cross-sensitivity with other phenomena, leading to inefficiently.

### 4.4.2 Flame detectors

*[Main reference: Handbook of Tunnel Fire Safety,2nd edition. Alan Beard. Paul Scott. Chapter 5]*

Flame is a radiation-emitting fire phenomenon. Different wavelengths of electromagnetic radiation, ranging from infrared to ultraviolet, can be detected by flame detectors. Flame detectors are light-sensitive sensors (calibrated for a certain wavelength) activated when the specific radiation is received (Fig 4-10). The flame detectors are installed at intervals of approximately 25 m.

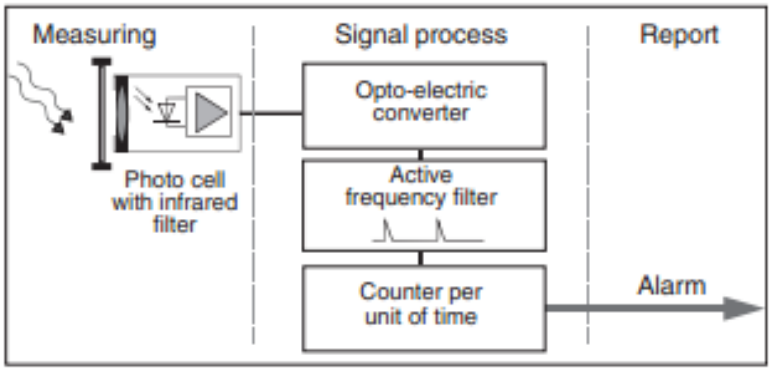


Fig 4-10 The principle of operation of flame detectors

In addition, flames can also be detected by video-image-processing systems; but again these systems suffer from a certain false alarm rate due to interference with other phenomena.

### 4.4.3 Heat detectors

*[Main reference: Handbook of Tunnel Fire Safety,2nd edition. Alan Beard. Paul Scott. Chapter 5]*

Reliable fire detection can be achieved by measuring the ambient temperature. When a preset maximum temperature is detected, the system activates an alarm. European Standards (EN 54-5) require evaluation of the rate of temperature rise in order to activate an alarm, even before the maximum temperature is reached (Fig 4-12).

There have two types of heat-detection systems: point detectors and line-type detectors.

Point heat detectors incorporate a heat sensor (heat-sensitive resistance) connected to an evaluation unit. Line-type heat detectors don't have longitudinal interruption between sensors, and measure, and in some cases even mathematically integrate the temperature increase. They thus provide higher accuracy of detection.

## 4.5 Ventilation in tunnels

Exposure to the products of combustion generated by vehicles travelling through a tunnel can cause discomfort and illness to vehicle occupants. Ventilation is a good solution, by providing a means to dilute the contaminants and to provide a respirable environment for the vehicle occupants. Visibility within the tunnel will be aided by the dilution effect of the ventilation air.

### 4.5.1 Natural ventilation

*[Main reference: Handbook of Tunnel Fire Safety,2nd edition. Art Bendelius Chapter 9]*

Tunnels that are naturally ventilated rely primarily on meteorological conditions and the piston effect of moving vehicles to maintain satisfactory environmental conditions in the tunnel. The chief meteorological conditions affecting tunnels is the pressure differential between the two tunnel portals created by differences in elevation, ambient temperatures or wind. But none of these factors can be relied upon for continued consistent results. The natural effects defined above are usually, in the majority of cases, not sufficiently reliable to be considered when addressing emergency ventilation during a fire except in short tunnels or in tunnels with unique potential smoke storage configurations.

Natural ventilated tunnels can be configured with airflow from portal to portal, from portal to shaft or from shaft to shaft (Fig 4-11).

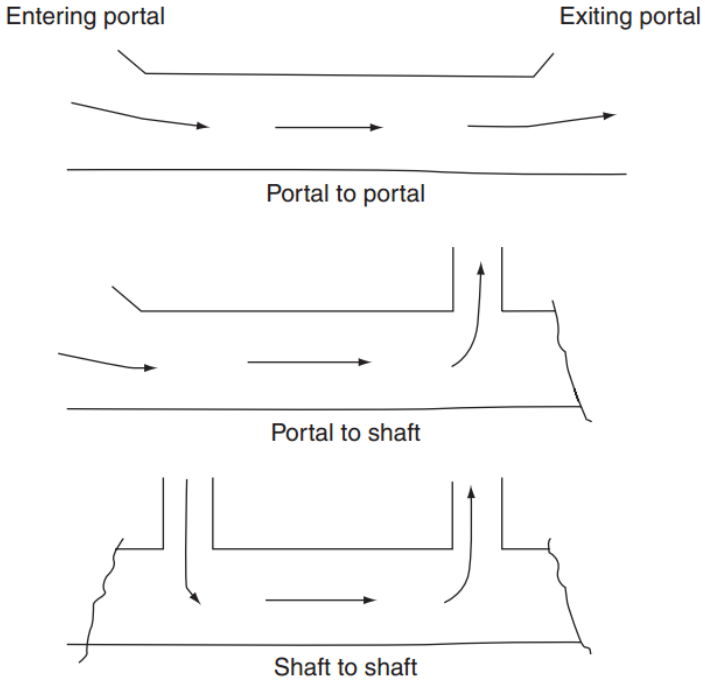


Fig 4-11 Natural ventilation configuration

### 4.5.2 Mechanical ventilation

Mechanical ventilation is required if the natural ventilation does not remove the heat adequately. However, the primary thrust of current tunnel ventilation design is tied to the requirement for ventilation during fire-based emergencies.

#### 4.5.2.1 Longitudinal ventilation systems

*[Main reference: Handbook of Tunnel Fire Safety,2nd edition. Art Bendelius Chapter 9]*

A longitudinal ventilation system is defined as any system where the air is introduced to or removed from the tunnel at a limited number of points, thus creating a longitudinal airflow within the tunnel.

The injection-type longitudinal system (Fig 4-12) used extensively in railway tunnels. Air is injected into the tunnel through a nozzle at one end of the tunnel, and then it mixes with the air brought in by the piston effect of the incoming traffic and induces additional longitudinal airflow. The air velocity within the tunnel is uniform throughout the tunnel length; the level of pollutants and/or temperature increase from ambient in the entering portal to a maximum at the exiting portal. Adverse external atmospheric conditions can reduce the effectiveness of this system. Pollutants and temperature levels increase as the airflow decreases or the tunnel length increases.

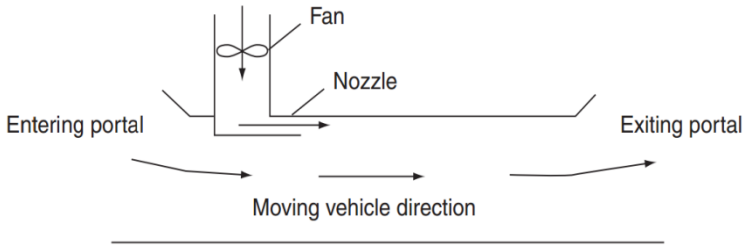


Fig 4-12 Nozzle longitudinal ventilation system

Jet fan longitudinal ventilation is based on the installation of a series of axial flow fans in series, within the tunnel, usually mounted at the tunnel ceiling or roof (Fig 4-13). The fans have a high discharge thrust and velocity, which in turn induce additional longitudinal airflow in the tunnel.

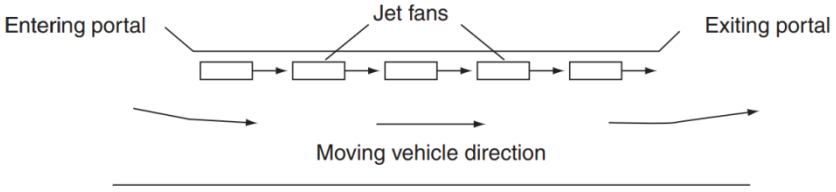


Fig 4-13 Jet fan longitudinal ventilation system

### 4.5.2.2 Transverse ventilation systems

*[Main reference: Handbook of Tunnel Fire Safety,2nd edition. Art Bendelius Chapter 9]*

Transverse ventilation system is defined by the uniform distribution of fresh air along the length of the tunnel. There are three systems in use: fully transverse, supply air semi-transverse and exhaust semi-transverse, as described below.

**Fully transverse ventilation systems** (Fig 4-14): Incorporates a full-length supply duct and a full-length exhaust duct, achieves a uniform distribution of supply and collection of air.

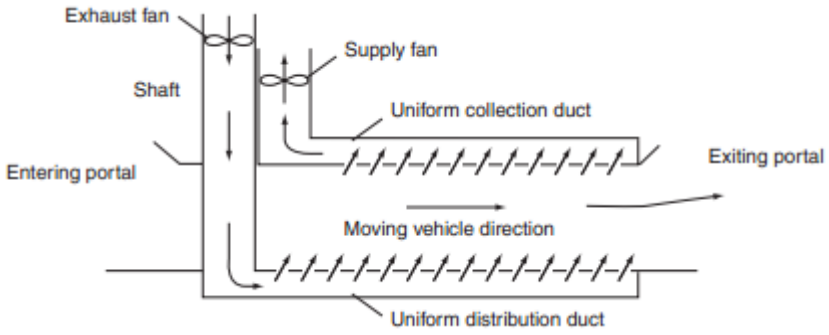


Fig 4-14 fully transverse ventilation system

**Supply air semi-transverse system** (Fig 4-15): Produce a uniform level of pollutants and temperature throughout the tunnel under the fact that the air and the vehicle-generated pollutants and heat enter the roadway area at the same relative rate.

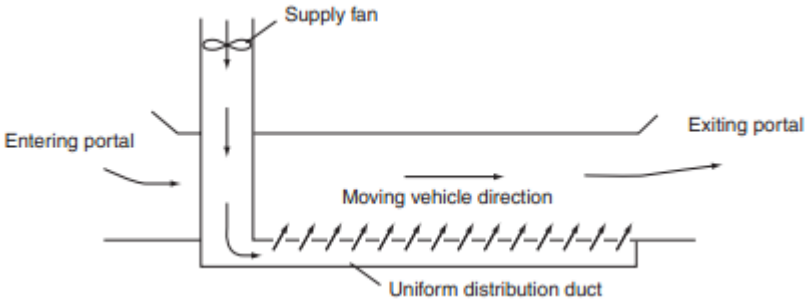


Fig 4-15 Supply semi-transverse ventilation system

**Exhaust semi-transverse system** (Fig 4-16): Produce a maximum level of pollutants and temperature at the exiting portal in the tunnel with unidirectional traffic.

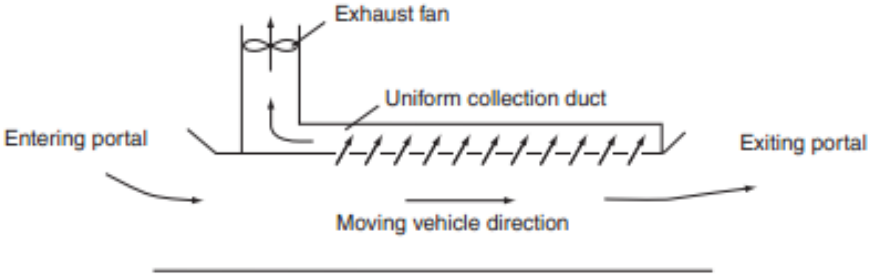


Fig 4-16 Exhaust semi-transverse ventilation system

# 5. Fire tests in tunnels

## 5.1 Introduction

Until the 1960s, research in tunnel fires had been largely concerned with fire safety in mine tunnels, and so the main fire loads that had been considered were coal, wooden structures and conveyor belts. The consequences of vehicle fires had never really been considered. In the early 1960s, a lot of transport tunnels were constructed, so in order to better understand what might happen if there were a fire, experimental testing of fires in vehicle tunnels began.

Fire tests have been carried out for a number of different reasons over the years, two main reasons are:

1. Gain an understanding of the fire dynamics and related phenomena in tunnels.
2. Test or commission tunnel installations, including ventilation systems, sprinkler systems and tunnel linings.

This chapter focuses primarily on the former type of tunnel-fire experiment. The conclusions and findings given in the following accounts are those of the people who conducted the tests.

## 5.2 Experimental testing on real tunnels

### 5.2.1 The Runehamar Tunnel fire test series, 2003

*[Main reference: Handbook of Tunnel Fire Safety,2nd edition. Richard Carvel. Guy Marlair Chapter 12]*

A series of four fire tests was carried out in a disused two-lane road tunnel in Norway in September 2003. The tunnel is 1.6 km long and has a rough rock cross-sectional area of 47–50 $m^2$. At the location of the fire experiments (approximately 1 km into the tunnel), a 75 m length of the tunnel was lined with fire-protective panels, and reduced the cross-sectional area of the tunnel to 32 $m^2$ in the vicinity of the fire (Fig 5-1). The objectives of the test were to investigate: (a) fire development in HGV cargo loads, (b) the influence of longitudinal ventilation on fire heat release rate and growth rate, (c) the production of toxic gases, (d) fire spread between vehicles, (e) fire-fighting possibilities, and (f) temperature development at the tunnel ceiling.


Fig 5-1 Fire experiment in the Runehamar Tunnel, Norway

Each of the tests comprised a fire load of equivalent size and shape to a standard HGV trailer (10.45 m long, 2.9 m wide and 4.5 m high).

For test 1, the fire load consisted of 10.9 tons of wooden pallets and plastic materials, and a 'target' object positioned 15 m downstream of the fire.

For test 2, the fire load consisted of 6.8 tons of wooden pallets, mattresses and plastic materials.

For test 3, the fire load consisted of 7.7 tons of furniture on wooden pallets, and ten tyres (800 kg) were positioned around the frame at the locations where they would be on a real HGV trailer.

For test 4, the fire load consisted of 3.1 tons of plastic cups in cardboard boxes on wooden pallets.

The conclusions from the test series including:

1. Ordinary' HGV cargoes could give rise to heat release rates comparable to fuel tanker fire scenarios.
2. Temperatures above 1300° C could be achieved in HGV tunnel fires.
3. When the fires reached full involvement, the ventilation flow reduced and back-layering occurred.
4. A 'pulsing' phenomenon was observed in tests 1 and 2.
5. The 'RWS fire curve' is the best standard fire curve to represent a HGV fire in a tunnel.

### 5.2.2 La Ribera del Folgoso Tunnel fire test series, 2009

*[Main reference: Handbook of Tunnel Fire Safety,2nd edition. Richard Carvel. Guy Marlair Chapter 12]*

A series of five fire tests was carried out in a 300 m long tunnel in Spain with a 50 $m^2$ cross-sectional area. The fuel source in each case was a 1 m × 2 m rectangular pool, with a peak HRR of approximately 5 MW. The test conditions were ostensibly identical, the idea being to investigate the variability of data within a single experimental configuration and to provide a robust set of experimental data for comparison with numerical models.

The tests show that approximately 10% variation in heat release rate and temperatures in the vicinity of the fire for experimental pool fire tests (Fig 5-2).

Fig 5-2 Pool fire test in La Ribera del Folgoso Tunnel

### 5.2.3 Project safety test: tests in the second Benelux Tunnel, The Netherlands, 2001

*[Main reference: Handbook of Tunnel Fire Safety,2nd edition. Richard Carvel. Guy Marlair Chapter 12]*

The high-profile accidental fires in several Alpine road tunnels in 1999 to 2001, a series of 26 fire tests was commissioned to investigate (a) the spread of heat and smoke from fire, (b) the influence of ventilation on fire size, (c) the influence of sprinklers, and (d) the capabilities of fire detectors during tunnel-fire incidents. These tests were carried out in the second Benelux Tunnel, Rotterdam, The Netherlands, before the tunnel was made operational. The test series included fires involving six fuel pools, three cars, one van, six stacked loads (to represent HGV fires; Fig 5-3) and ten small fuel basins (to test the fire detectors). These tests included with natural ventilation and forced longitudinal ventilation.

Fig 5-3 Fire experiment with wooden pallets and an aluminum covering carried out in the second Benelux Tunnel, The Netherlands.

The main conclusions from the test series including:

1. Under high levels of heat radiation, conditions were lethal within 6 m of a fully developed passenger-vehicle fire. For a small HGV fire this distance increased to 12 m. No threat to life from carbon monoxide at such locations due to convection and stratification of the fumes.
2. Both with and without longitudinal ventilation there was poor visibility due to smoke at 100–200 m from the fire location. Toxicity limits were not exceeded at these locations.
3. High ventilation rates retarded the development of a fire involving a passenger car by up to 30 minutes, the fire starting at the front of the vehicle and the ventilation blowing from the rear. High ventilation rates tended to enhance the burning of the 'HGV' fires by up to 20 MW, but temperatures in the locality of the vehicles were reduced due to the ventilation.
4. Sprinklers substantially reduced the air temperature and the temperature of vehicles in the vicinity of the fires. For the vehicles tested, lethal temperatures were not observed and fire spread was controlled. The formation of steam was not observed.
5. Linear fire detectors, in general, activated an alarm more than 5 minutes after the start of the fire. For rapidly growing fires at this time was reduced to 3 minutes. Under natural ventilation conditions, a fire would generally be detected by a sensor less than 5 m away; with forced ventilation the activated detector may even be as much as 20 m.
6. Escape-route signage became invisible very quickly in smoke. It was recommended that the signs be situated at low level.

## 5.3 Experimental testing on a smaller scale

*[Main reference: Handbook of Tunnel Fire Safety,2nd edition. Richard Carvel. Guy Marlair Chapter 12]*

Fire tests including full-size fires in full-size tunnels are very expensive. The high cost seriously limits the number of full-size experimental tests that are conducted. Many fundamental questions about the behavior of fire and smoke in tunnels have not been answered by full-scale tests. In order to be able to combat these questions at a lower price, and sometimes to model a specific tunnel design, reduced scale experiments have been carried out.

In order to let small-scale experiments to be useful, there must be a well-defined similarity between the scale model and the full-scale case of interest. If there is a strong similarity then a scale model can be used to investigate specific aspects of the behavior for fire or smoke. If the similarity is not so strong, then the behavior of the fire can only provide information in general terms. To scale between a real situation and a scale model with a strong similarity, it is necessary to consider the gas flow around the fire.

Gas flow can be classified using certain non-dimensional numbers. The Froude number may be used to classify fire type:

$$Fr = U^2 / gL \tag{5-1}$$

Where U is the velocity of the gases, g is the acceleration due to gravity, and L is a characteristic dimension of the system.

Other non-dimensional numbers are also used to classify flow behavior, including: the Reynolds number:

$$\mathrm{Re} = UL / v \tag{5-2}$$

Where v is the viscosity; the Richardson number:

$$\mathrm{R}i = gL\Delta\rho / U^2\rho \tag{5-3}$$

Where $\rho$ is the density of the plume gases, and $\Delta\rho$ is the difference between this and the density of the surrounding air; and the Grashof number:

$$Gr = gL^3\Delta\rho / v^2\rho \tag{5-4}$$

Each of these numbers should be the same in the scale model as in the real situation. Models are usually scaled assuming conservation of the Froude number only.

### 5.3.1 Tunnel fire experiments for the EGSI STES project, IN ERIS, France, 2006– 2009

*[Main reference: Handbook of Tunnel Fire Safety,2nd edition. Richard Carvel. Guy Marlair Chapter 12]*

The INERIS fire galley was again modified to reproduce a realistic tunnel section in one-third scale. A roof was installed to obtain a modified section of 5.4 $m^2$ with smoke duct positioned above. The resulting section was 3 m wide and 1.8 m high, and experiments carried out with both longitudinal and semi-transverse ventilation systems. A large series of experiments was carried out to investigate smoke behavior in both of back-layering and in the downstream smoke layer, and also the smoke behavior in the presence of perturbations.

The fires tested were different sized heptane pool fires, with a fuel-control system to obtain constant burning. The fire properties then studied, with a particular focus on the radiated heat fraction, and two fire positions were used to study the upstream and downstream smoke layers. The stability of the two layers was studied with regard to the influence of jet fans located upstream and the influence of vehicles located upstream or downstream of the fire. In both cases, different ventilation schemes were used to study various configurations corresponding to the French ventilation practice.

The main conclusions of this project listed below.

1. Upstream jet fans affect only the fastest part of the back-layering. The flow close to the fire layer is not significantly affected, the temperature in the plume is independent of the velocity gradient upstream.
2. Vehicle blockages upstream of the fire influence back-layering, primarily due to the velocities around them increased, due to blockage effects.
3. At low ventilation velocities, vehicle blockages downstream of the fire don't reduce the smoke stratification.

### 5.3.2 Pool fire tests at the Londonderry Occupational Safety Cent re, Australia, 1990

*[Main reference: Handbook of Tunnel Fire Safety,2nd edition. Richard Carvel. Guy Marlair Chapter 12]*

A series of five kerosene pool fire tests was carried out in a 130 m long, 5.4 m wide, 2.4 m high ‘mine roadway’ tunnel near Londonderry, NSW, Australia. The longitudinal ventilation in the tunnel was maintained by two exhaust fans at one end, with a rectangular grid for ‘flow straightening’ nears the other end. Three tests were carried out using a 1 m diameter pool and

ventilation velocities ranging from minimal (0~0.5 m/s) to 2 m/s. Tests were also carried out using 0.57 and 2 m diameter pools. An extensive array of thermocouples and airflow probes was arranged around, and mass loss was measured by load cells under the pool tray. 2 video cameras were also used to record the experiments. The experiments were carried out to test a numerical model. Some of the observations from the study include the following:

1. Increasing the ventilation from 0.5 to 2.0 m/s caused a 25% decrease in the HRR of the 1 m diameter fire.
2. The observed decrease in the heat release rate is due to the fact that less of the plume is above the fuel surface at higher air velocities.
3. The rate of mass loss rate in larger fires is proportionately higher than that in smaller fires (subject to ventilation velocities of about 0.9 m/s).
4. significant back-layering at 0.85 m/s, but this is 'arrested' by 2 m /s airflow.

### 5.3.3 Test series carried out by FOA, the Swedish Defense Agency, 1997

*[Main reference: Handbook of Tunnel Fire Safety,2nd edition. Richard Carvel. Guy Marlair Chapter 12]*

A series of 24 fire tests was carried out in a 100 m long 'blasted rock tunnel', approximately 3 m wide and 3 m high. The tunnel was open to the air at one end and had a large chimney at the other. No mechanical ventilation system installed in the tunnel, but different ventilation rates were achieved by restricting the inflow of air in some tests and using two different fire locations within the tunnel. The experiments included fire tests of heptane pools (12 tests), methanol pools (2 tests), kerosene pools (occasionally incorrectly referred to in the report as 'diesel' pools) (2 tests), polystyrene cups in cardboard boxes (2 tests), wooden cribs (3 tests), and heptane pools contained within a dummy vehicle (2 tests) and a car. Although the tests were primarily carried out to provide experimental data for testing of CFD codes, which conclusions are:

1. All fire tests showed some correlation between the degree of ventilation and the heat release rate of fire. This effect was more apparent for solid fire loads than for liquid pools.
2. Measurements of optical density and gas concentrations indicated there was a correlation between these two parameters. However, a parameter for the fuel type must be included.
3. In a confined space the heat release rate of a small car reached 4 MW for a short time.

### 5.3.4 Model scale tunnel fire tests with longitudinal ventilation

*[Main reference: Ingason, H. and ZhenLi, Y., "Model Scale Tunnel Fire Tests with Longitudinal ventilation",]*

#### 5.3.4.1 Introduction

Test results from a series of tests in a model tunnel (1:23) are presented. Tests were carried out with longitudinal ventilation under different fire conditions. Wood cribs used to simulate the fire source, which was designed to correspond to a scaled-down HGV (Heavy Goods Vehicle) fire load. The parameters tested: the number of wood cribs, type of wood cribs, the longitudinal ventilation rate and the ceiling height. The HRR, fire growth rate, maximum gas temperature beneath the ceiling, temperature distribution, and total heat flux at floor level, flame length, and back-layering length were investigated. Correlations for these parameters were investigated and proposed for longitudinal flow.

#### 5.3.4.2 Experimental procedure

Ingason carried out a total of 12 tests in a 1:23 scale model tunnel, as shown in Fig 5-4.

Fig 5-4 A photo of the 1:23 model-scale tunnel

The tunnel itself is 10 m long, 0.4 m wide and with two heights: 0.2 and 0.3 m, respectively, as shown in Fig 5-5. The lower height (0.2 m) was created by using a false ceiling with the same material. The model was constructed using non-combustible boards with a thickness of 15 mm. The manufacture of the boards provide the following technical data: the density of the boards is 870 kg/m$^3$, the heat capacity is 1130 J/kg K and the heat conduction is 0.175 W/m K. The floor, ceiling and one of the vertical walls, the front side of the tunnel was covered with a fire resistant window glaze. The 5 mm thick window glaze (0.6 m wide and 0.35 m high) mounted in steel frames which measured 0.67 m by 0.42 m.

Fig 5-5 Schematic diagram of the model scale test-rig in Tests 1–9 (dimensions in mm).

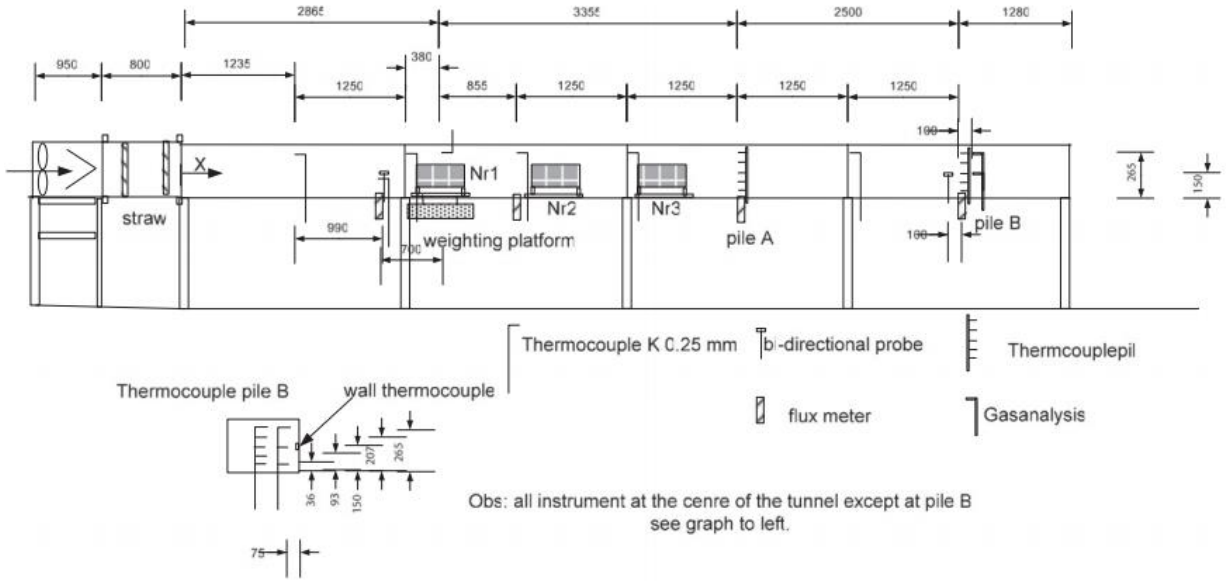


Longitudinal flow was supplied using an electrical axial fan attached to the entrance of the model tunnel, as shown in Fig 5-4. The fan itself was 0.95 m long with an inner diameter of 0.35 m and a 0.8 HP motor yielding a maximum capacity of 2000 m$^3$/h (at 1400 rpm and 7.5 mm$H_2O$). The rotation speed, and thereby the capacity, could be controlled using an electrical device coupled to the motor. A 0.8 m long rectangular plywood box with the dimension 0.4 wide and 0.3 m high, mounted between the fan and the tunnel entrance to create a uniform flow at the entrance of the tunnel. The swirls were dampened by filling the plywood box with straw fibers. Longitudinal ventilation velocities of 0.34–0.85 m/s were used in the test series. The corresponding large scale velocities are 1.6–4.1 m/s. To measure the tunnel ventilation velocity, two bi-directional probes were used. Detailed descriptions of wood crib A and wood crib B are given in Fig 5-6. A cube of fiberboard measuring 0.03, 0.03 and 0.024 m which was soaked in heptane (9 mL) was placed at the upstream edge of the wood crib as shown in Fig 5-7.

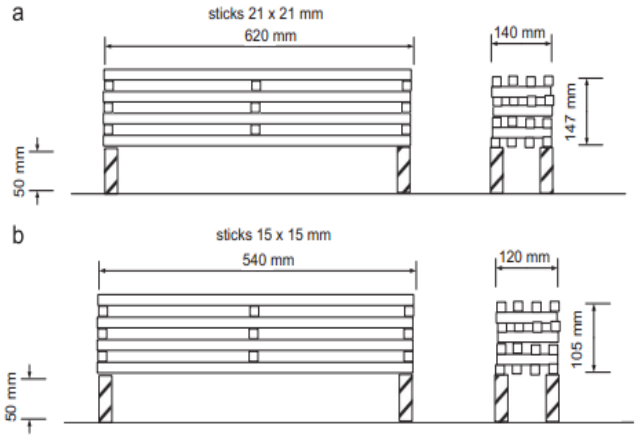


Fig 5-6 Detailed drawing of the wood cribs (a) Wood crib A. (b) Wood crib B.

Fig 5-7 A photo from test 5 showing a fully developed fire of wood crib A

### 5.3.4.3 Test result

A fundamental aim of this study was to investigate the influence of ventilation on the maximum heat release rate and the fire growth rate for solid fuels (wood cribs in this case). One important aspect is to study fuels that are comparable from a porosity point of view. The fuel mass loss rate per unit fuel surface area is a very weak function of the ventilation velocity. The fuel mass loss rate per unit fuel surface area in a tunnel fire test is in a range of 1.4–1.55 times the value measured in free burning test. At 10 m/s the fire will probably be 10 times larger. The ventilation rates used in this study, converted to large scale, are in the range of 2–5 m/s. Fuel that nder-ventilated during ambient conditions has been used in the comparison. The maximum heat release rate per unit fuel surface area has the same trend as the fuel mass loss rate per unit fuel surface area.

The fire growth rate is highly sensitive to the longitudinal ventilation velocity. The increase at a velocity corresponding to 2.9 m/s (0.60 m/s) in large scale is in the order of 2 times the fire growth rate in ambient conditions and for 4.3 m/s (0.9 m/s) it is of the order of 3. Increasing longitudinal ventilation rate increases the fire growth rate. And the fire growth rate is one of the most important design parameters for tunnel safety these results are considered important.

The maximum excess temperature lays mainly in a range of 900–1100 ° C. The flame length increases linearly with the heat release rate, and is insensitive to the ventilation velocity.

## 5.4 Concluding comments

*[Main reference: Handbook of Tunnel Fire Safety,2nd edition. Richard Carvel. Guy Marlair Chapter 12]*

Experimental fire test in tunnels has greatly increased our understanding of tunnel-fire phenomena and led to the development of better sustainable tunnel-fire prevention, protection and mitigation technologies. If the lessons of the earlier tunnel-fire experiments had not been learned, catastrophes like the fires in the Mont Blanc Tunnel and the St. Gotthard Tunnel may be far more frequent than they have been. It is only through experimental testing and learning from experience that incidents on this scale will be prevented in the future.

Fire tests in operational tunnels, like those described in this chapter, will undoubtedly become more common in the future. Indeed, there have a regulation in France which states that tunnel operators must organize full-scale exercises to test emergency procedures at least once a year. These exercises include fire scenarios, and it has induced a significant increase in the number of fire tests in French tunnels since the last decade. It is expected that other countries will implement similar requirements in the future.

Large-scale fire tests will always be expensive and involve highly qualified specialists, but they remain of importance to provide essential information for understanding fire behavior, investigating fire suppression and protection possibilities (ventilation design, water-based suppression systems, etc.), training fire-fighters and tunnel operation personnel, and also to provide data for testing computer models.

Finally, the booming interest in the use of alternative energy sources in the transport sector might trigger the need for testing new vehicle types and fuel sources. Design fire scenarios, will need to be considered. Indeed, fire development in ‘plug-in’ electric vehicles and fully electric vehicles, as well as the behavior of a fire on a Heavy Good Vehicle carrying a cargo of rechargeable lithium-based batteries in tunnel configurations, need to be assessed, due to the special thermal and chemical risk profiles of the new electric storage systems. It should be noted that lithium batteries are classified as dangerous goods according to international TDG regulations. A facility at INERIS in France is currently being developed to test the systems.

# 6. Small scale experiment

## 6.1 Introduction

*[Reference: Fire safety in concrete tunnels-First results on small scale tests. Mahmoud Mohamed Kamal Ahmed, chapter 4]*

In this chapter some former results from small scale experiments are summarized, in order to form the basis for comparisons with the numerical model that is the object of this thesis. The tests were performed by Mahmoud Mohamed Kamal Ahmed, in the framework of his thesis work at Politecnico di Milano.

Generally speaking, with regard to reduced scale fire tests, it is not possible to rigorously apply a scientific scaling procedure in order to carry out them, for there are too many non-dimensional quantities that should be preserved, e.g. Reynolds Number, Froude Number, fire size, and so on. In fact, when considering combustion phenomena there are about thirty likely dimensionless groups, and scaling keeping all of these groups constant is obviously impossible. More limited scaling procedure may be carried out if the governing groups can be identified. Froude scaling criteria may not apply to fires in tunnels smaller than about 1 m in diameter, and small-scale pool fires may behave substantially differently from the full-scale counterparts. For example, a pool of a hydrocarbon fuel will exhibit 'transitional' flame behavior if its diameter is less than about 1 m, and larger pools will exhibit fully turbulent flame behavior.

Fire tests in tunnels are important in order to understand the effect of fire on tunnel elements like lining segments, temperature distribution and behavior of smoke. Test scaling is a promising tool to assist the development of new approaches for fighting fires in tunnels and perform parametric studies by varying the input quantities. The survey of experiments were already implemented before is also of a high importance in order to be able to understand the advantages and disadvantages of different approaches, evaluate each procedure to running the experiments, which materials are better to use and to have the ability to judge the results of test. As long as the limitations of these small-scale experiments are borne, laboratory scale experiments can yield useful results and help improve the understanding of the features of

tunnel-fire dynamics.

## 6.2 Scaling theory

The method of scaling being used in the tests is the most widely used Froude scaling. Clearly, it is impossible and not necessary to preserve all the terms obtained by scaling theory simultaneously in model scale tests. The terms that are most important and most related to the study can be preserved. The thermal inertia of the involved material, turbulence intensity and radiation are not explicitly scaled, but we scale the HRR, time, flow rates, energy content and mass (Fig 6-1). The heat of combustion is assumed to be the same in both scales.

| Type of unit | Scaling | equation number |
|---|---|---|
| Heat Release Rate (HRR) (kW) | $Q_M/Q_F = (L_M/L_F)^{5/2}$ | (1) |
| Velocity (m/s) | $V_M/V_F = (L_M/L_F)^{1/2}$ | (2) |
| Time (s) | $t_M/t_F = (L_M/L_F)^{1/2}$ | (3) |
| Energy (kJ) | $E_M/E_F = (L_M/L_F)^3$ | (4) |
| Mass (kg) | $m_M/m_F = (L_F/L_M)^3$ | (5) |
| Temperature (K) | $T_F/T_M = 1$ | (6) |

Fig 6-1 A list of scaling correlations for the model tunnel

Where L is the length scale and index M is related to the model scale and index F to large scale.

*[Ingason, H. and ZhenLi, Y., "Model Scale Tunnel Fire Tests with Longitudinal ventilation",]*

## 6.3 Experiment description and running

The small scale tunnel test is carried out mainly to check the parameters of relationship between HRR data and distribution of the temperature. Then the results will be checked and compared with the results of numerical analysis using a multi-zone concept with MATLAB script, and the numerical analysis process will be shown in the following chapter. Finally, all main results followed by a comparison between experimental and numerical model concluding with the achieved results and the research recommendations, will discussed in the chapter 8.

### 6.3.1 Concrete tube description

The test will be applied on a long reinforced concrete tube with a density of 2400 kg/m$^3$, the thickness of the tube is 7.5 cm and inner diameter of 1 m of the radial section. The concrete tube consists of 12 segments with a length of 1 m for each segment as shown in the following (Fig 6-2). This concrete tube will behave as a scaled tunnel during the test.


Fig 6-2 Schematic sketch of tube segment arrangement during the test

### 6.3.2 Experiment apparatus

#### 6.3.2.1 Combustion material

There are many kinds of fuel that can be used to perform fires tests. Among them, Diesel chosen because it is a very common material and all of its parameters are known, so achieving precise results will be easily and comparing it with numerical model results will be more sufficient here are the properties of the material which consideration in the experiment and numerical stage. Mass burning rate: 0.045 kg/m$^2$/sec; Effective heat of combustion: 44400 kJ/kg; Fuel density: 918 kg/m$^3$. Then the pans used to containing fuel during the test have different diameters and depth (Fig 6-3)

Fig 6-3 Sample of metal fuel container used (with diameter 26 cm and weight 350 g)

#### 6.3.2.2 Temperature measurement

During the experiment, the temperature will be monitored by thermocouples (Fig 6-4) which are made of high conductive steel covered with anti-fire textile material to measure the temperature at specific points where the steel part is subjected directly to fire. Regarding the fixation of these thermocouples, high temperature resistance glue is used. The tube is drilled from outside in a way that keeps most of the wire area covered out the test tube while keeping the metal part of thermocouples only inside the tube in order to assure that the temperature measurements are only based on the internal temperature

Fig 6-4 Thermocouples and the way of fixation

The benefit of these thermocouples is to measure the temperature distribution along the upper profile of the tube where the major rise in temperature during the test occurs. In addition to that, the temperature distribution is also measured along the section levels by trees (Fig 6-5) that can be defined as a group of thermocouples connected together at the same section with different levels to be able to know the temperature from lower to upper points.

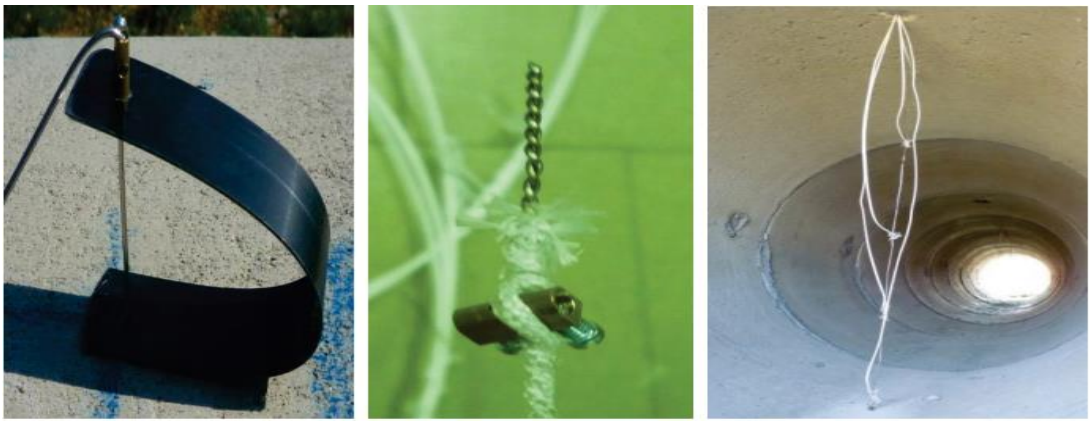

Fig 6-5 The way of fixation and distribution of the trees

In order to check the true fixation and arrangement of wires, a polarity check is done by investigating their electrical connectivity. All thermocouples are completely checked before running the test to assure accurate results. The method of tree fixation is based on putting the wire under tension while fixing the tree thermocouples at different levels to measure the temperature in different heights.

#### 6.3.2.3 Weight measurement

One of the methods to determine HRR as mentioned before is to determine the mass loss rate of fuel. The weight gauge (Fig 6-6) in this case is used to determine the rate of mass loss. The heat release rate is assumed to be directly proportional to the fuel mass loss rate. The unit weight gauge is based on the electrical sign that indicated differences in voltages. The distance is proportionally increasing with weight and vice versa as shown in the following. The capacity of the weight gauge is 3 kg.


Fig 6-6 Electrical weight gauge

#### 6.3.2.4 Ventilation unit

A ventilation unit with different velocities was used, as indicated in the following (Fig 6-7), to investigate the effect of wind on smoke and temperature distributions. In order to control the wind speed and swirling effect, barriers (Fig 6-7) have been used. By increasing the number of barriers, the wind effect is decreased.

Fig 6-7 Ventilator and barriers

### 6.3.3 Test preparation and running

Unit weight gauges are connected with data logger to measure weight loss rate with time during test running. A pan filled with fuel is hanged to a weight scale gauge horizontally without any friction with the drilled hole in concrete tube (Fig 6-8). Specific software is used for collecting and analyzing received information from data logger.

Fig 6-8 concrete tube cross section showing method of fuel hang an electrical weight gauge

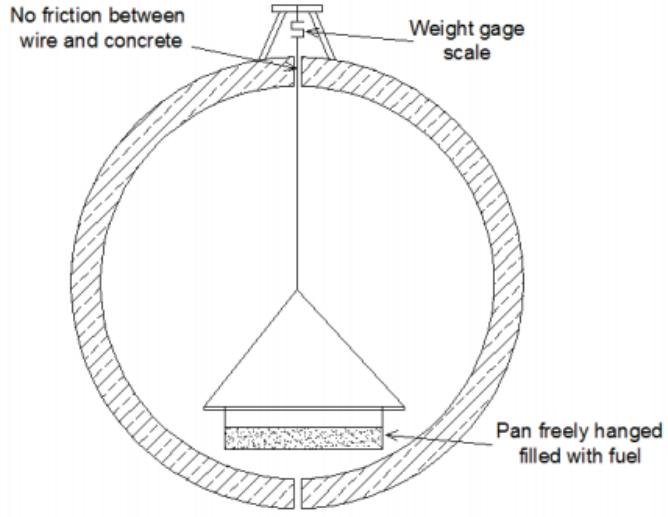


All test units are arranged in proper way to prevent conflict of measurements and insure accurate results. All gauges are installed as indicated in the following (Fig 6-9) that shows the procedures of data collection. 24 thermocouples are used in both single temperature and tree measurements. Each 8 thermocouples are connected to a data logger which in turn is connected to a USB hub. The USB hub supports a computer unit for data collection and analysis. The main function of these thermocouples is to measure the temperature distribution along the tube, the air and concrete temperatures.

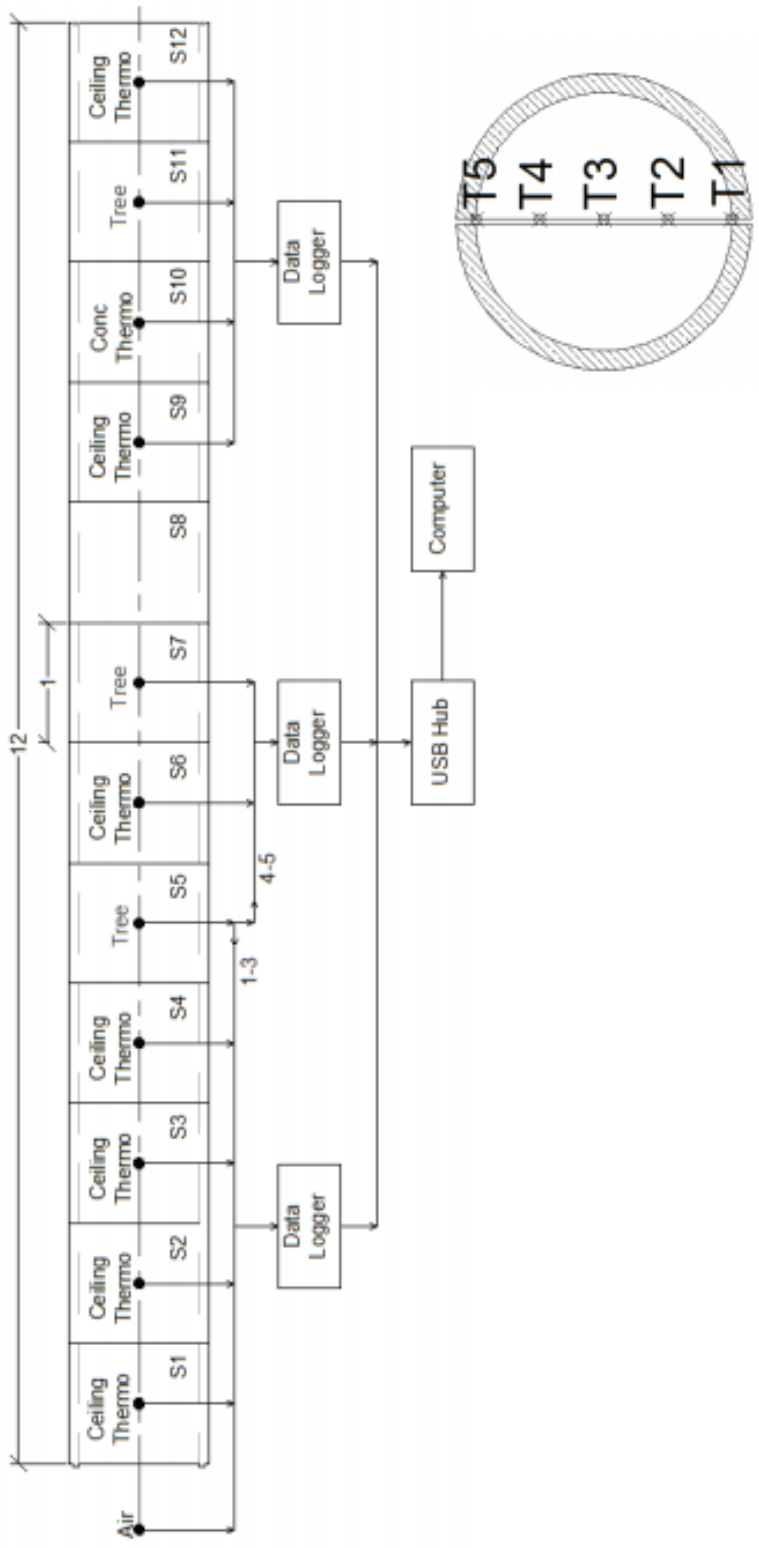


Fig 6-9 Schematic diagrams for test gauges setup and thermocouples levels

The test is repeated several times using different parameters in order to make parametric studies and check effect of input change on temperature and smoke behavior.

All data were collected by computer with time step 10 seconds. The measured data include the temperature measured y thermocouples to show the distribution of temperature along the tube and the temperature measured by trees to show temperature distribution with levels change and the weight mass loss to calculate the heat release rate for test with time, following figure shows the tube with fire (Fig 6-10).

Fig 6-10 Concrete tube with fire

## 6.4 Test results

The main results related to the maximum heat release rate, fire growth rate, distribution of temperature and total heat flux.

There are 4 tests repeated in the experiment, considering changing the weight of the burning fuel, the diameter of the mass container pan and also the ventilation condition like the wind velocity and the ventilation starting time.

After finish these tests a parametric study can be performed then check effect of input change on temperature and smoke behavior, the test results are showing in the following:

### 6.4.1 First test results

The first test is performed using a 26 cm diameter stainless steel pan filled with a quantity of diesel fuel (1400 gram) and the test was performed in non-ventilation condition.

**Mass loss rate:**

The weight gauge (Fig 6-6) in this case is used to determine the rate of mass loss (Fig 6-11).

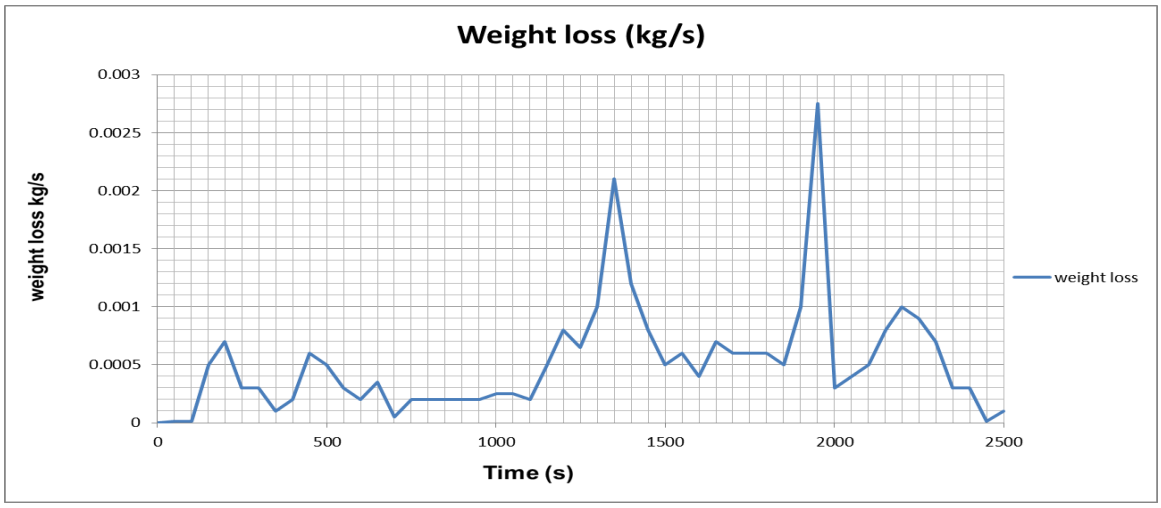


Fig 6-11 Fuel mass loss rate (g) per time (sec) in the first test

**Heat release rate:**

By calculating the heat release rate using the equation mentioned before that is based on rate of fuel mass loss, following figure shows the result (Fig 6-12):

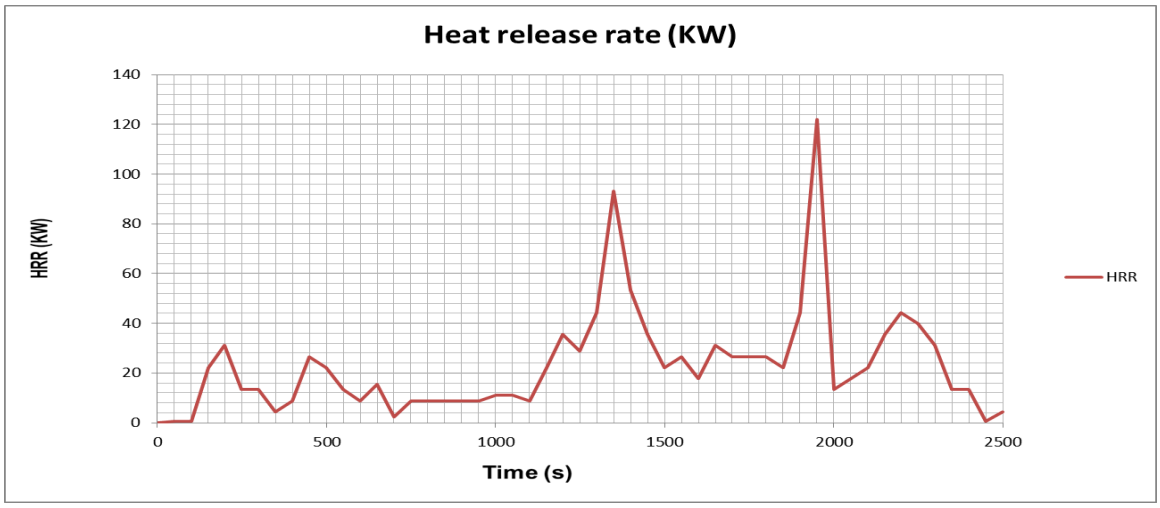


Fig 6-12 Heat release rate (KW) per time (sec) in the first test

**Temperature distribution:**

All temperature distribution change with time are monitored by thermocouples and shown in the following figure (Fig 6-13):

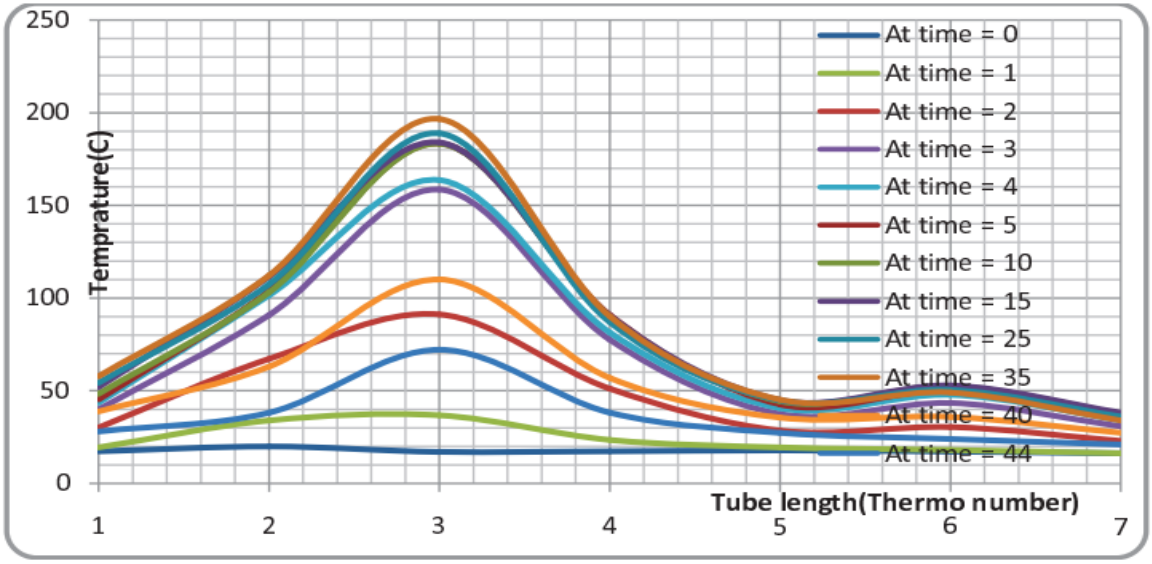


Fig 6-13 Temperature changes with tube length during the first test stages

Temperature monitoring in each segment separately shows in following figure (Fig 6-14)

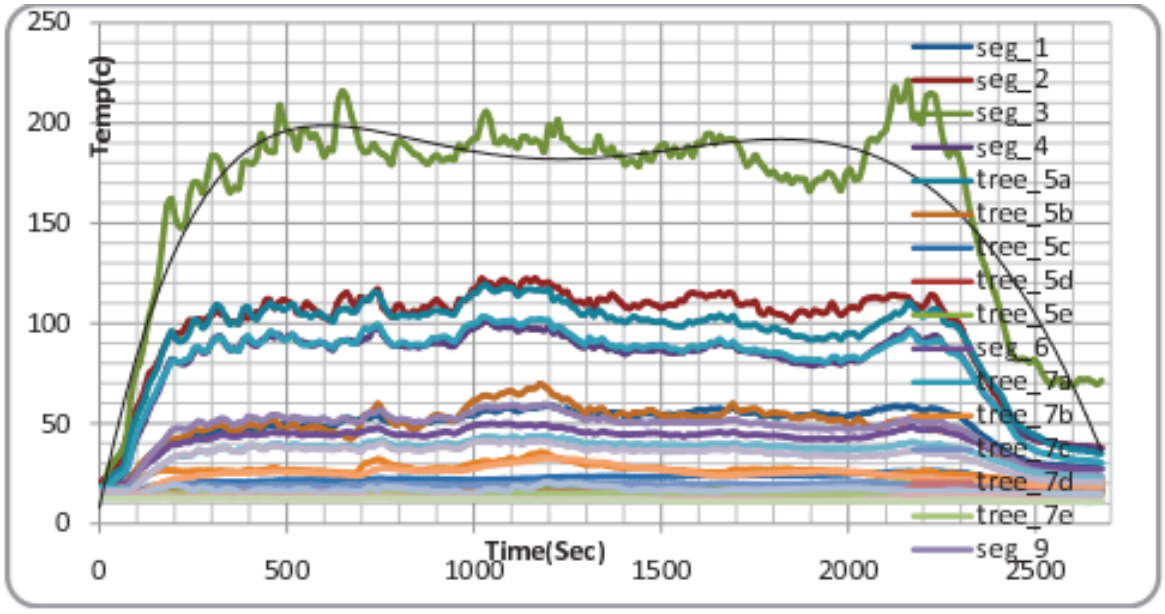


Fig 6-14 Temperature monitoring in each segment separately

Regarding the temperature distribution along change of levels, they are monitored by trees in different stations in tube and shown in the next figures (Fig 6-15 – Fig 6-17):

**Tree at segment 5**

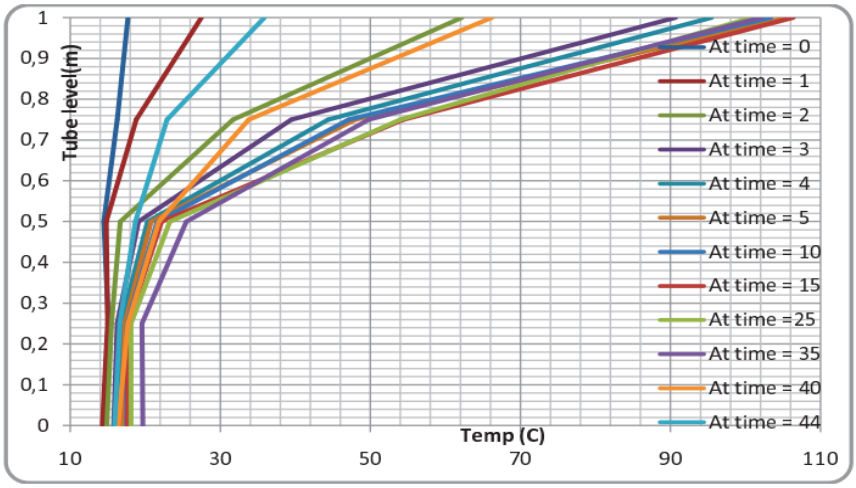


Fig 6-15 Temperature changes with tube level according to different time stages in segment 5

**Tree at segment 7**

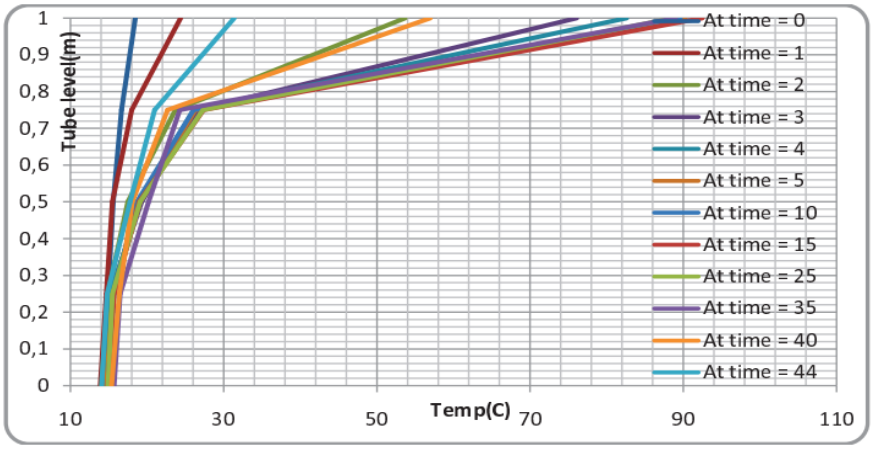


Fig 6-16 Temperature changes with tube level according to different time stages in segment 7

**Tree at segment 11**

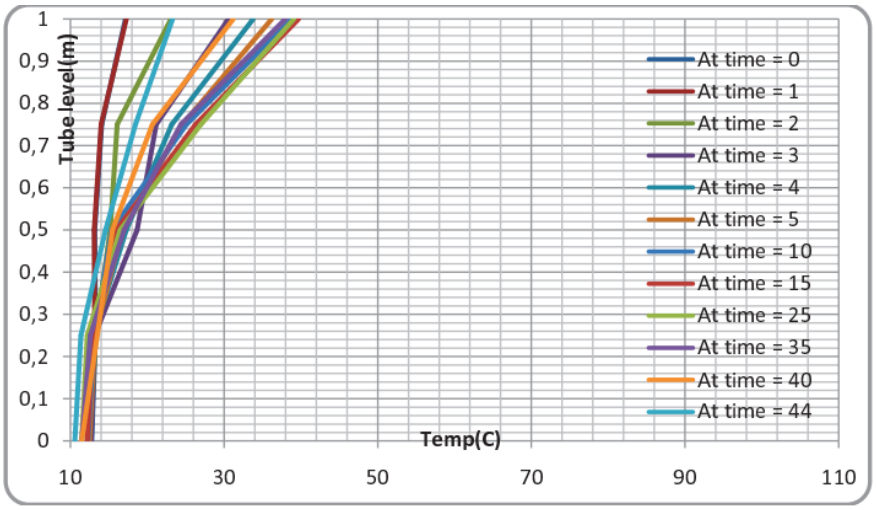


Fig 6-17 Temperature changes with tube level according to different time stages in segment 11

### 6.4.2 Second test results

The second test is performed using a 26 cm diameter stainless steel pan filled with a quantity of diesel fuel (700 gram) and the test was performed in non-ventilation condition.

**Mass loss rate:**

The weight gauge (Fig 6-6) in this case is used to determine the rate of mass loss (Fig 6-18).

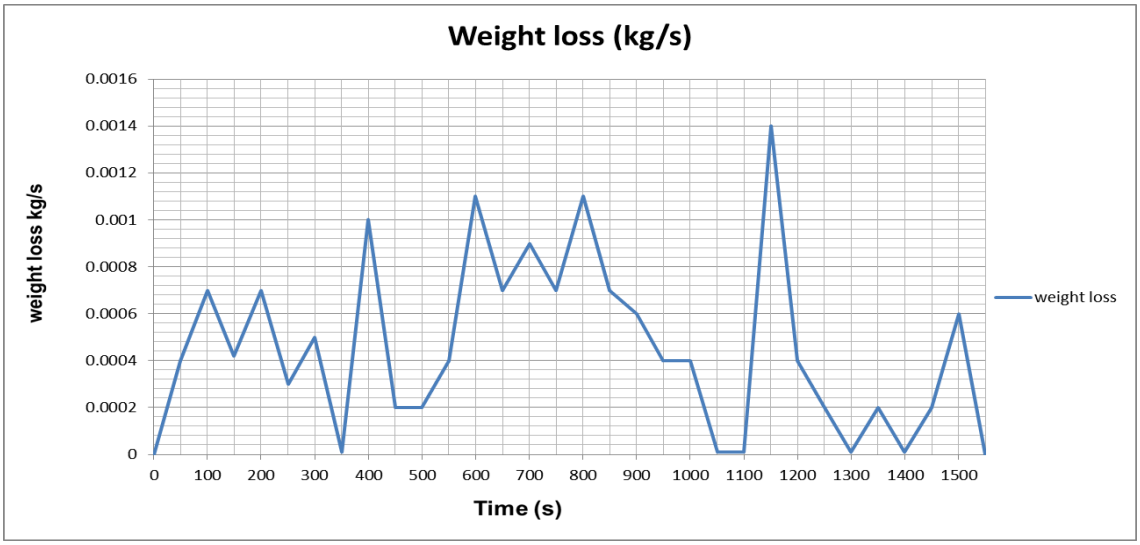


Fig 6-18 Fuel mass loss rate (g) per time (sec) in the second test

**Heat release rate:**

By calculating the heat release rate using the equation mentioned before that is based on rate of fuel mass loss, following figure shows the result (Fig 6-19):

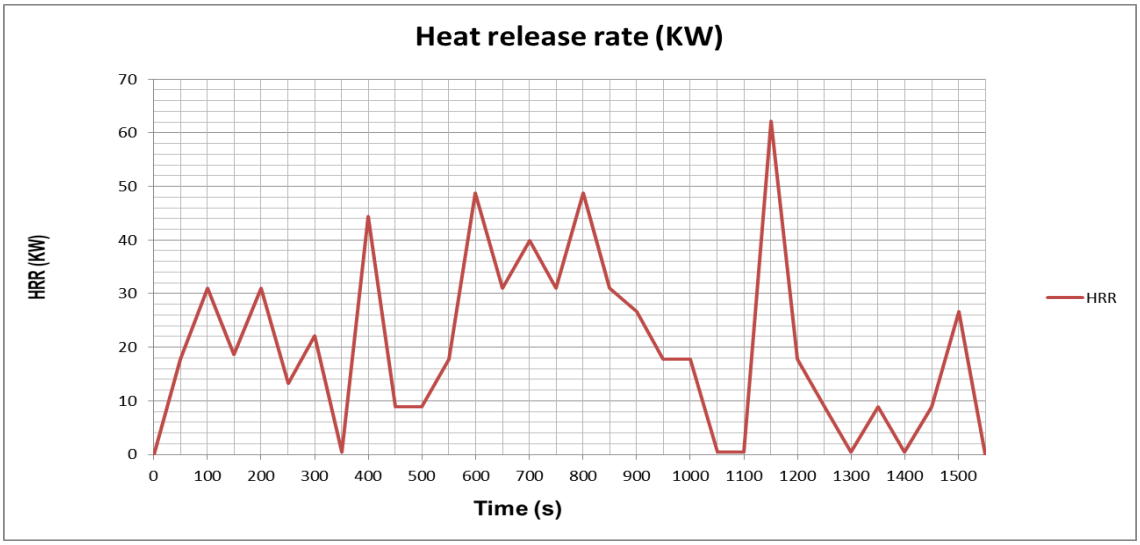


Fig 6-19 Heat release rate (KW) per time (sec) in the second test

**Temperature distribution:**

All temperature distribution change with time are monitored by thermocouples and shown in the following figure (Fig 6-20):

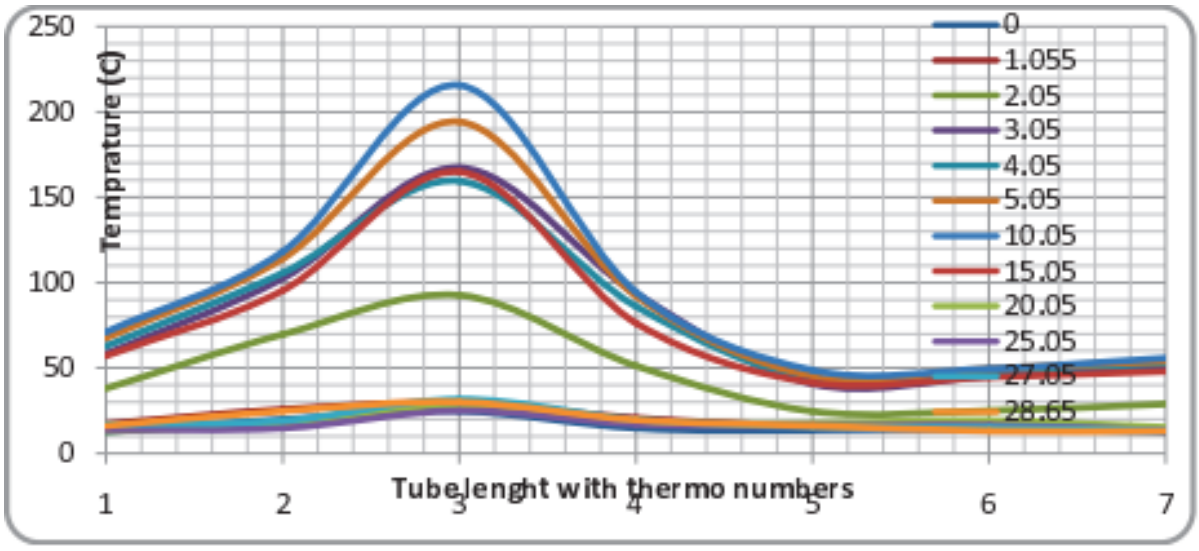


Fig 6-20 Temperature changes with tube length during the second test stages

Temperature monitoring in each segment separately shows in following figure (Fig 6-21)

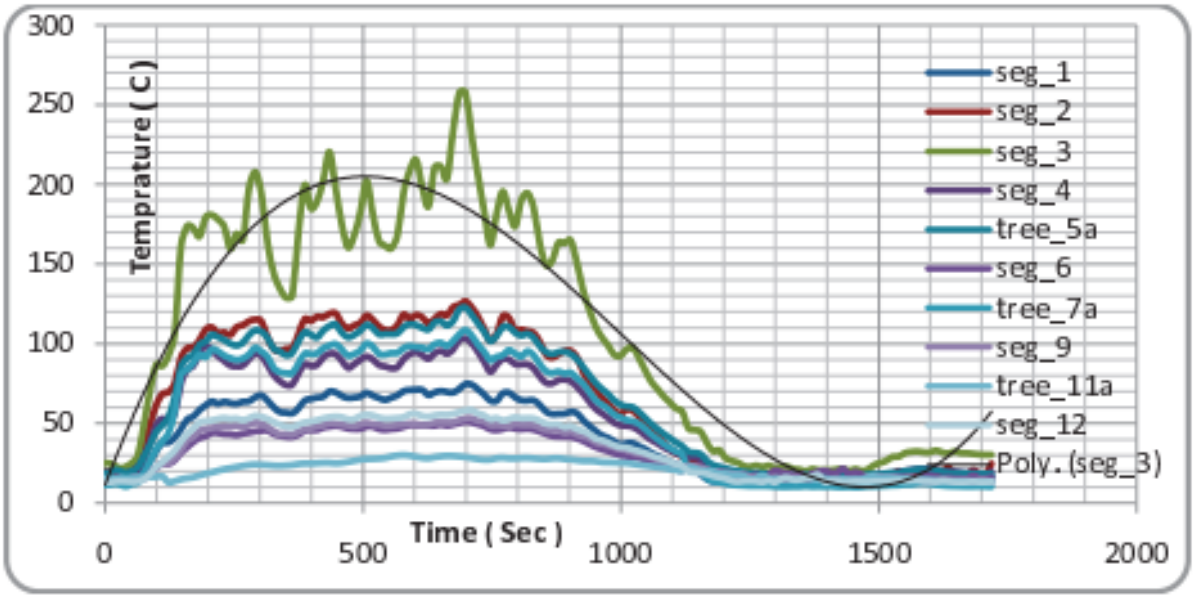


Fig 6-21 Temperature monitoring in each segment separately

Regarding the temperature distribution along change of levels, they are monitored by trees in different stations in tube and shown in the next figures (Fig 6-22 – Fig 6-24):

**Tree at segment 5**

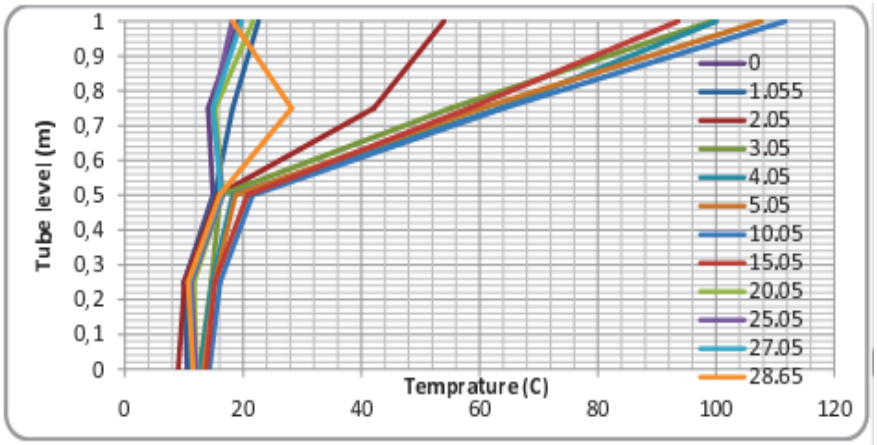


Fig 6-22 Temperature changes with tube level according to different time stages in segment 5

**Tree at segment 7**

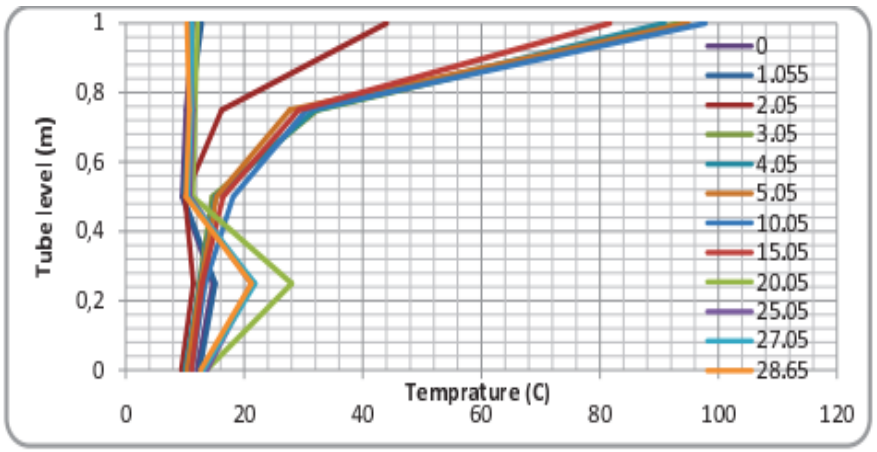


Fig 6-23 Temperature changes with tube level according to different time stages in segment 7

**Tree at segment 11**

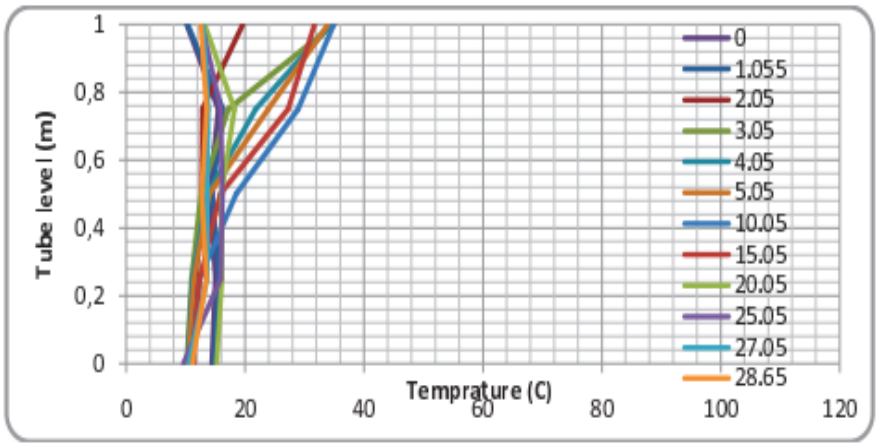


Fig 6-24 Temperature changes with tube level according to different time stages in segment 11

### 6.4.3 Third test results

The third test is performed using a 26 cm diameter stainless steel pan filled with a quantity of diesel fuel (900 gram) and the ventilation started at the 2 minute of testing time with a value of more than 2.5m/s.

**Mass loss rate:**

The weight gauge (Fig 6-6) in this case is used to determine the rate of mass loss (Fig 6-25).


Fig 6-25 Fuel mass loss rate (g) per time (sec) in the third test

**Heat release rate:**

By calculating the heat release rate using the equation mentioned before that is based on rate of fuel mass loss, following figure shows the result (Fig 6-26):

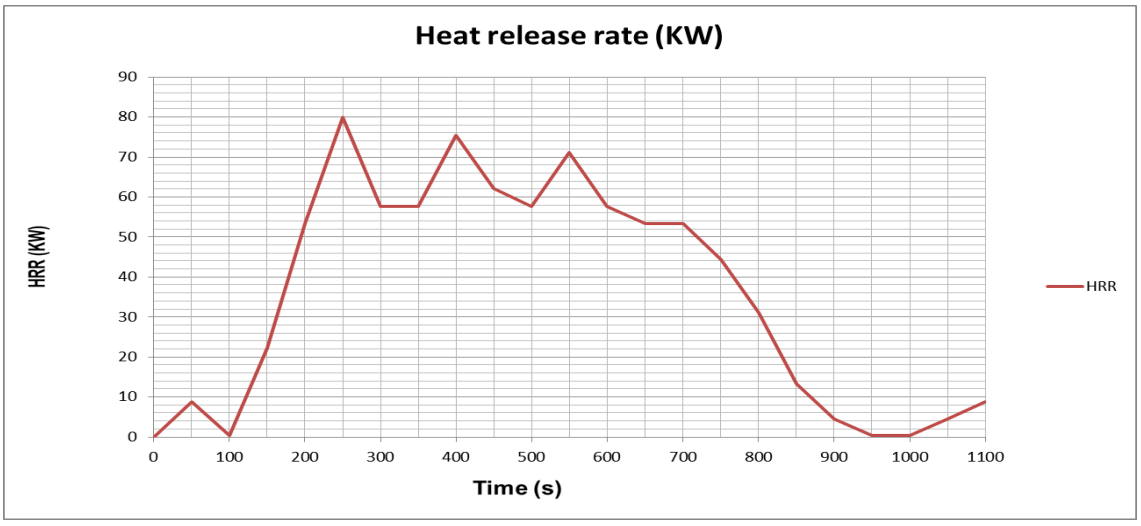


Fig 6-26 Heat release rate (KW) per time (sec) in the third test

**Temperature distribution:**

All temperature distribution change with time are monitored by thermocouples and shown in the following figure (Fig 6-27):

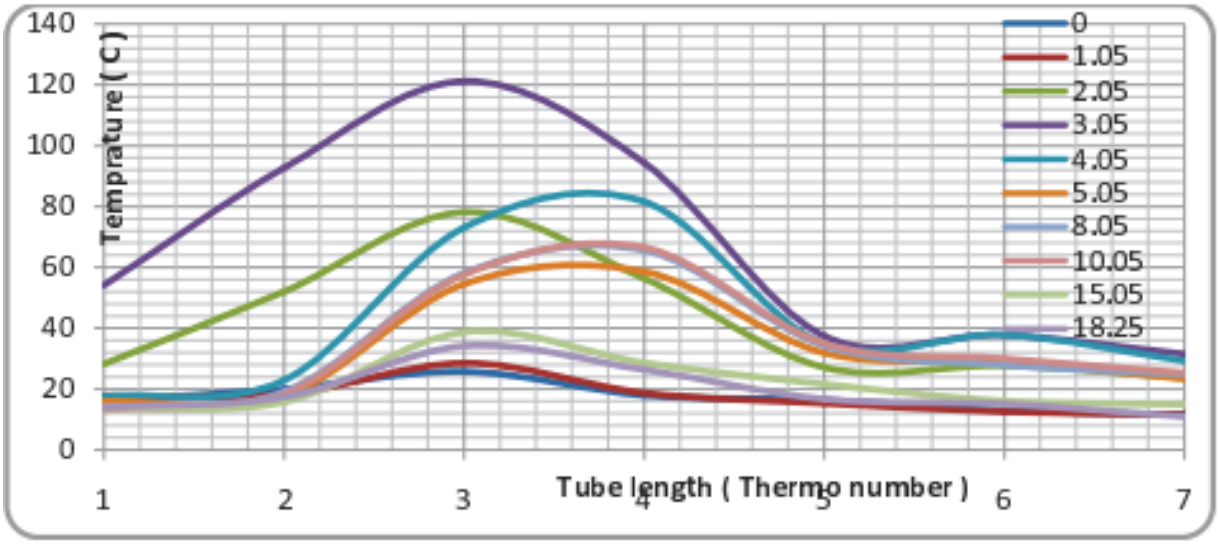


Fig 6-27 Temperature changes with tube length during the third test stages

Temperature monitoring in each segment separately shows in following figure (Fig 6-28)

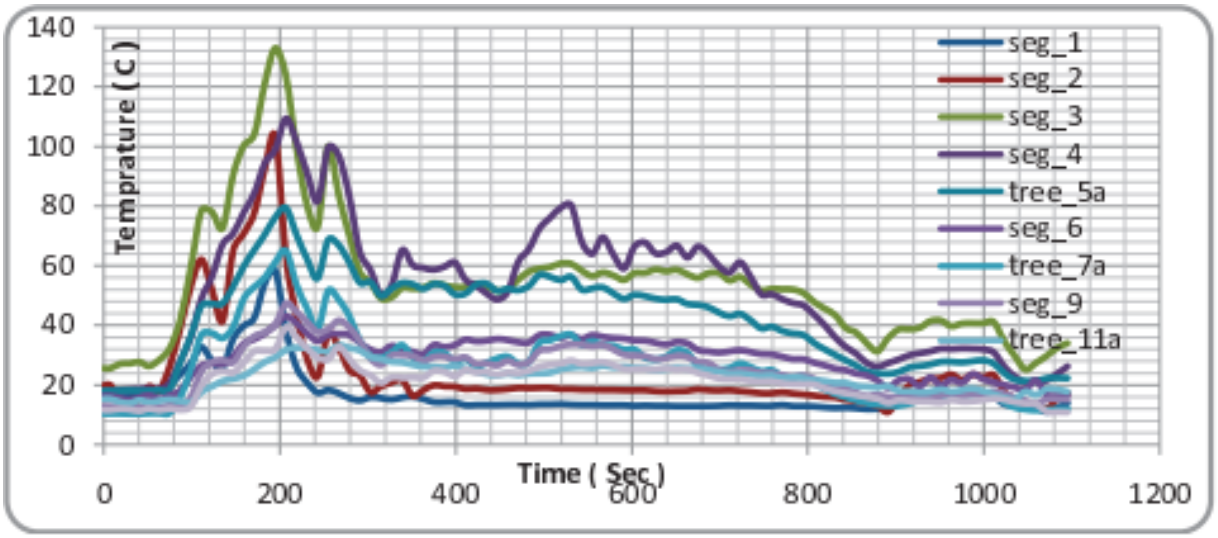


Fig 6-28 Temperature monitoring in each segment separately

Regarding the temperature distribution along change of levels, they are monitored by trees in different stations in tube and shown in the next figures (Fig 6-29 – Fig 6-31):

**Tree at segment 5**

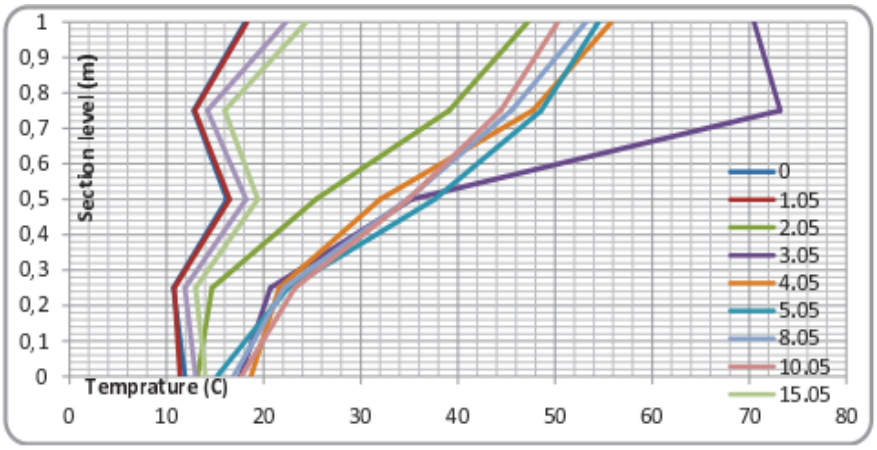


Fig 6-29 Temperature changes with tube level according to different time stages in segment 5

**Tree at segment 7**

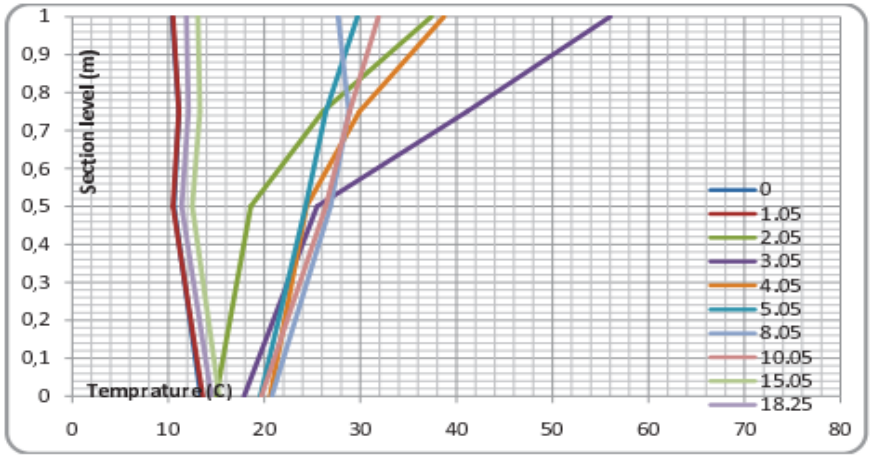


Fig 6-30 Temperature changes with tube level according to different time stages in segment 7

**Tree at segment 11**

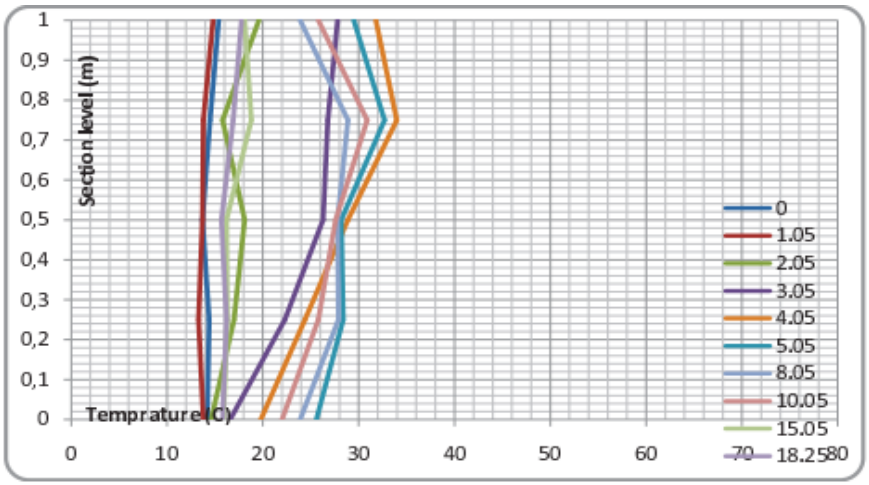


Fig 6-31 Temperature changes with tube level according to different time stages in segment 11

### 6.4.4 Fourth test results

The fourth test is performed using a 18 cm diameter stainless steel pan filled with a quantity of diesel fuel (790 gram) and the ventilation started at the 30 minute of testing time with a value of 2.5m/s

**Mass loss rate:**

The weight gauge (Fig 6-6) in this case is used to determine the rate of mass loss (Fig 6-32).

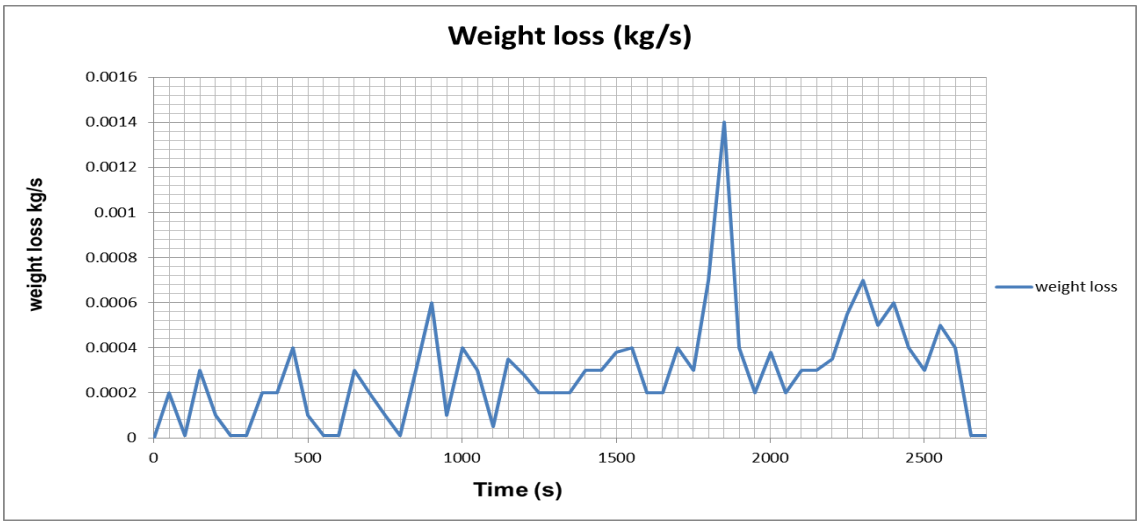


Fig 6-32 Fuel mass loss rate (g) per time (sec) in the fourth test

**Heat release rate:**

By calculating the heat release rate using the equation mentioned before that is based on rate of fuel mass loss, following figure shows the result (Fig 6-33):

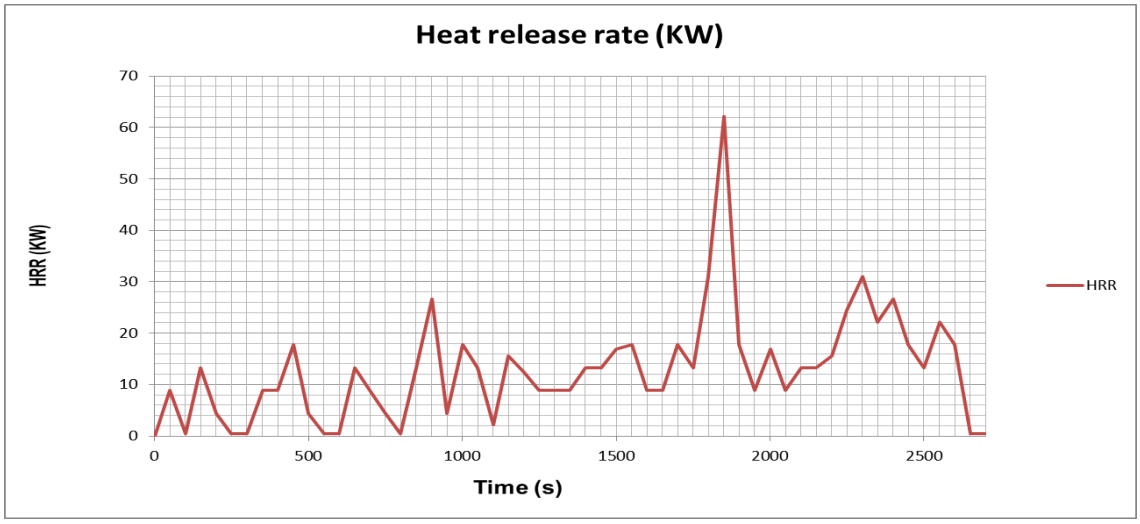


Fig 6-33 Heat release rate (KW) per time (sec) in the fourth test

**Temperature distribution:**

All temperature distribution change with time are monitored by thermocouples and shown in the following figure (Fig 6-34):

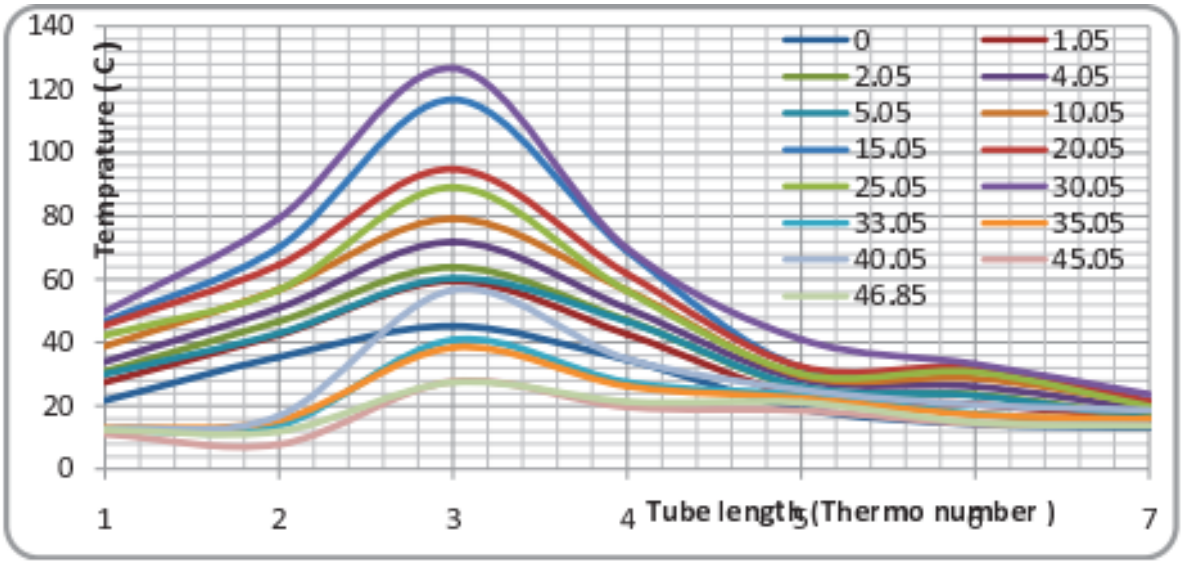


Fig 6-34 Temperature changes with tube length during the fourth test stages

Temperature monitoring in each segment separately shows in following figure (Fig 6-35)

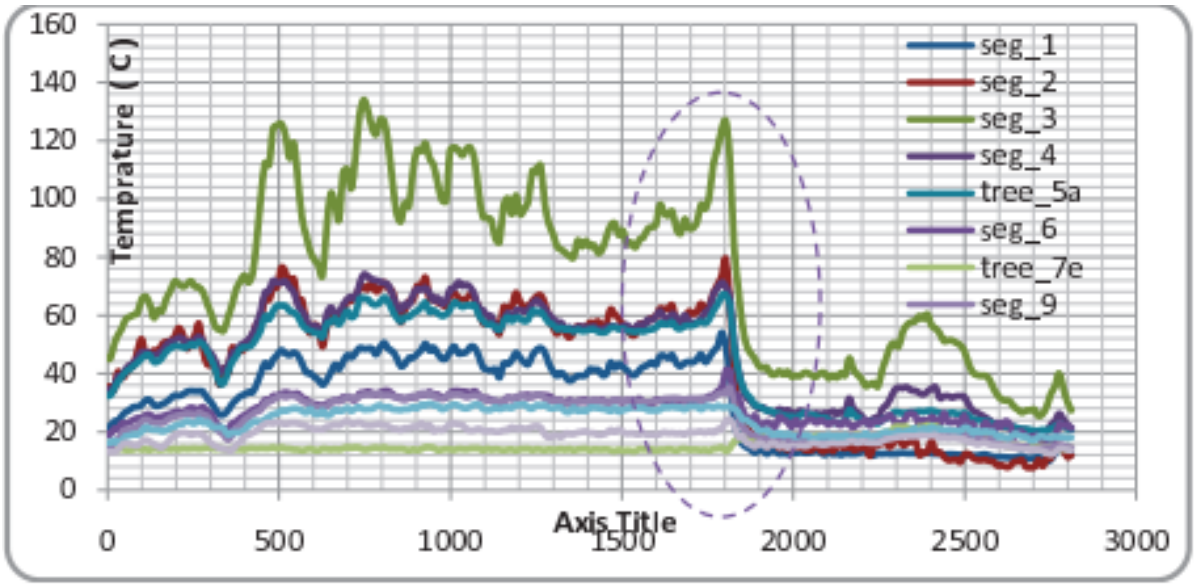


Fig 6-35 Temperature monitoring in each segment separately

Regarding the temperature distribution along change of levels, they are monitored by trees in different stations in tube and shown in the next figures (Fig 6-36 – Fig 6-38):

**Tree at segment 5**

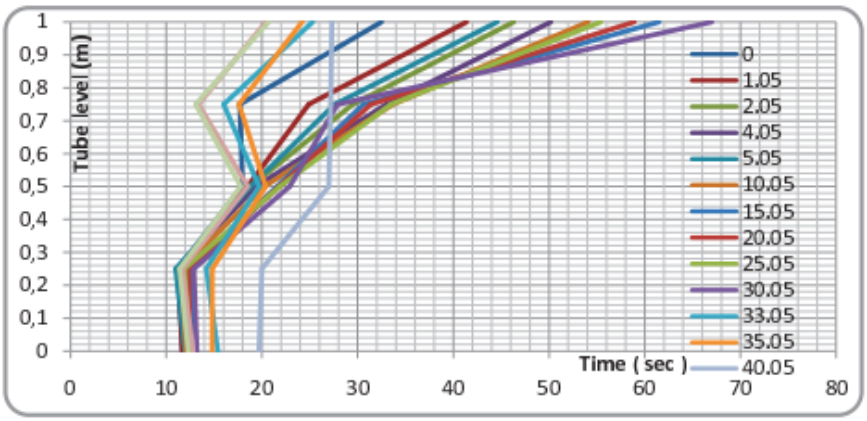


Fig 6-36 Temperature changes with tube level according to different time stages in segment 5

**Tree at segment 7**

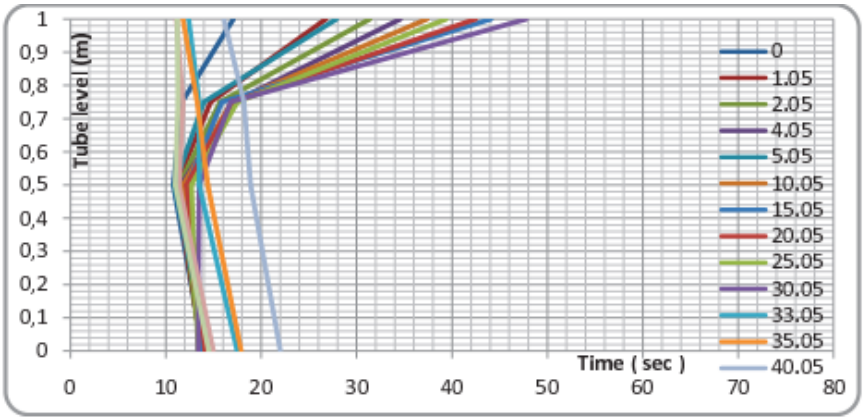


Fig 6-37 Temperature changes with tube level according to different time stages in segment 7

**Tree at segment 11**

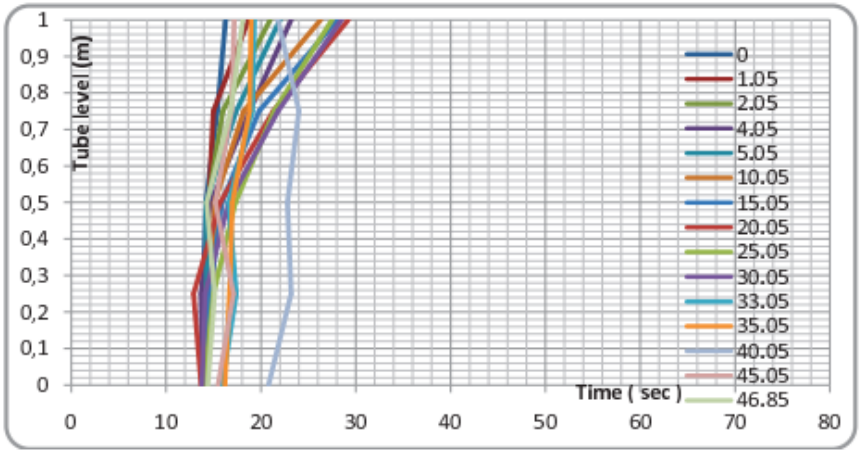


Fig 6-38 Temperature changes with tube level according to different time stages in segment 11

# 7. Numerical modeling

## 7.1 Introduction

*[Main reference: Handbook of Tunnel Fire Safety, 2nd edition, David Charters, Chapter 16]*

Control volume modeling is an approach for predicting various aspects of fires in tunnels and often known as 'zone' modeling. The approach works by dividing the tunnel system into a series of control volumes (or zones). Each control volume represents a part of the system that is homogeneous in nature, i.e. one control volume assumed to have the same properties (e.g. temperature, velocity, density, species concentration). Conservation equations are applied to each control volume to predict the fire or plume, and processes between control volumes, such as convective heat transfer, affect the control volumes properties. Figure 7-1 denotes how the tunnel-fire domain can be divided up into different control volumes

Fig 7-1 A typical tunnel fire control volume model

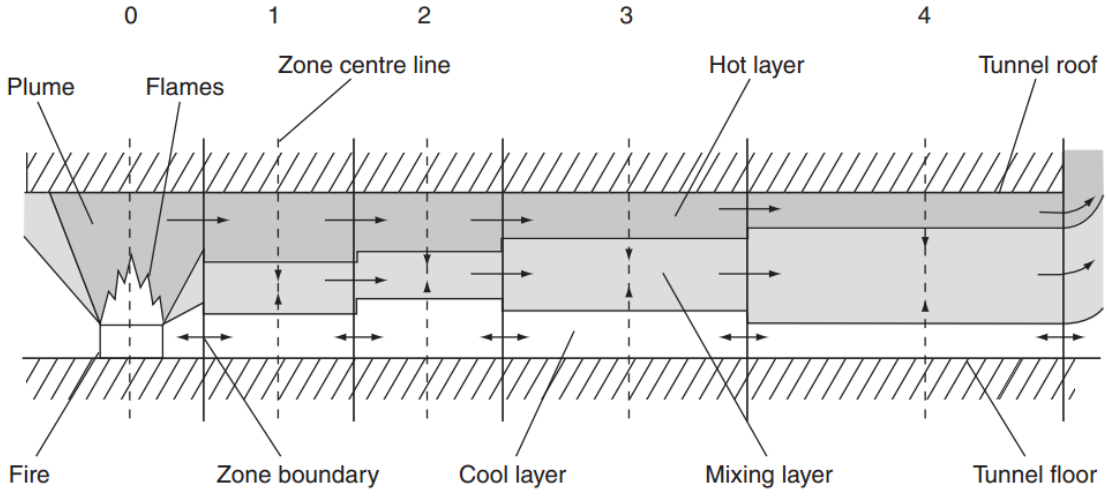


Control volume modeling of tunnel fires is built on three types of model: conservation equations, source terms, and mass and heat transfer sub-models. The kinds of assumptions that are typical of control volume modeling include:

1. All properties in the control volume are homogeneous.
2. The gas is treated as an ideal gas (usually as air).
3. Combustion is treated as the source term of heat and mass.
4. Mass transport times within a control volume are instant.
5. Heat transfer to tunnel contents, such as a vehicle, is neglected.
6. The cross-section of the tunnel is constant and the tunnel is horizontal.

In this research, a new zone modeling approach, called a Multi-Layer Zone (MLZ) model was extended adapt to predict smoke movement in a tunnel fire, including vertical distributions of temperature. In this model the volume of a tunnel is divided into multiple of areas and each of them is further divided into multiple layers as the control volumes (Fig 7-2). The physical properties, such as temperature, in each layer of each area are assumed to be uniform. Boundary walls are also divided into segments at uniform temperature in accordance with the layer division. Radiation heat transfer between the layers and between the layers and the wall segments is neglected, and the convective heat transfer between the layers and the wall segments is calculated. Air entrainment into the fire plume, considering the effect of the horizontal flow around it, is calculated with a simple set of equations. This model retains the advantage of zone models in terms of computational load; hence it is expected to be useful for practical applications associated with fire safety design in tunnels. For calibration and verification of the model, comparisons of the predictions by this model are presented against measurements in small scale concrete tube experiments.

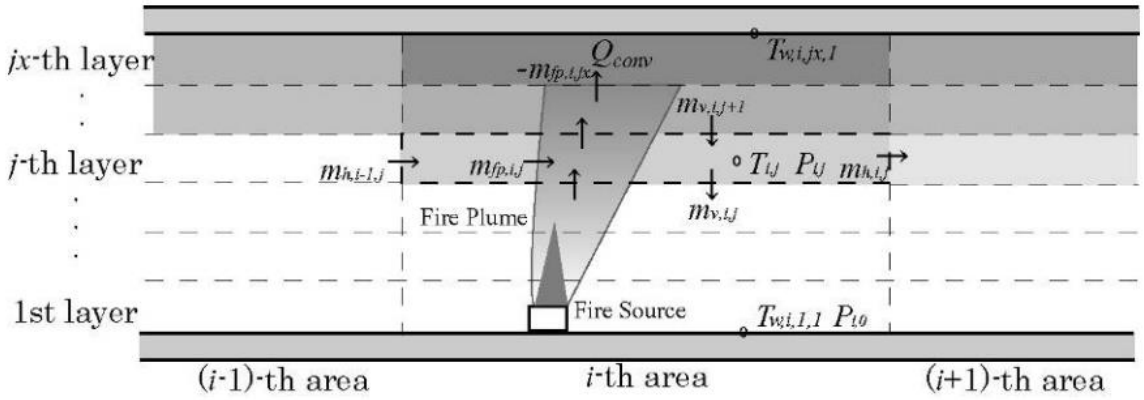


Fig 7-2 Multi-Layer Zone (MLZ) model to a tunnel fire

*[Suzuki, Keichi. Tanaka, Takeyoshi, et al., 2004. An application of a multi-layer zone model to a tunnel fire]*

## 7.2 Nomenclature listing

$A_w$: area of wall ($m^2$)

$C_p$: specific heat of gas (kJ/kg/K)

$C_w$: specific heat of wall (kJ/kg/K)

d: hydraulic diameter of tunnel (m)

$F_f$: friction force

$H_h$: horizontal enthalpy flow rate (KW)

$H_v$: vertical enthalpy flow rate (KW)

$k_w$: thermal conductivity of wall (KW/mK)

$M_{fp}$: mass flow rate into fire plume (kg/s)

$M_v$: vertical mass flow rate (kg/s)

$M_h$: horizontal mass flow rate (kg/s)

P: pressure difference (Pa)

$P_v$: dynamic pressure (Pa)

$Q_c$: convective heat release rate (KW)

$Q_w$: convection heat transfer to wall (KW)

$\alpha_c$: convective heat transfer coefficient ($KW/m^2/K$)

b: width of the opening (m)

$\varphi_i$: fraction of radiation to each layer

$\Delta x$: length of area (m)

$\Delta z$: depth of layer (m)

$\lambda$: coefficient of friction

$\rho$: density of gas ($kg/m^3$)

$\rho_w$: density of wall ($kg/m^3$)

T: gas temperature (K)

$T_w$: wall temperature (K)

u: horizontal velocity (m/s)

V: volume of layer ($m^3$)

t: time (s)

g: gravity acceleration ($m/s^2$)

f: area number with fire

i: area number

j: layer number

iN: maximum area number

jN: maximum layer number

$F_r$: fraction of radiation

## 7.3 Governing equations for zone properties

The concept of the multi-layer zone model is denoted in Fig 7-2. One of the notable differences of the concept of the model from the two-layer zone models is that the fire plume flow does not mix with the upper layer as soon as it penetrates a layer interface but continues to rise until it hits the ceiling, after it pushes down the gases in the top layer. The principal equations of ordinary two-layer zone models were derived from the equations for mass and energy conservation in the upper and lower layers. In the case of the multi-layer zone model, the conservation equations for each laminated horizontal layer are also the bases to derive the equations.

The principal equations for gas temperature in the MLZ model, called zone governing equations, are derived from the conservation equations for mass and internal energy and equation of state in each layer.

### 7.3.1 Mass conservation

Fig 7-3 shows a mass balance condition in a control volume of the tunnel ($i^{th}$ area, $j^{th}$ layer).

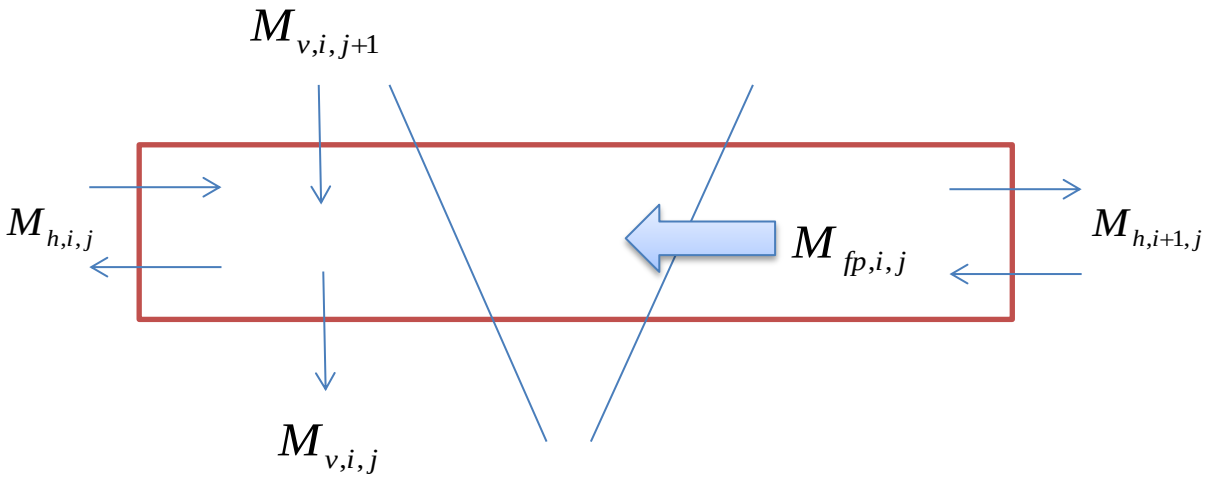


Fig 7-3 Mass conservation of $i^{th}$ area, $j^{th}$ layer

From Fig 7-3:

$$\frac{d}{dt}(\rho_{i,j}V_{i,j}) = -M_{fp,i,j} + M_{v,i,j+1} - M_{v,i,j} + M_{h,i,j} - M_{h,i+1,j} \quad (7\text{-}1)$$

Where $\rho_{i,j}$ and $V_{i,j}$ are the density and the volume of the control volume, $M_{fp,i,j}$ is the flow rate of mass entrained to the fire plume, which is a positive value, $M_{v,i,j}$ is the net mass flow rate from the jth layer to the (j-1)th through the surface outside of the fire plume. $M_{h,i,j}$ is the horizontal mass flow rate in the left side of the control volume, positive means mass flow into the control volume, negative means flow out the control volume. $M_{h,i+1,j}$ is the horizontal mass flow rate in the right side of the control volume, positive means mass flow out the control volume, negative means flow into the control volume.

For the top layer, considering that the mass rate of gas entrained into the fire plume is eventually transported to the layer, and $M_{fp,i,jN}$ is a negative value, the mass conservation becomes:

$$\frac{d}{dt}(\rho_{i,jN}V_{i,jN}) = -M_{fp,i,jN} - M_{v,i,jN} + M_{h,i,jN} - M_{h,i+1,jN} \tag{7-2}$$

### 7.3.2 Energy conservation

Some documents assumed that all the heat released by the fire rises to the top layer. But in fact, about 30 percent of the fire's heat is radiated. So it can be assumed that as default that 70 percent rises to the top layer and other is transferred to each layer by radiation.

Fig 7-4 shows a energy balance condition in a control volume of the tunnel ($i^{th}$ area, $j^{th}$ layer).

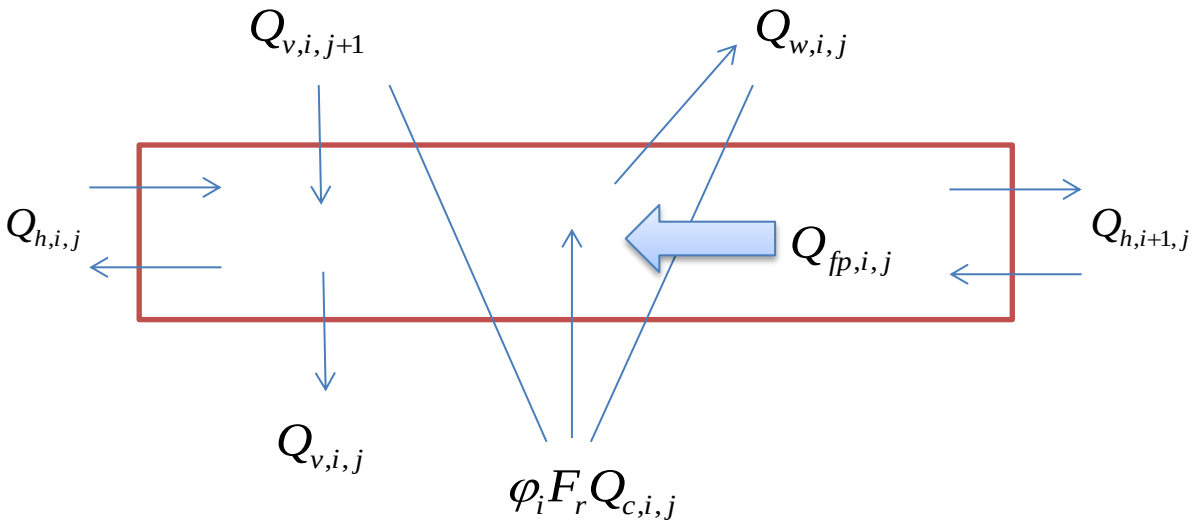


Fig 7-4 Energy conservation of $i^{th}$ area, $j^{th}$ layer

From Fig 7-4:

$$\begin{aligned}\frac{d}{dt}(C_p\rho_{i,j}V_{i,j}T_{i,j}) = &-C_pM_{fp,i,j}T_{i,j} + C_p\{\max(M_{v,i,j+1}T_{i,j+1},0)+\min(M_{v,i,j+1}T_{i,j},0)\}\\ &-C_p\{\max(M_{v,i,j}T_{i,j},0)+\min(M_{v,i,j}T_{i,j-1},0)\}\\ &+C_p\{\max(M_{h,i,j}T_{i-1,j},0)+\min(M_{h,i,j}T_{i,j},0)\}\\ &-C_p\{\max(M_{h,i+1,j}T_{i,j},0)+\min(M_{h,i+1,j}T_{i+1,j},0)\}\\ &-Q_{w,i,j}+\varphi_iF_rQ_{c,i,j}\end{aligned} \tag{7-3}$$

Where $C_p$ is the specific heat, $T_{i,j}$ is the temperature of the control volume, $Q_{w,i,j}$ is the convection heat loss to the wall surface. The second and the third terms shows that if $M_{v,i,j+1}$ is positive, the net flow through the interface of the (j+1) th and the jth layers is downward, otherwise upward. The fourth term shows that if $M_{h,i,j}$ is positive, the net flow through the interface of the (i-1) th and the ith layers is into the volume, otherwise outflow. The fifth term shows that if $M_{h,i+1,j}$ is positive, the net flow through the interface of the ith and the (i+1)th layers is flow out the volume, otherwise inflow. $Q_{c,i,j}$ is the heat released by fire. $F_r$ is the fraction of radiation default that is equal to 0.3; it is a fuel-dependent parameter. $\varphi_i$ is the fraction of radiation to each layer. $\varphi_i = 4/3jN$ when $j \le jN/2$ and $\varphi_i = 2/3jN$ when $j > jN/2$.

For the top layer, the energy conservation is written as:

$$\begin{aligned}\frac{d}{dt}(C_p\rho_{i,jN}V_{i,jN}T_{i,jN}) = &-C_pM_{fp,i,jN}T_{i,jN}\\ &-C_p\{\max(M_{v,i,jN}T_{i,jN},0)+\min(M_{v,i,jN}T_{i,jN-1},0)\}\\ &+C_p\{\max(M_{h,i,jN}T_{i-1,jN},0)+\min(M_{h,i,jN}T_{i,jN},0)\}\\ &-C_p\{\max(M_{h,i+1,jN}T_{i,jN},0)+\min(M_{h,i+1,jN}T_{i+1,jN},0)\}\\ &-Q_{w,i,jN}+(1-F_r)Q_{c,i,jN}\end{aligned} \tag{7-4}$$

### 7.3.3 The ideal gas state equation

Considering that a fire is basically a phenomenon at atmospheric pressure, the equation of state of the ideal gas in this model is simplified as follows:

$$\rho_{i,j}T_{i,j} = const. = 1.205\times 293 \tag{7-5}$$

### 7.3.4 Zone governing equations

Noting that the left-hand side of equation (7-3) can be expanded as follows:

$$\frac{d}{dt}(C_p\rho_{i,j}V_{i,j}T_{i,j}) = C_p\rho_{i,j}V_{i,j}\frac{dT_{i,j}}{dt} + C_pT_{i,j}\frac{d}{dt}(\rho_{i,j}V_{i,j}) \tag{7-6}$$

Then finally the zone governing equation for temperature of each layer is derived by substituting equations (7-1) and (7-3) in to equation (7-6) and arranging as follows:

$$\begin{aligned}\frac{dT_{i,j}}{dt} = \frac{1}{C_p\rho_{i,j}V_{i,j}}\times[&(H_{v,i,j+1} - C_pM_{v,i,j+1}T_{i,j}) - (H_{v,i,j} - C_pM_{v,i,j}T_{i,j})\\ &+(H_{h,i,j} - C_pM_{h,i,j}T_{i,j}) - (H_{h,i+1,j} - C_pM_{h,i+1,j}T_{i,j})\\ &-Q_{w,i,j} + \varphi_i F_r Q_{c,i,j}]\end{aligned} \tag{7-7}$$

Where $H_v$ and $H_h$ are the vertical and horizontal enthalpy flow rate, are changed by flow direction, the computation method will be discussed later.

For the top layer, substituting equations (7-2) and (7-4) in to equation (7-6) and arranging as follows:

$$\begin{aligned}\frac{dT_{i,jN}}{dt} = \frac{1}{C_p\rho_{i,jN}V_{i,jN}}\times[&(C_p\sum_{j=1}^{jN-1}M_{fp,i,j}T_{i,j} - C_pT_{i,jN}\sum_{j=1}^{jN-1}M_{fp,i,j})\\ &-(H_{v,i,jN} - C_pM_{v,i,jN}T_{i,jN})\\ &+(H_{h,i,jN} - C_pM_{h,i,jN}T_{i,jN}) - (H_{h,i+1,jN} - C_pM_{h,i+1,jN}T_{i,jN})\\ &-Q_{w,i,jN} + (1-F_r)Q_{c,i,jN}]\end{aligned} \tag{7-8}$$

Equation (7-7) and (7-8) are the governing equation of temperature, according to the equation, the temperature at every control volume at any time can be computed through assume a small time step, but the rate terms in the equations must be formulated based on the relevant modeling of component processes of fire. Then deals with the rate terms will be introduced as follows.

## 7.4 Tunnel geometry and control volume determination

To start the numerical modeling, the geometry of the tunnel and the determination of the control volume will be first considered. The modeling will be applied on a long reinforced concrete tube; the length is 12m with a density of 2400 kg/m$^3$, just the same with the small scale test, and the inner diameter of 1 m of the radial section. The control volume in the tunnel can be divided at any number, following picture (Fig 7-5, Fig7-6 and Fig 7-7) shows an example of totally number of 60 control volumes which the tunnel have 12 areas and 5 layers.

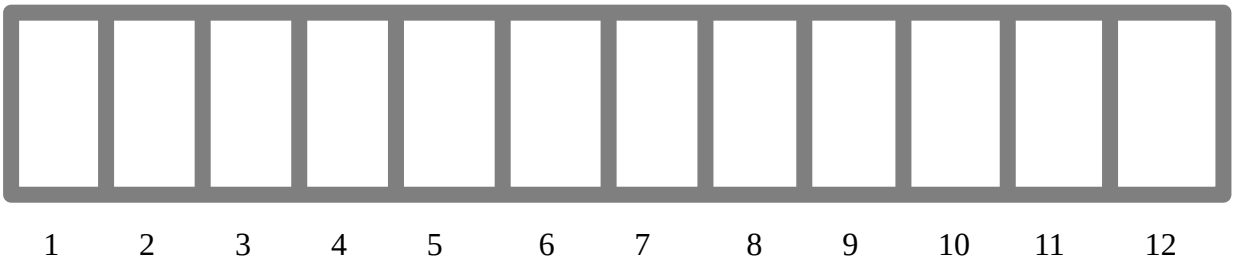


Fig 7-5 Area number in the tunnel

Fig 7-6 5 layer number in the tunnel

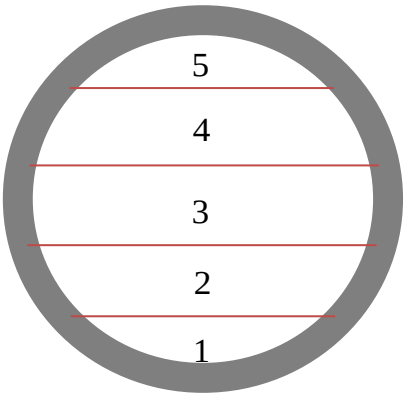


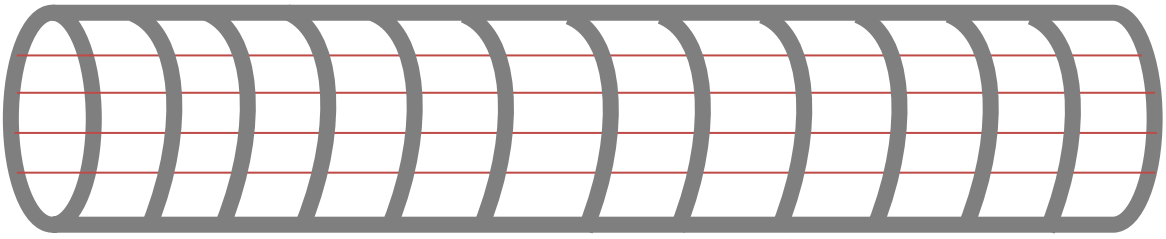

Fig 7-7 Totally 60 control volumes divided in the tunnel

## 7.5 Convection heat transfer to wall $Q_w$

The convection heat transfer to wall related to the temperature of the gas temperature in the control volume T, and the temperature of the wall $T_w$, and the areas of the wall surface around $A_w$, and a constant parameter $\alpha_c$ (0.035 KW/m$^2$/K). The equation shows below:

$$Q_w = \alpha_c (T - T_w) A_w \tag{7-9}$$

In which the temperature of the wall surface is assumed to be related to the temperature of the gas in the control volume by:

$$T_w = T_{amb} + U_w (T - T_{amb}) \tag{7-10}$$

Where $U_w = e^{-\beta (K_w \rho_w C_w)^B}$ (7-11)

And $T_{amb}$ is the temperature of ambient air, the value is assumed to 293K. And $K_w$ is the thermal conductivity of the wall, $\rho_w$ is the density of the wall, $C_w$ is specific heat of the wall, $\beta$ (0.539) and B (0.338) are constants.

The expression for $U_w$ is based upon the assumption that a relatively high value of $U_w$ correlates with a relatively low value of the thermal inertia $K_w \rho_w C_w$. This has been done in order to directly relate $U_w$ to material properties, the value of $U_w$ is within the range $0 \le U_w \le 1$. That is, $T_w$ cannot be less than $T_a$ or greater than T.

## 7.6 Plume entrainment $M_{fp}$

Fire-induced buoyant plume entrainment is a very important factor in modeling fire growth and smoke spread in a building. Following equations show the results:

$$M_{p,i,j} = 0.21 \left( \frac{\rho_{amb}^{\ 2} g}{C_p T_{amb}} \right)^{(\frac{1}{3})} Q_{c,i,j}^{\ (\frac{1}{3})} z_{i,j}^{\ (\frac{5}{3})} \tag{7-12}$$

$$M_{fp,i,j} = M_{p,i,j} - M_{p,i,j-1} \tag{7-13}$$

Where $\rho_{amb}$ and $T_{amb}$ is the density and temperature of ambient air, $Q_c$ (KW) is the heat release rate, z is height from floor.

## 7.7 Mass flow rate through vertical boundaries $M_h$

Adding the energy conservation equations of all layers and the equation of state, then get the mass conservation equations of each area at each time step, as follows:

$$\sum_{j=1}^{jN} C_p \frac{M_{h,i,j} + \left|M_{h,i,j}\right|}{2} T_{i-1,j} + \sum_{j=1}^{jN} C_p \frac{M_{h,i,j} - \left|M_{h,i,j}\right|}{2} T_{i,j}$$
$$- \sum_{j=1}^{jN} C_p \frac{M_{h,i+1,j} + \left|M_{h,i+1,j}\right|}{2} T_{i,j} - \sum_{j=1}^{jN} C_p \frac{M_{h,i+1,j} - \left|M_{h,i+1,j}\right|}{2} T_{i+1,j} + \sum_{j=1}^{jN} Q_{w,i,j} + \sum_{j=1}^{jN} Q_{c,i,j} = 0 \quad (7\text{-}14)$$

The pressure differences, $P_{i,j}$, are computed simply from the pressure difference at the standard level, $P_{i,0}$, and gravity as:

$$P_{i,j} = P_{i,0} - g\sum_{k=1}^{j} \rho_{i,k} \Delta z \quad (7\text{-}15)$$

Then the velocities of horizontal flow through the boundary from the ith layer to the ( i+1)th layer, $u_{i+1,j}$, are computed by equation (7-16), which is obtained by arranging the equation of Bernoulli.

$$u_{i+1,j} = \begin{pmatrix} \sqrt{\dfrac{2(P_{i,j} - P_{i+1,j} + P_v - F_f)}{\rho_{i+1,j}}}, (P_{i,j} - P_{i+1,j} + P_v - F_f \geq 0) \\ -\sqrt{\dfrac{-2(P_{i,j} - P_{i+1,j} + P_v - F_f)}{\rho_{i,j}}}, (P_{i,j} - P_{i+1,j} + P_v - F_f < 0) \end{pmatrix} \quad (7\text{-}16)$$

Mass flow rate through vertical boundaries $M_{h,i,j}$ is shown by:

$$M_{h,i,j} = \begin{pmatrix} b\Delta z u_{i,j} \rho_{i-1,j}, (u_{i,j} \geq 0) \\ b\Delta z u_{i,j} \rho_{i,j}, (u_{i,j} < 0) \end{pmatrix} \quad (7\text{-}17)$$

$F_f$ is the friction with the walls, the ceilings and the floors, becomes:

$$F_f = \frac{\lambda}{2d} \rho_{i,j} \Delta x u_{i,j} \left|u_{i,j}\right| \frac{A_{w,i,j}}{\sum_{j=1}^{jN} A_{w,i,j}} \quad (7\text{-}18)$$

The dynamic pressure $P_v$ is calculated from the higher velocity of both adjacent boundaries:

$$P_v = \begin{pmatrix} (1/2)\rho_{i,j} {u_{i,j}}^2, (\left|\max(u_{i,j}, 0)\right| \geq \left|\min(u_{i+2,j}, 0)\right|) \\ (1/2)\rho_{i+1,j} {u_{i+2,j}}^2, (\left|\max(u_{i,j}, 0)\right| < \left|\min(u_{i+2,j}, 0)\right|) \end{pmatrix} \quad (7\text{-}19)$$

There are many loops to implementation the computation of the mass flow rate through the vertical boundaries, so just discuss the method to let these loops work.

1. Firstly, at the very beginning stage, the temperature in every control volume in the tunnel is in the ambient condition, just equal to 293K, and for the boundary velocity (no ventilation), just equal to 0 m/s, but after a small time step (0.1 s), some convective heat release rate and convection heat transfer to wall will let equation (7-14) unbalance, so the velocity in every area and every layer boundary according to this unbalance value need be changed, in every layer jut change the same value, in changing the velocity loop, the velocity will become steady, and the equation (7-14) is almost equal to 0, then shift to the next loop to compute the pressure.

2. Secondly, according to the steady velocity, the relative steady pressure under this velocity using equation (7-16) with Gauss-Seidel model can be found, due to change the velocity the same value in each layer before, the pressure calculate here is just a steady value, not the truly value at this time because it will not follow the density and gravity integration law (equation 7-15), so the pressure need to be changed: using the lowest control volume position pressure in the tunnel to compute the whole pressure in the tunnel at this time by using equation (7-15), then call this new pressure distribution $P_1$, then using the highest control volume position pressure in the tunnel to compute the whole pressure in the tunnel at this time by using equation (7-15), and call this new pressure distribution $P_2$, then the average value of $P_1$ and $P_2$ will the pressure need to start in the next loop.

3. Thirdly, according to the average pressure value which just computed before, by using Gauss-Seidel model again with equation (7-16), the steady velocity at this pressure distribution can be got, then this velocity distribution will not fulfill the equation (7-14), so return to step 1 again, then during some loops, the pressure and velocity are close to the real one in one time step.

After finish these loops the velocity distribution can be got at this time step , then continue the computation of the rest rate terms just shows below and finish calculating the temperature at this time step finally shift to the next time step will discuss later.

## 7.8 Horizontal enthalpy flow rate $H_h$

Horizontal enthalpy flow rate $H_{h,i,j}$ is shown by:

$$H_{h,i,j} = \begin{pmatrix} C_p M_{h,i,j} T_{i-1,j}, (M_{h,i,j} \geq 0) \\ C_p M_{h,i,j} T_{i,j}, (M_{h,i,j} < 0) \end{pmatrix} \tag{7-20}$$

## 7.9 Vertical enthalpy flow rate $H_v$

The enthalpy flow rate through the surface of the top layer to the lower layer outside of the fire plume is shows as:

$$\begin{aligned} H_{v,i,jN} = & -C_p M_{fp,i,jN} T_{i,jN} + \frac{(\mathrm{H}_{h,i,jN} + |\mathrm{H}_{h,i,jN}|)}{2} - \frac{(|\mathrm{H}_{h,i,jN}| - \mathrm{H}_{h,i,jN})}{2} \\ & + \frac{(|\mathrm{H}_{h,i+1,jN}| - \mathrm{H}_{h,i+1,jN})}{2} - \frac{(|\mathrm{H}_{h,i+1,jN}| + \mathrm{H}_{h,i+1,jN})}{2} - Q_{w,i,jN} + Q_{c,i,jN} \end{aligned} \tag{7-21}$$

The enthalpy flow rate through the interface of the (i+1)th and the ith layer is calculated layer by layer, using the enthalpy flow rate through the upper surface as follows:

$$\begin{aligned} H_{v,i,j} = & -C_p M_{fp,i,j} T_{i,j} + \frac{(\mathrm{H}_{h,i,j} + |\mathrm{H}_{h,i,j}|)}{2} - \frac{(|\mathrm{H}_{h,i,j}| - \mathrm{H}_{h,i,j})}{2} \\ & + \frac{(|\mathrm{H}_{h,i+1,j}| - \mathrm{H}_{h,i+1,j})}{2} - \frac{(|\mathrm{H}_{h,i+1,j}| + \mathrm{H}_{h,i+1,j})}{2} - Q_{w,i,j} + Q_{c,i,j} + H_{v,i,j+1} \end{aligned} \tag{7-22}$$

## 7.10 Mass flow rate through horizontal boundaries $M_v$

Vertical mass flow rate $M_{v,i,j}$ is shown by:

$$M_{v,i,j} = \begin{pmatrix} \frac{H_{v,i,j}}{C_p T_{i,j}}, (H_{v,i,j} \geq 0) \\ \frac{H_{v,i,j}}{C_p T_{i,j-1}}, (H_{v,i,j} < 0) \end{pmatrix} \tag{7-23}$$

## 7.11 Ventilation control

Changing ventilation condition is just changing the ambient velocity condition at boundaries, and ventilation changing with time is implement by adding a new velocity matrix to the old one in different time, the process will be shown in the appendix MATLAB script. And the result will be shown in the Chapter 8- Results Analysis.

## 7.12 Temperature computation

Equation (7-7):

$$\frac{dT_{i,j}}{dt} = \frac{1}{C_p \rho_{i,j} V_{i,j}} \times [(H_{v,i,j+1} - C_p M_{v,i,j+1} T_{i,j}) - (H_{v,i,j} - C_p M_{v,i,j} T_{i,j}) + (H_{h,i,j} - C_p M_{h,i,j} T_{i,j}) - (H_{h,i+1,j} - C_p M_{h,i+1,j} T_{i,j}) - Q_{w,i,j} + \varphi_i F_r Q_{c,i,j}]$$

Equation (7-8):

$$\frac{dT_{i,jN}}{dt} = \frac{1}{C_p \rho_{i,jN} V_{i,jN}} \times [(C_p \sum_{j=1}^{jN-1} M_{fp,i,j} T_{i,j} - C_p T_{i,jN} \sum_{j=1}^{jN-1} M_{fp,i,j}) - (H_{v,i,jN} - C_p M_{v,i,jN} T_{i,jN}) + (H_{h,i,jN} - C_p M_{h,i,jN} T_{i,jN}) - (H_{h,i+1,jN} - C_p M_{h,i+1,jN} T_{i,jN}) - Q_{w,i,jN} + (1 - F_r) Q_{c,i,jN}]$$

They are the governing equation of temperature, according to the equation, the temperature at every control volume at any time can be computed through assume a small time step (0.1 s), at the same time, the rate terms in the equations have already be understood before, so now what should do is just assume the temperature and the velocity is in the ambient condition at Time=0, after a small time step (0.1 s), a new temperature at every control volume in the tunnel can be got by using the method which just mention before, then this temperature is a new start point to calculate the next time step temperature, finally, the temperature distribution at the ending time can be computed. Different results are related to the inputting convective heat release rate data, the ventilation condition, and the weight of the burning fuel and the diameter of the mass container pan. There are 4 tests repeated in the experiment which mentioned before, and for the numerical computation, all initial condition should be consistence with the experiment condition, then by comparing the results, the parametric analysis can be achieved.

## 7.13 Software organization

The computation flow diagram of the MATLAB script is illustrated in Fig. 7-8. Firstly input the boundary conditions and initial state in the tunnel, after a small time step, a new temperature at every control volume in the tunnel can be got by solving the governing equations, and this temperature is a new start in the whole computation loop.

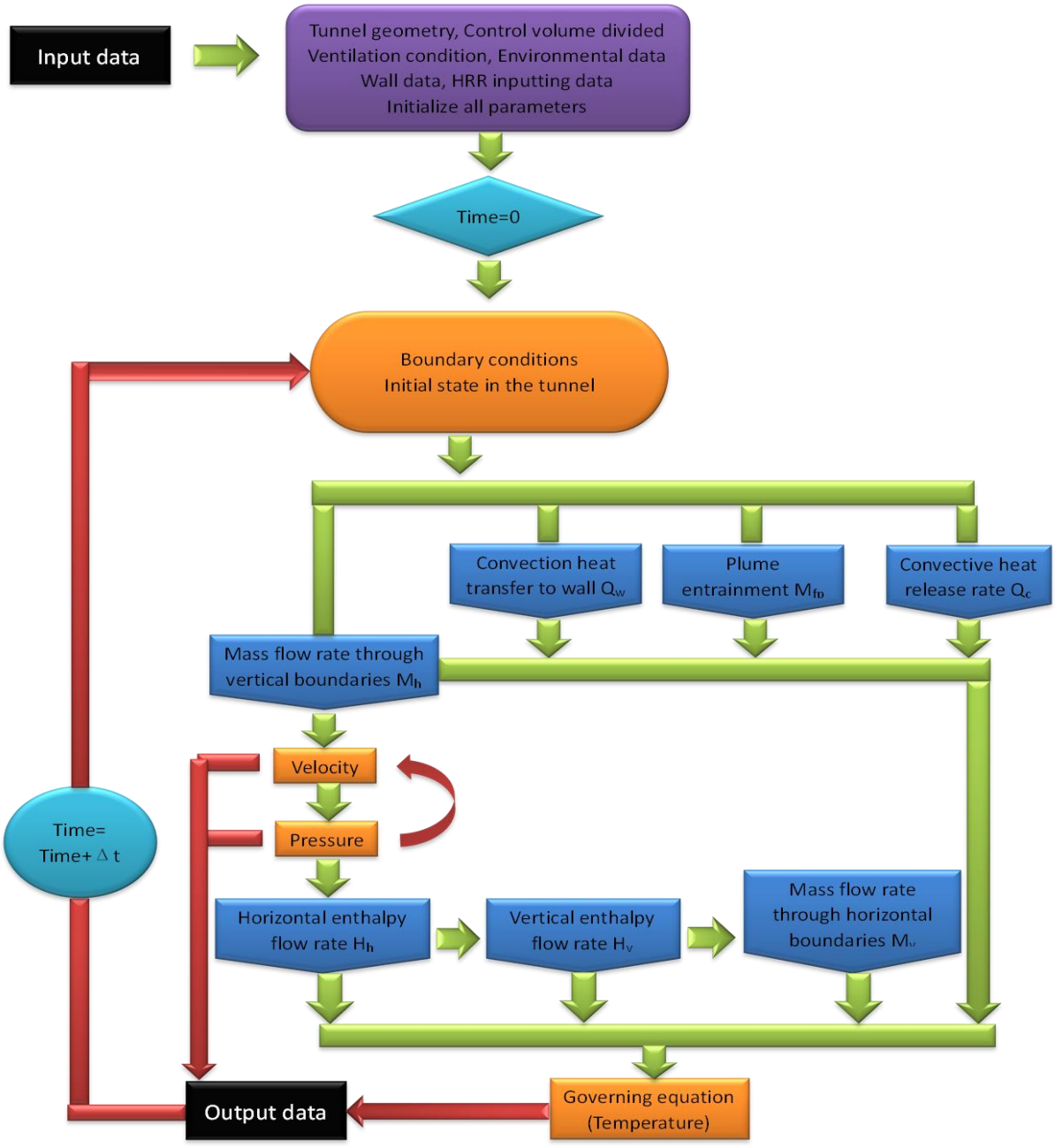


Fig 7-8 Computation flow diagram in MATLAB script

## 7.14 Modeling results

There are two different kinds of results; the first one is to provide the program with actual heat release rate ($Q_c$) curve produced by experimental test. The second is to provide the program with the theoretical heat release curve without fluctuation of HRR values and check the result.

### 7.14.1 First test results

The first test is modeled using a 26 cm diameter stainless steel pan filled with a quantity of diesel fuel (1400 gram) and the test was performed in non-ventilation condition.

**Actual heat release rate**

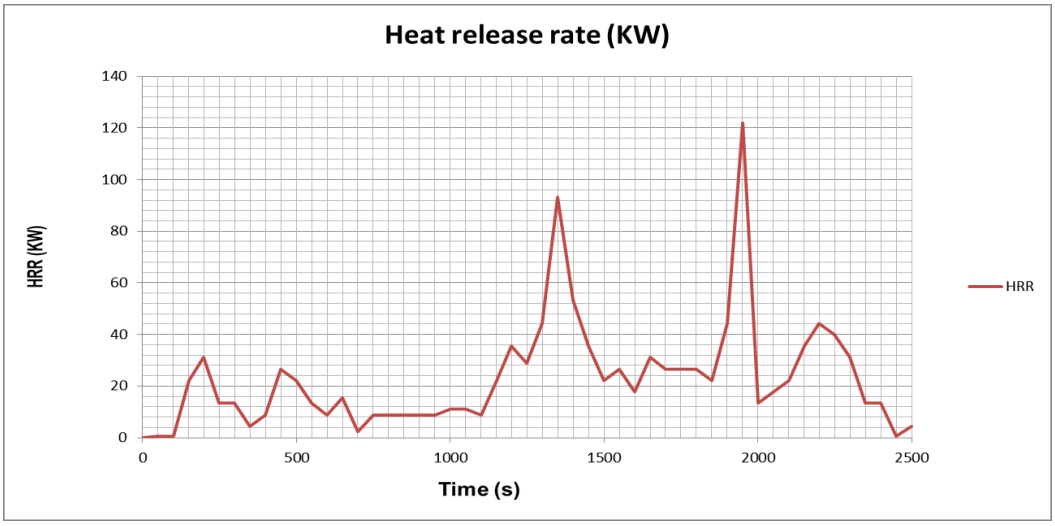


Fig 7-9 Actual heat release rate of first test

**Theoretical heat release rate**

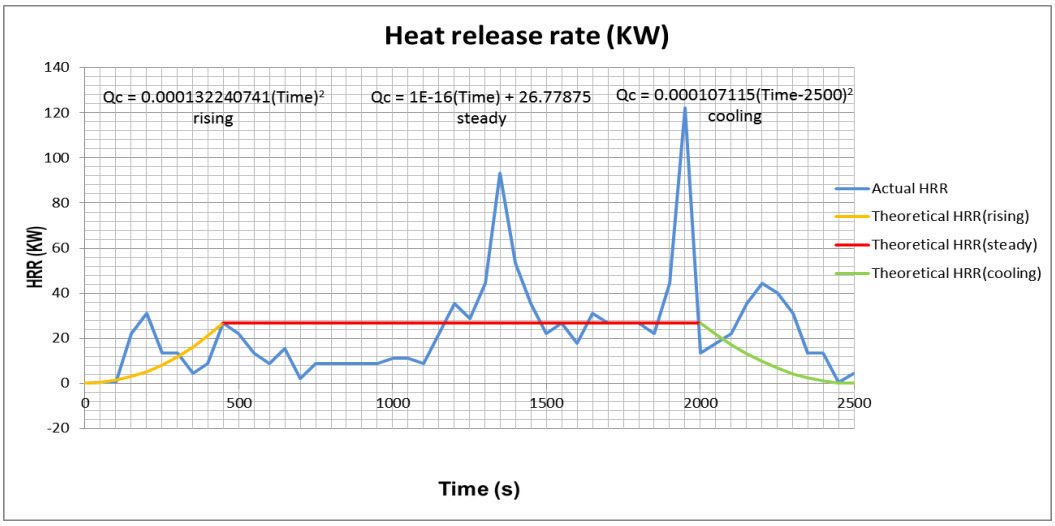


Fig 7-10 Theoretical heat release rate of first test

**Temperature distribution (Actual $Q_c$):**

All temperature distribution change with time are monitored by the program and shown in the following figure (Fig 7-11):

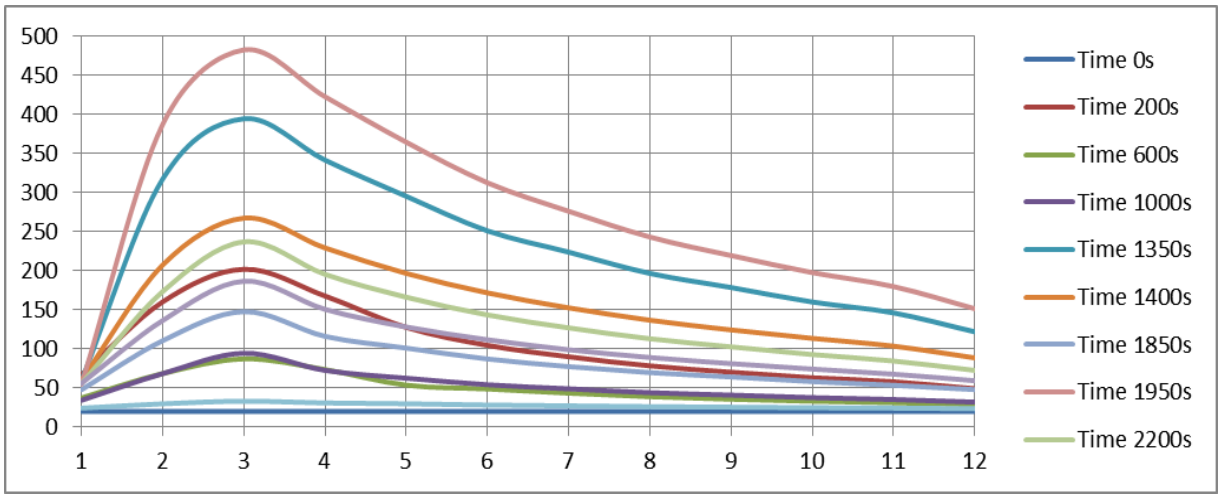


Fig 7-11 Temperature (℃) changes with tube length (m) during the first modeled stages

Temperature monitoring in each segment separately shows in following figure (Fig 7-12)

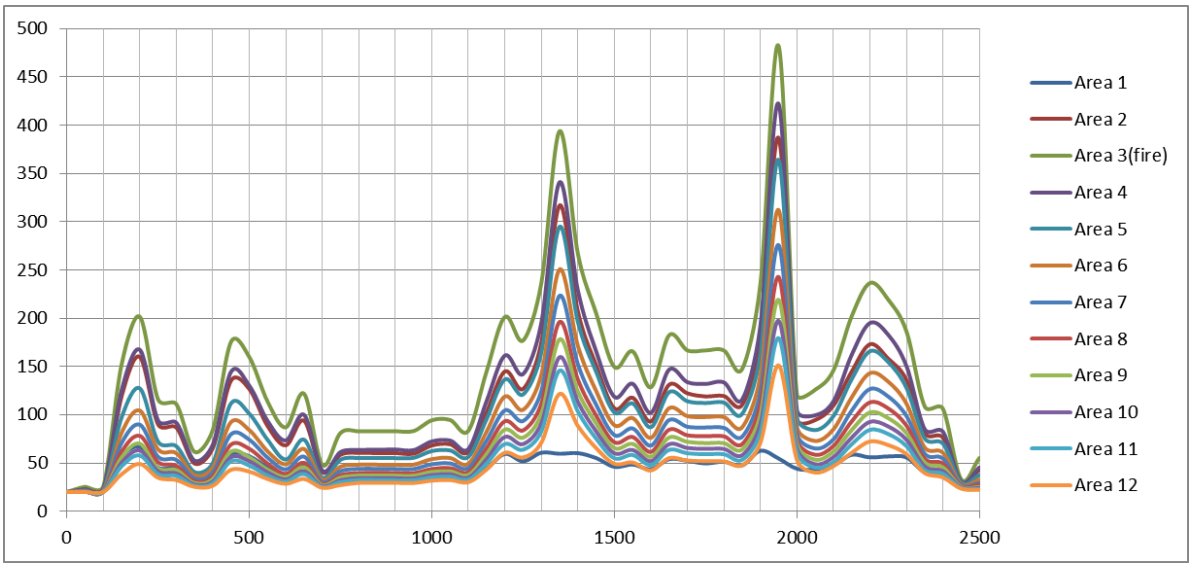


Fig 7-12 Temperature(℃) monitoring in each segment separately during different time(s)

Regarding the temperature (℃) distribution along change of levels, they are monitored by trees in different stations in tube and shown in the next figures (**Actual $Q_c$**): (Fig 7-13 – Fig 7-15):

**Tree at segment 5**

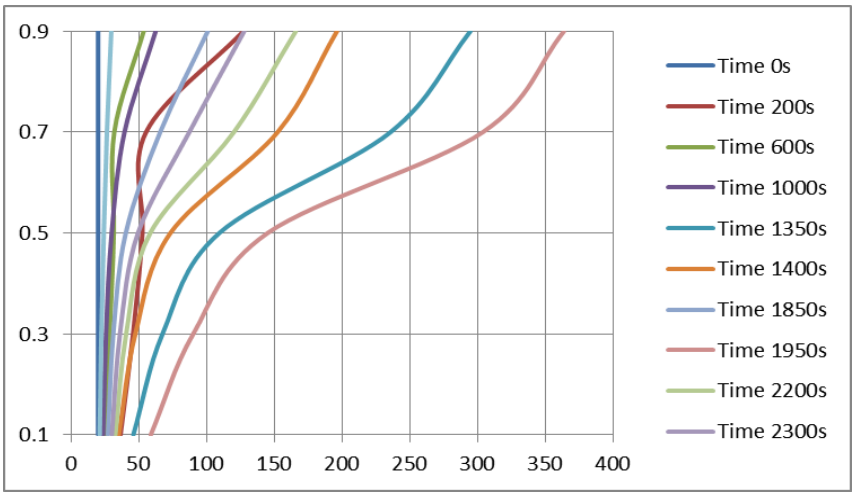


Fig 7-13 Temperature (℃) changes with tube level (m) according to different time stages in segment 5

**Tree at segment 7**

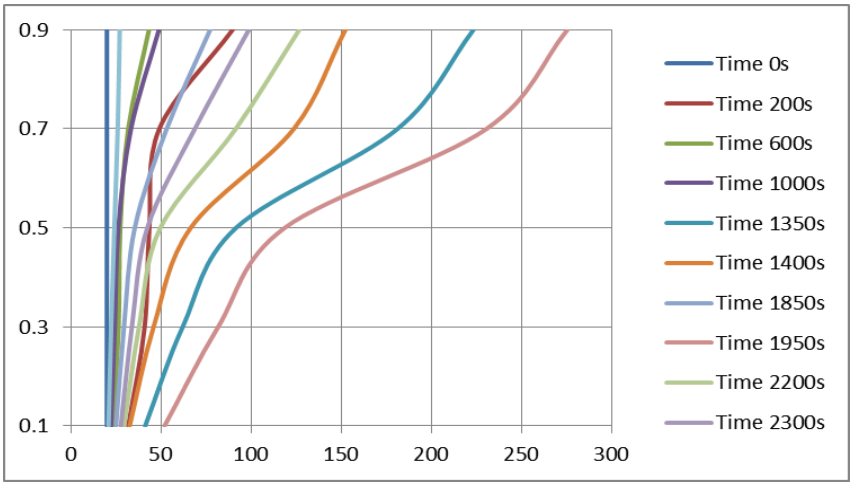


Fig 7-14 Temperature (℃) changes with tube level (m) according to different time stages in segment 7

**Tree at segment 11**

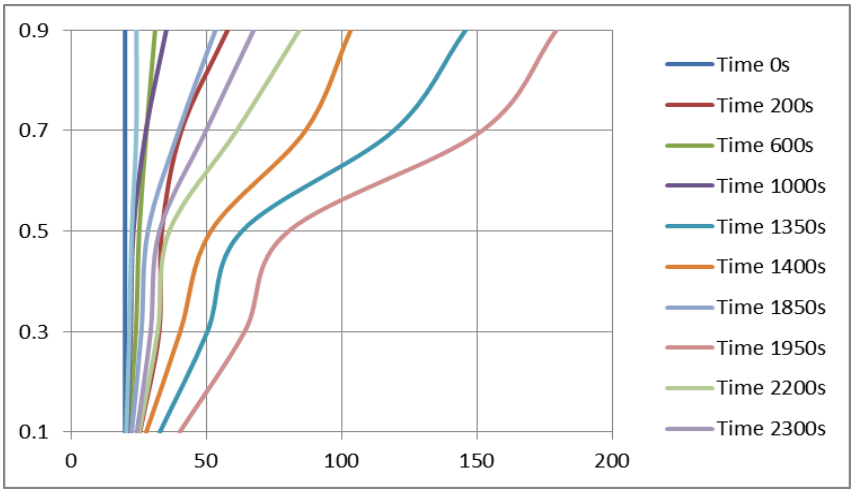


Fig 7-15 Temperature (℃) changes with tube level (m) according to different time stages in segment 11

**Temperature distribution (Theoretical $Q_c$):**

All temperature distribution change with time are monitored by the program and shown in the following figure (Fig 7-16):

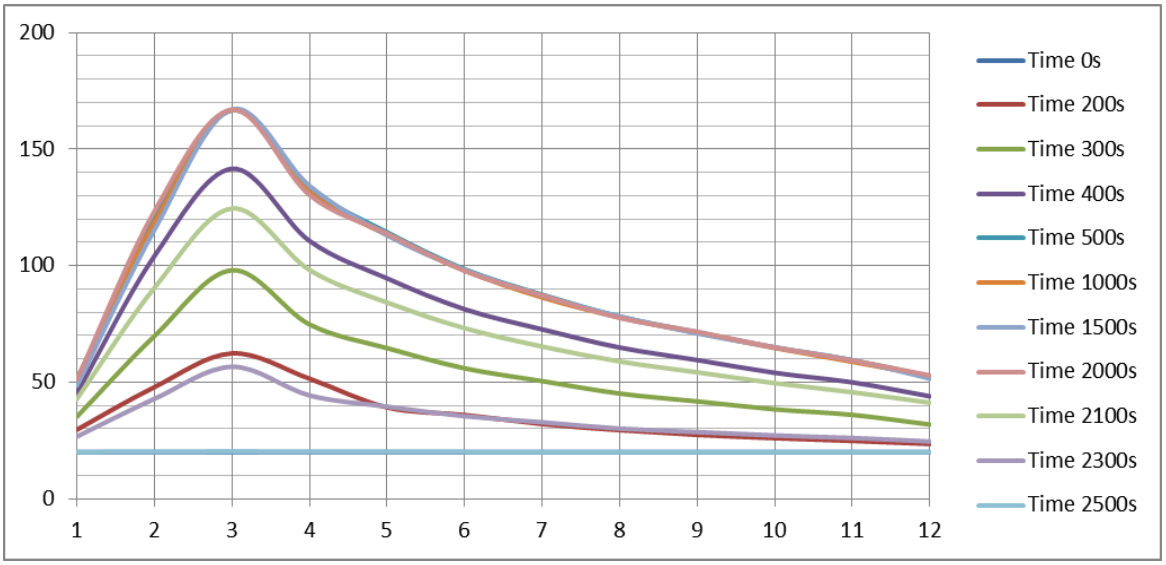


Fig 7-16 Temperature (℃) changes with tube length (m) during the first modeled stages

Temperature monitoring in each segment separately shows in following figure (Fig 7-16)

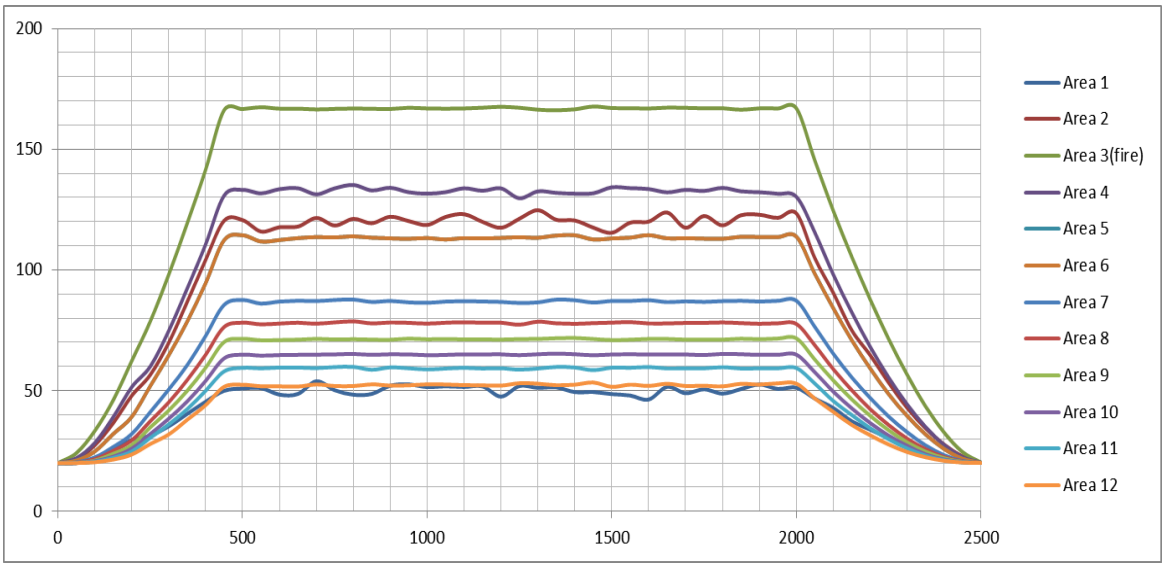


Fig 7-17 Temperature(℃) monitoring in each segment separately during different time(s)

Regarding the temperature distribution along change of levels, they are monitored by trees in different stations in tube and shown in the next figures (**Theoretical $Q_c$**): (Fig 7-18– Fig 7-20):

**Tree at segment 5**

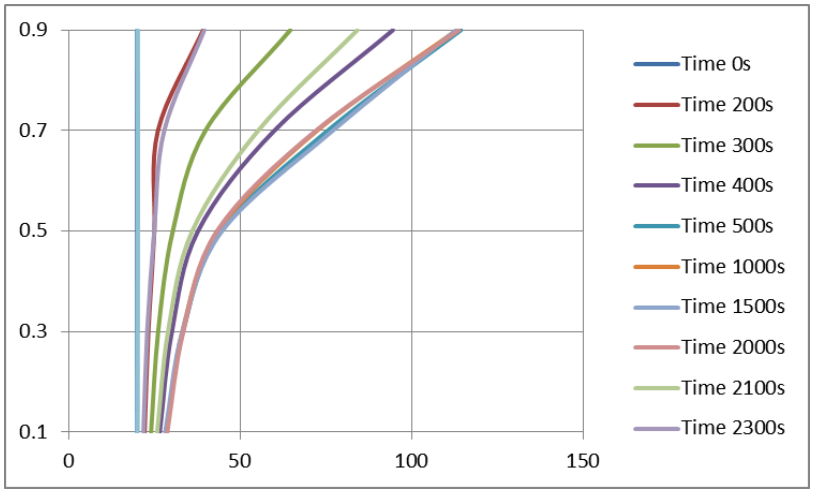


Fig 7-18 Temperature (℃) changes with tube level (m) according to different time stages in segment 5

**Tree at segment 7**

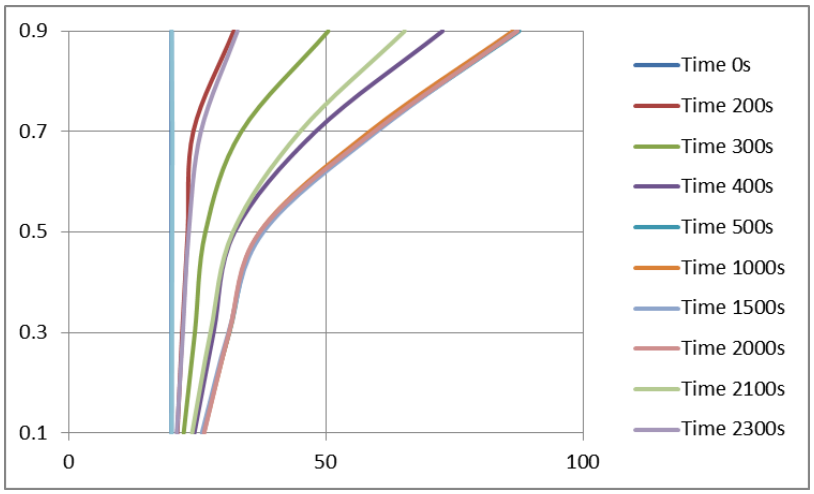


Fig 7-19 Temperature (℃) changes with tube level (m) according to different time stages in segment 7

**Tree at segment 11**

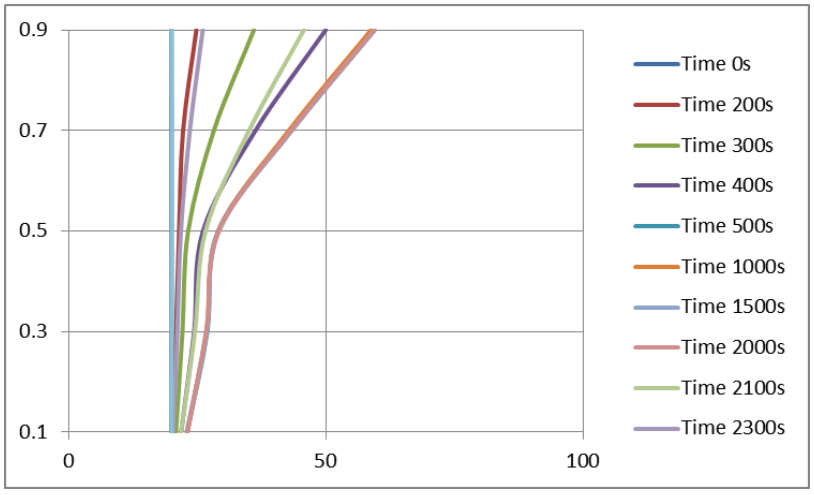


Fig 7-20 Temperature (℃) changes with tube level (m) according to different time stages in segment 11

### 7.14.2 Second test results

The second test is performed using a 26 cm diameter stainless steel pan filled with a quantity of diesel fuel (700 gram) and the test was performed in non-ventilation condition.

**Actual heat release rate**

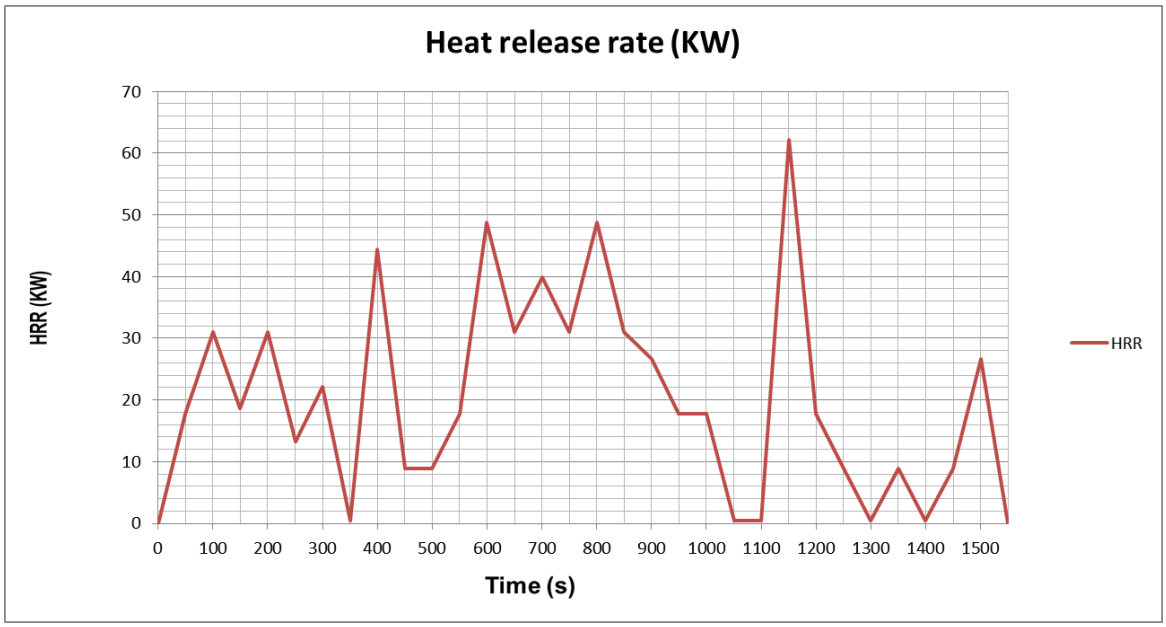


Fig 7-21 Actual heat release rate of second test

**Theoretical heat release rate**

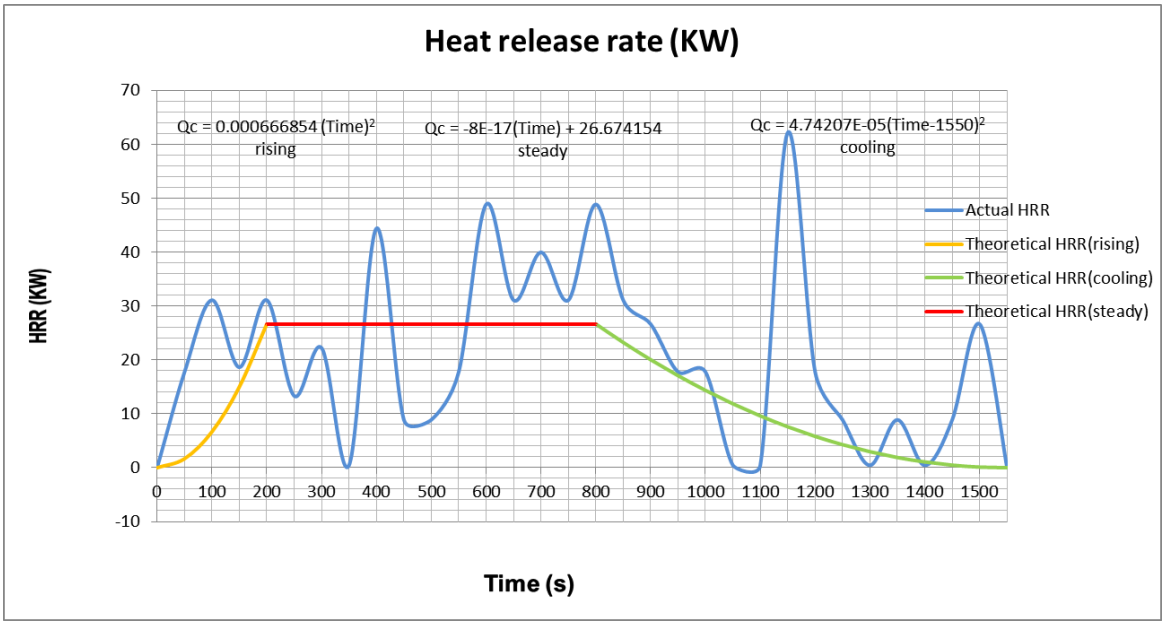


Fig 7-22 Theoretical heat release rate of second test

**Temperature distribution (Actual $Q_c$):**

All temperature distribution change with time are monitored by the program and shown in the following figure (Fig 7-23):

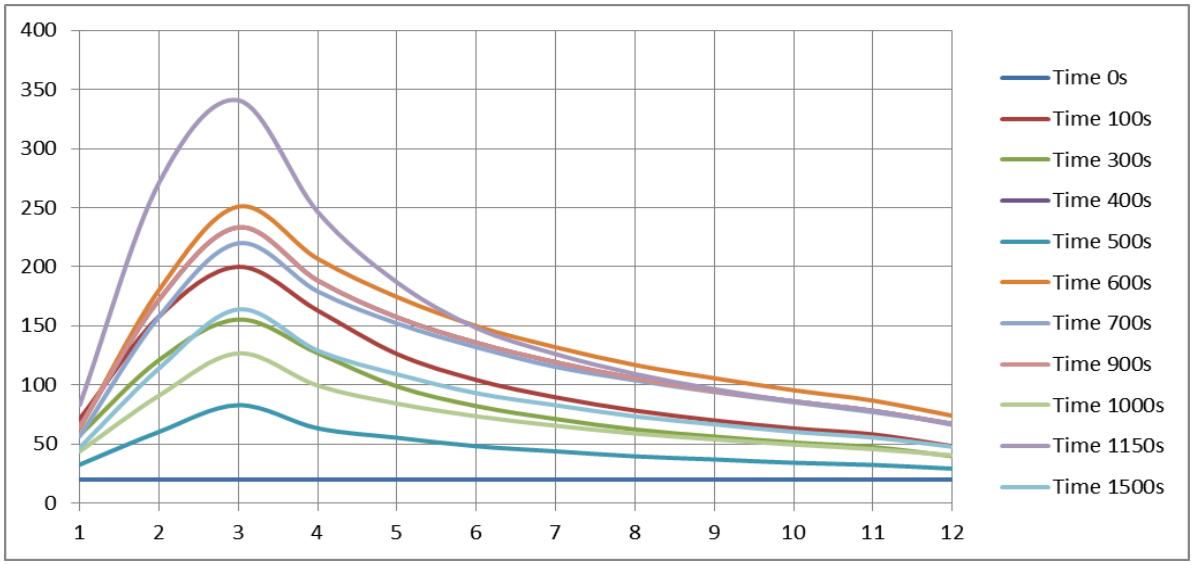


Fig 7-23 Temperature (℃) changes with tube length (m) during the second modeled stages

Temperature monitoring in each segment separately shows in following figure (Fig 7-24)

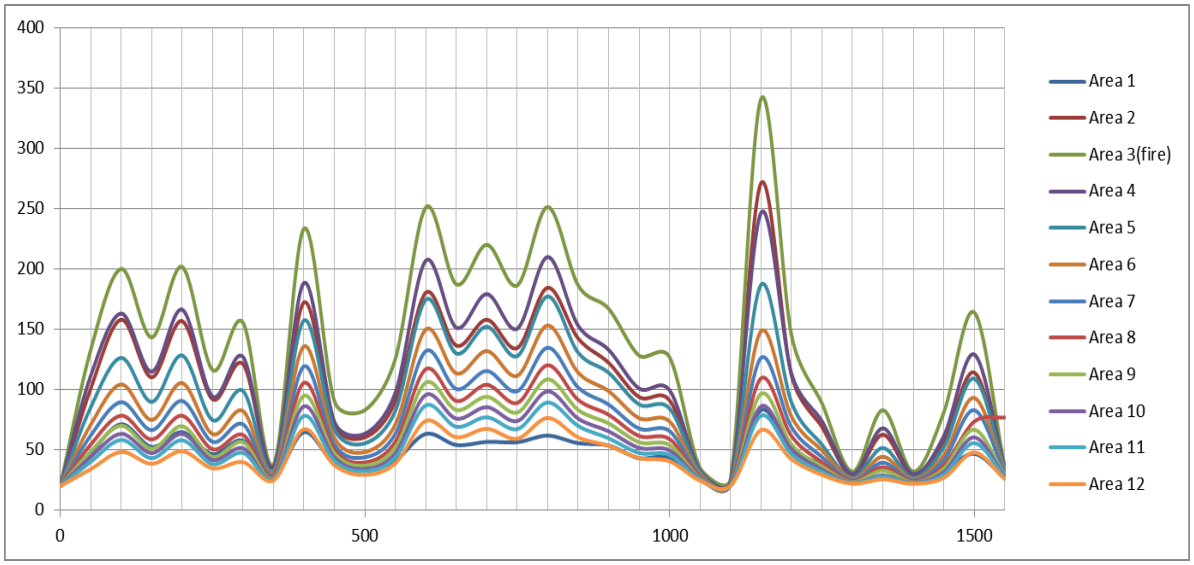


Fig 7-24 Temperature(℃) monitoring in each segment separately during different time(s)

Regarding the temperature distribution along change of levels, they are monitored by trees in different stations in tube and shown in the next figures (**Actual $Q_c$**): (Fig 7-25 – Fig 7-27):

**Tree at segment 5**

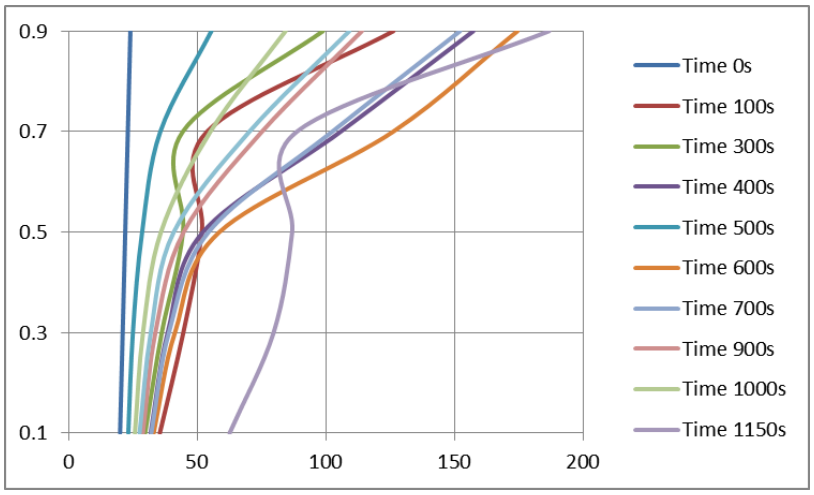


Fig 7-25 Temperature (℃) changes with tube level (m) according to different time stages in segment 5

**Tree at segment 7**

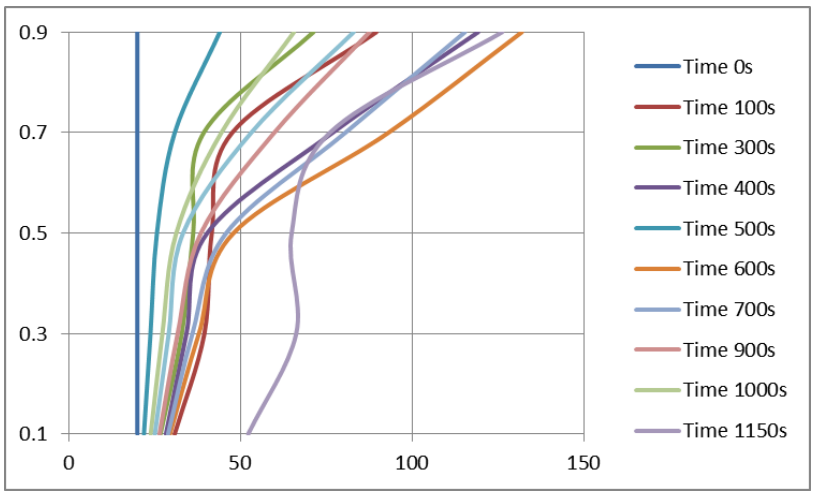


Fig 7-26 Temperature (℃) changes with tube level (m) according to different time stages in segment 7

**Tree at segment 11**

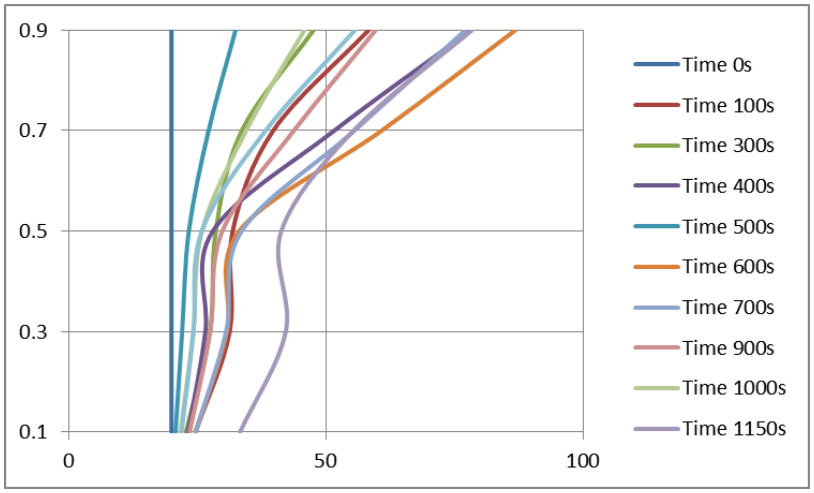


Fig 7-27 Temperature (℃) changes with tube level (m) according to different time stages in segment 11

**Temperature distribution (Theoretical $Q_c$):**

All temperature distribution change with time are monitored by the program and shown in the following figure (Fig 7-28):

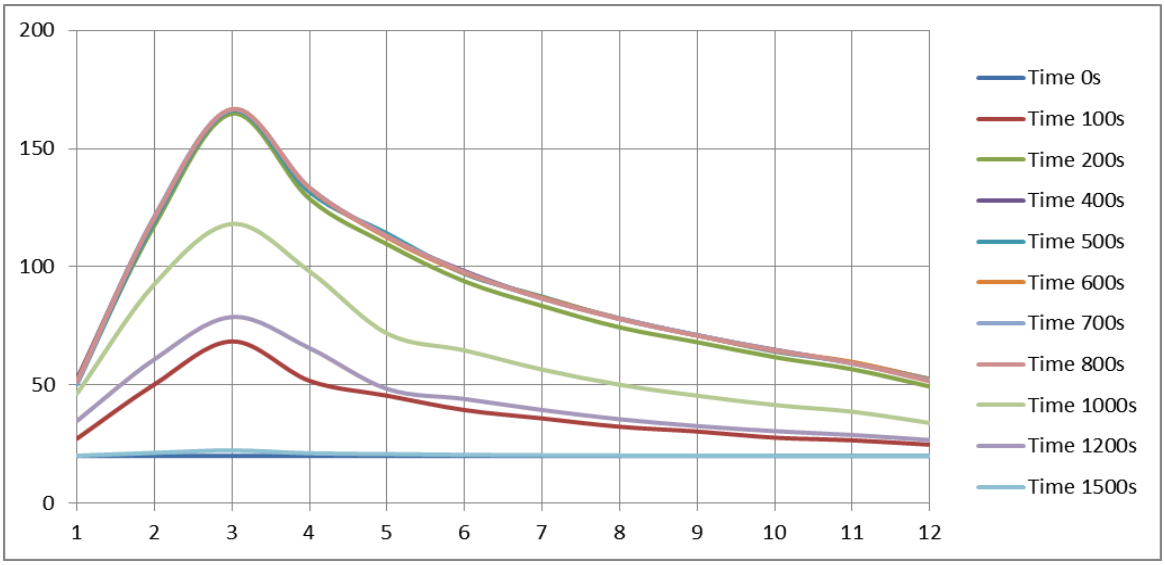


Fig 7-28 Temperature (℃) changes with tube length (m) during the second modeled stages

Temperature monitoring in each segment separately shows in following figure (Fig 7-29)

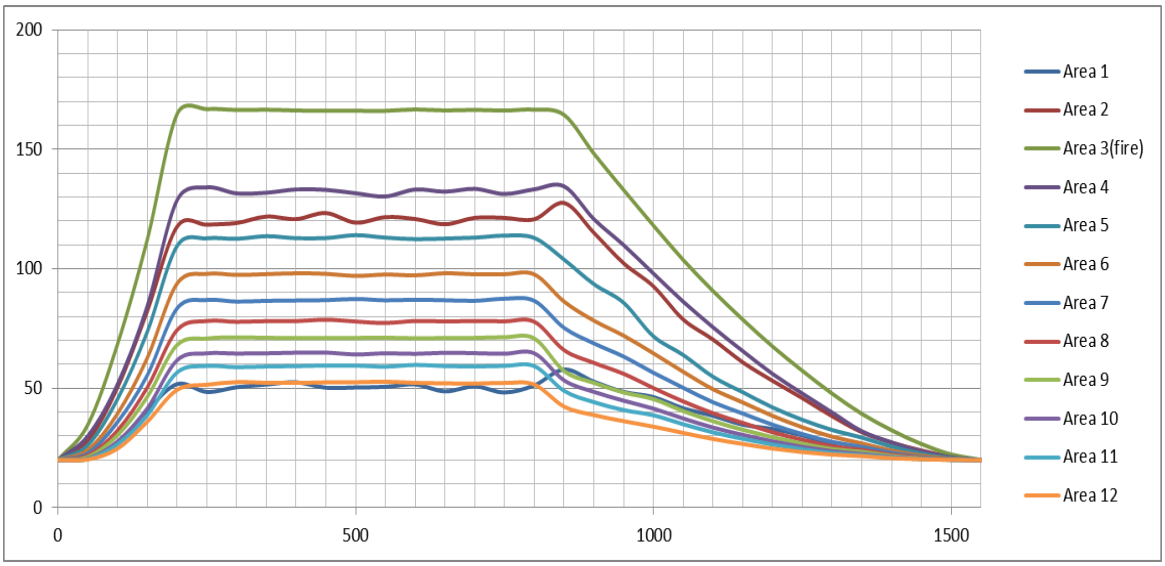


Fig 7-29 Temperature(℃) monitoring in each segment separately during different time(s)

Regarding the temperature distribution along change of levels, they are monitored by trees in different stations in tube and shown in the next figures (**Theoretical $Q_c$**): (Fig 7-30– Fig 7-32):

**Tree at segment 5**

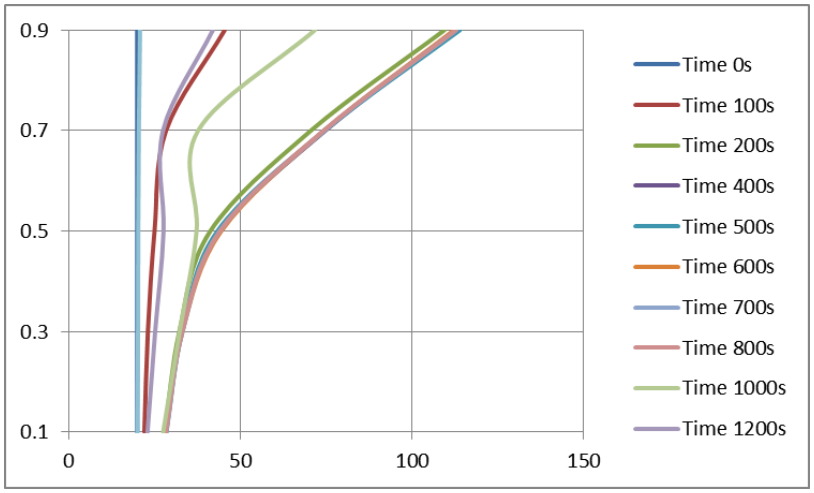


Fig 7-30 Temperature (℃) changes with tube level (m) according to different time stages in segment 5

**Tree at segment 7**

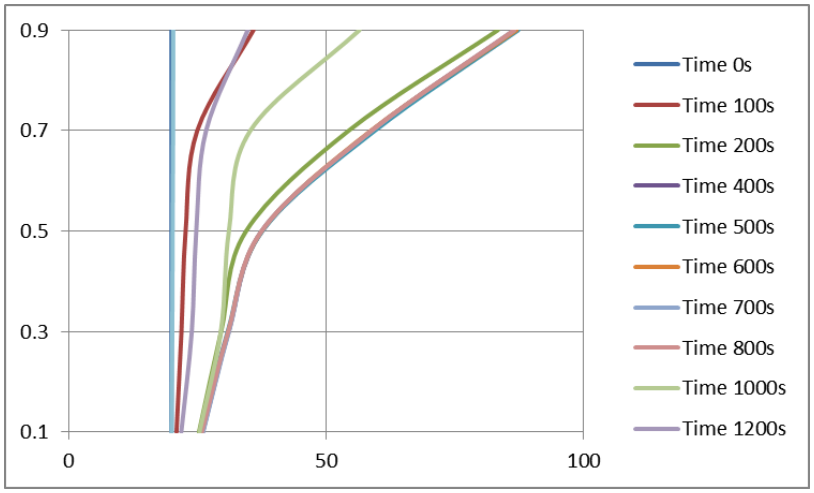


Fig 7-31 Temperature (℃) changes with tube level (m) according to different time stages in segment 7

**Tree at segment 11**

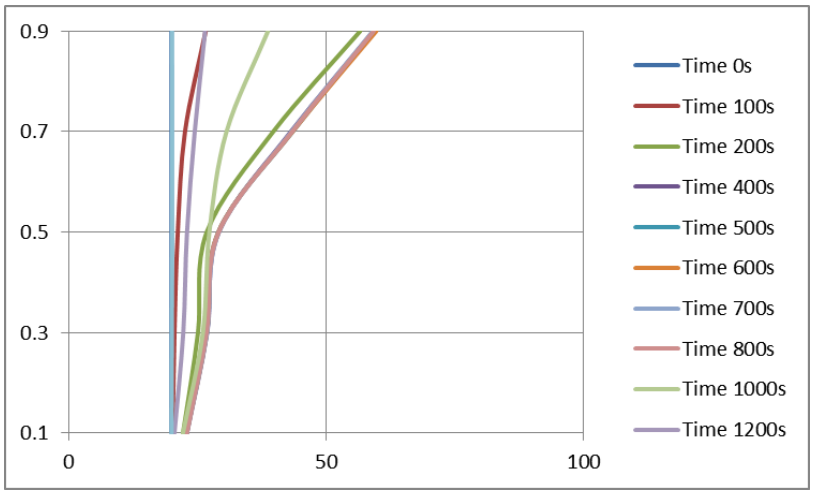


Fig 7-32 Temperature (℃) changes with tube level (m) according to different time stages in segment 11

### 7.14.3 Third test results

The third test is performed using a 26 cm diameter stainless steel pan filled with a quantity of diesel fuel (900 gram) and the ventilation started at the 2 minute of testing time with a value of more than 2.5m/s.

**Actual heat release rate**

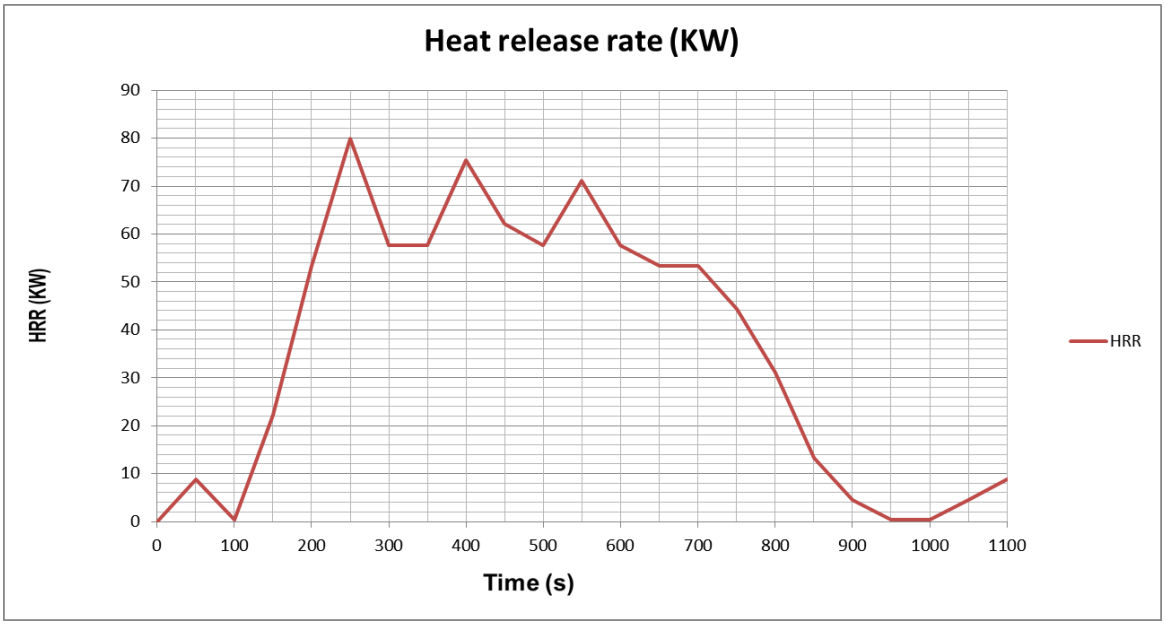


Fig 7-33 Actual heat release rate of third test

**Theoretical heat release rate**

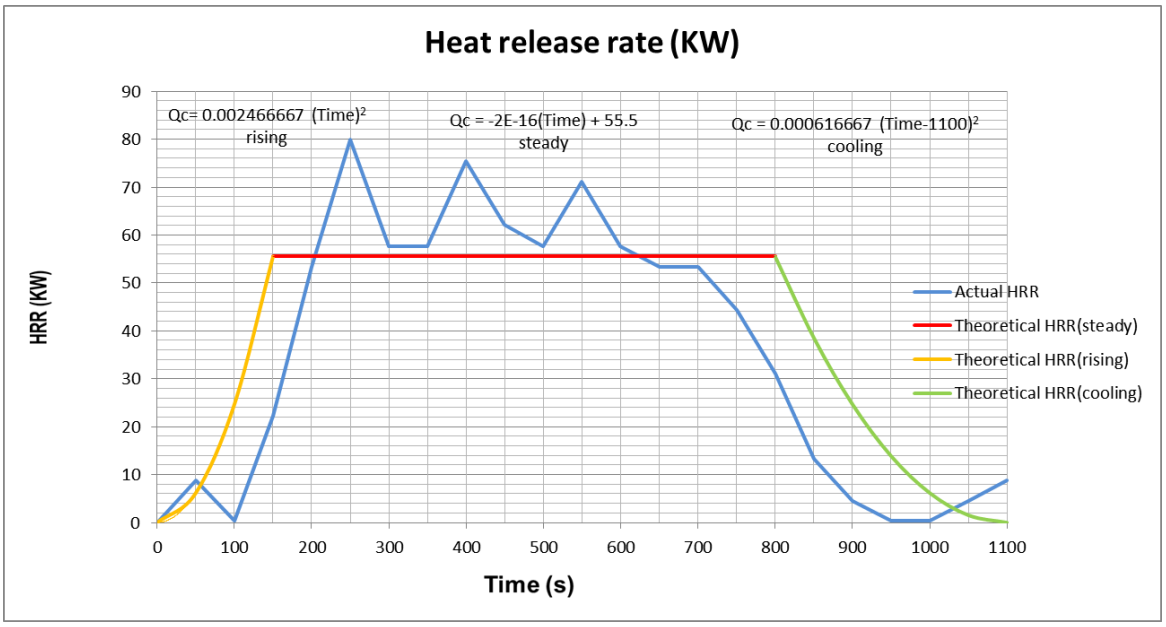


Fig 7-34 Theoretical heat release rate of third test

**Temperature distribution (Actual $Q_c$):**

All temperature distribution change with time are monitored by the program and shown in the following figure (Fig 7-35):

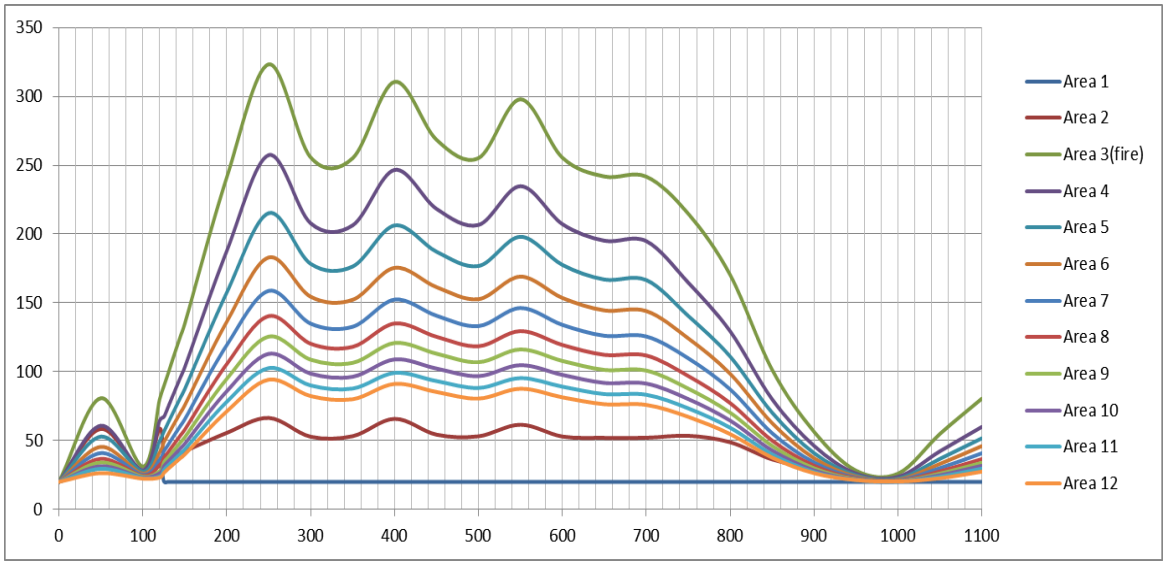


Fig 7-35 Temperature (℃) changes with tube length (m) during the third modeled stages

Temperature monitoring in each segment separately shows in following figure (Fig 7-36)

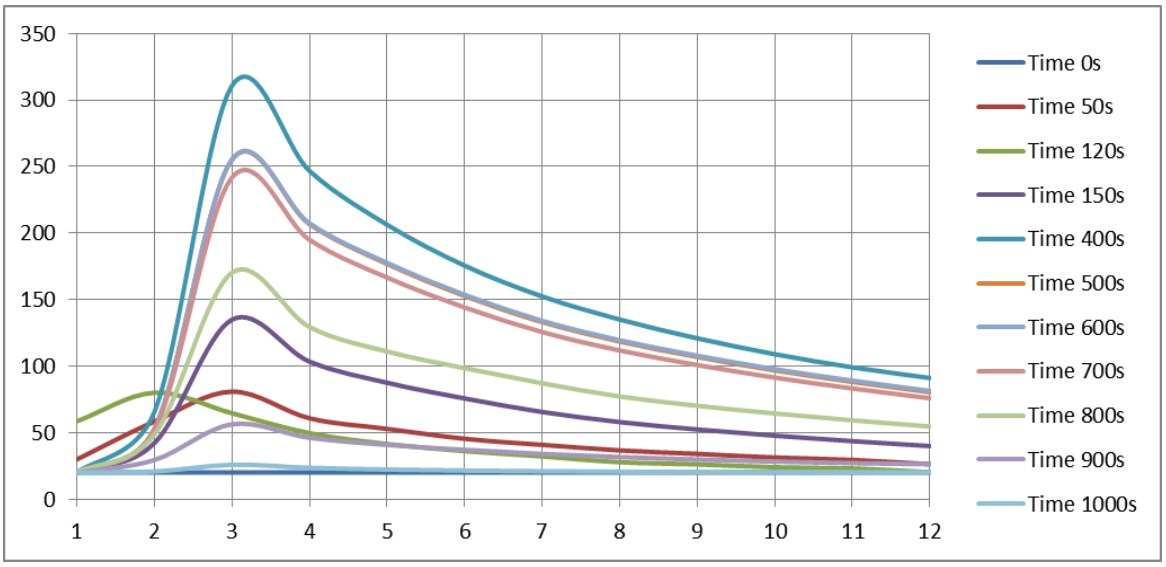


Fig 7-36 Temperature(℃) monitoring in each segment separately during different time(s)

Regarding the temperature distribution along change of levels, they are monitored by trees in different stations in tube and shown in the next figures (**Actual $Q_c$**): (Fig 7-37 – Fig 7-39):

**Tree at segment 5**

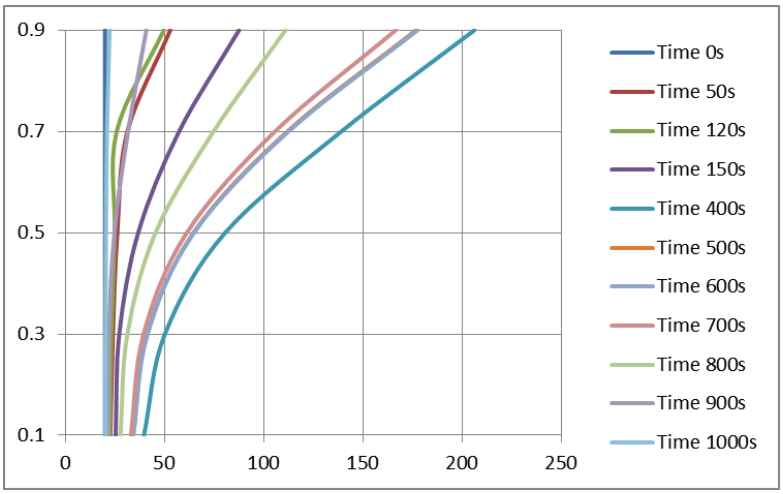


Fig 7-37 Temperature (℃) changes with tube level (m) according to different time stages in segment 5

**Tree at segment 7**

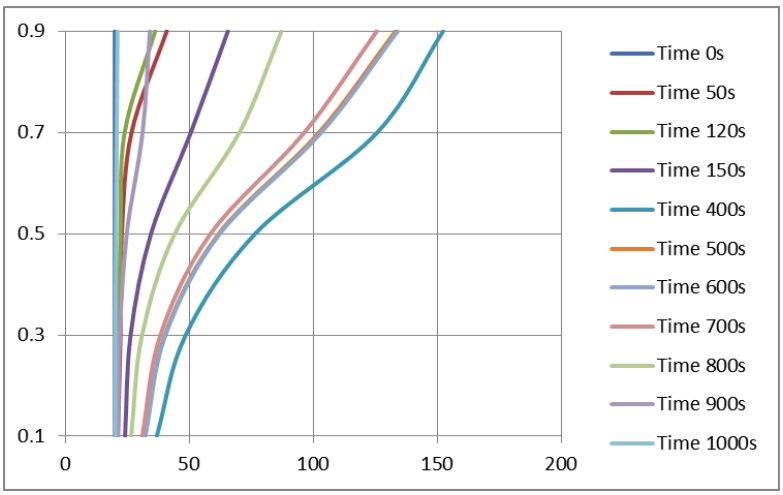


Fig 7-38 Temperature (℃) changes with tube level (m) according to different time stages in segment 7

**Tree at segment 11**

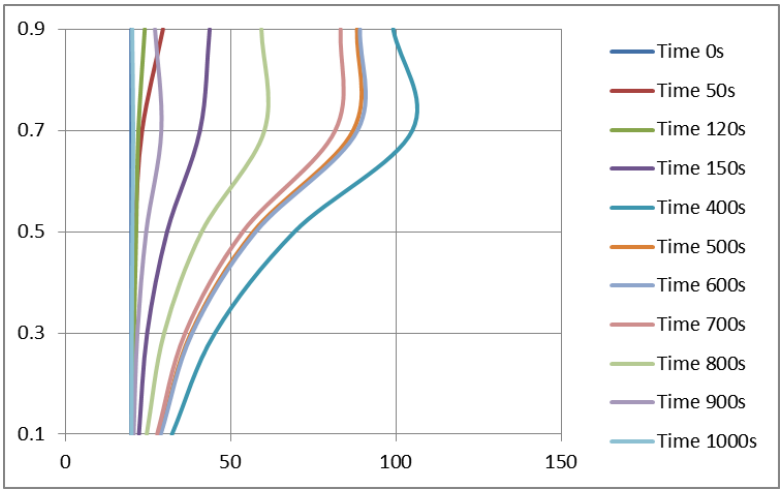


Fig 7-39 Temperature (℃) changes with tube level (m) according to different time stages in segment 11

**Temperature distribution (Theoretical $Q_c$):**

All temperature distribution change with time are monitored by the program and shown in the following figure (Fig 7-40):

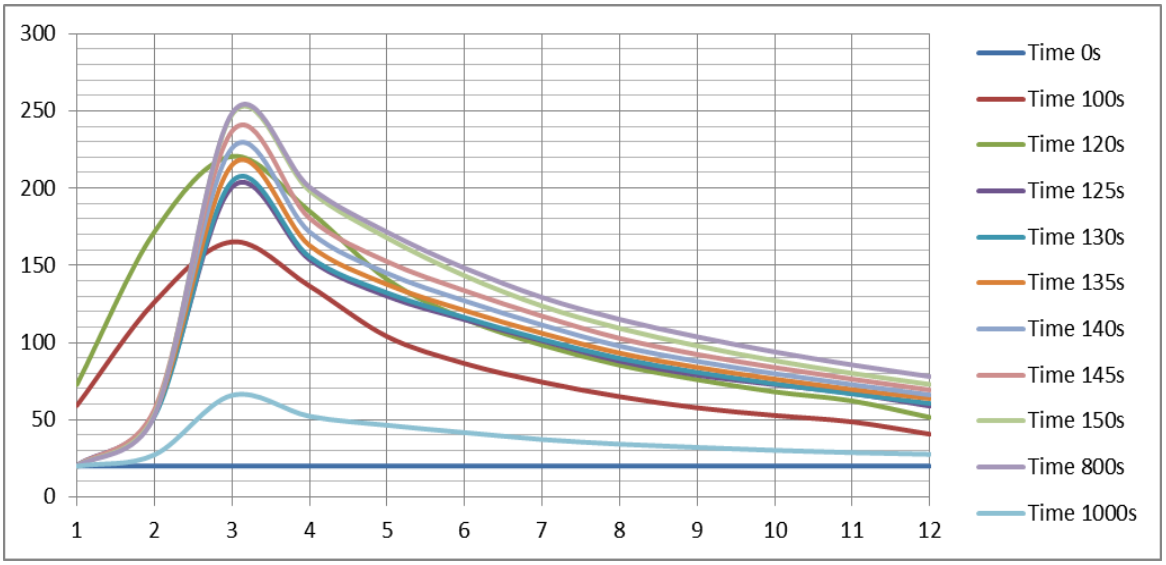


Fig 7-40 Temperature (℃) changes with tube length (m) during the third modeled stages

Temperature monitoring in each segment separately shows in following figure (Fig 7-41)

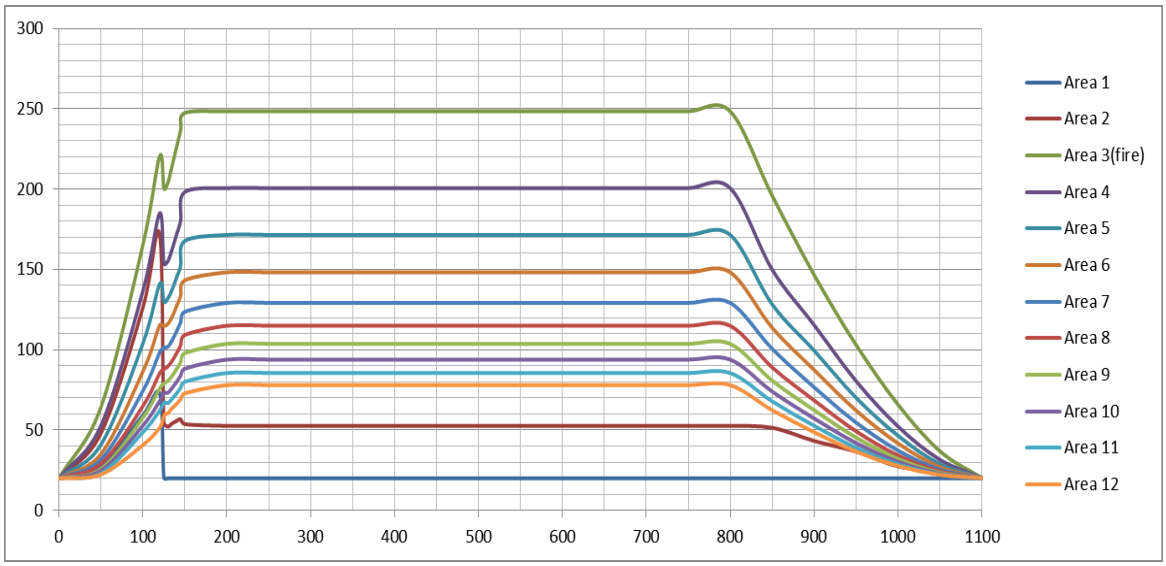


Fig 7-41 Temperature(℃) monitoring in each segment separately during different time(s)

Regarding the temperature distribution along change of levels, they are monitored by trees in different stations in tube and shown in the next figures (**Theoretical $Q_c$**): (Fig 7-41– Fig 7-43):

**Tree at segment 5**

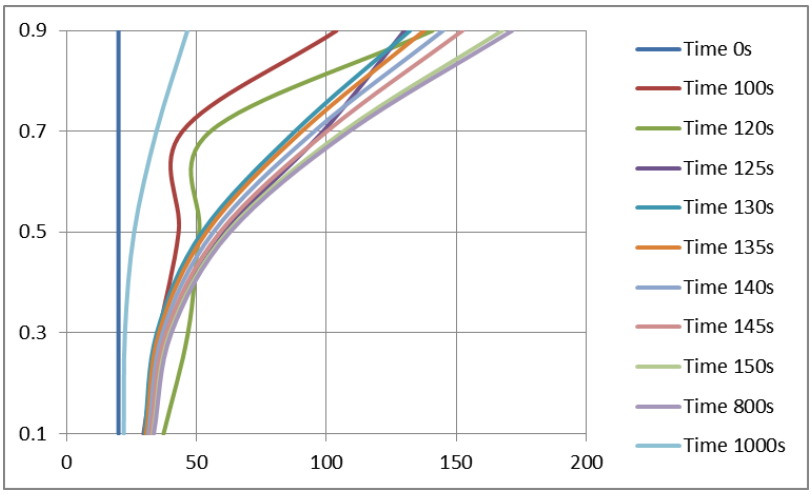


Fig 7-41 Temperature (℃) changes with tube level (m) according to different time stages in segment 5

**Tree at segment 7**

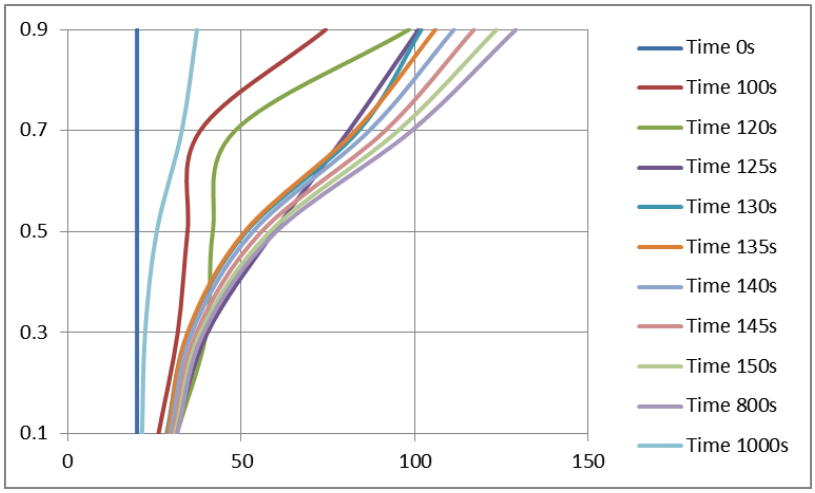


Fig 7-42 Temperature (℃) changes with tube level (m) according to different time stages in segment 7

**Tree at segment 11**

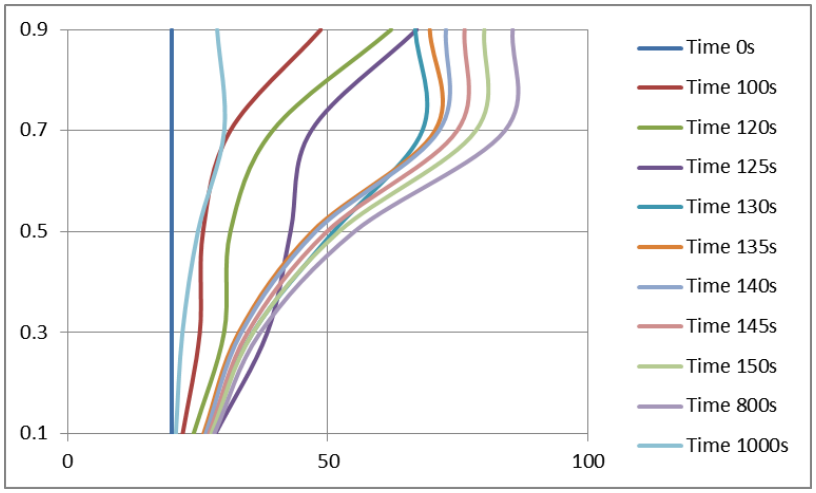


Fig 7-43 Temperature (℃) changes with tube level (m) according to different time stages in segment 11

### 7.14.4 Fourth test results

The fourth test is performed using a 18 cm diameter stainless steel pan filled with a quantity of diesel fuel (790 gram) and the ventilation started at the 30 minute of testing time with a value of 2.5m/s

**Actual heat release rate**

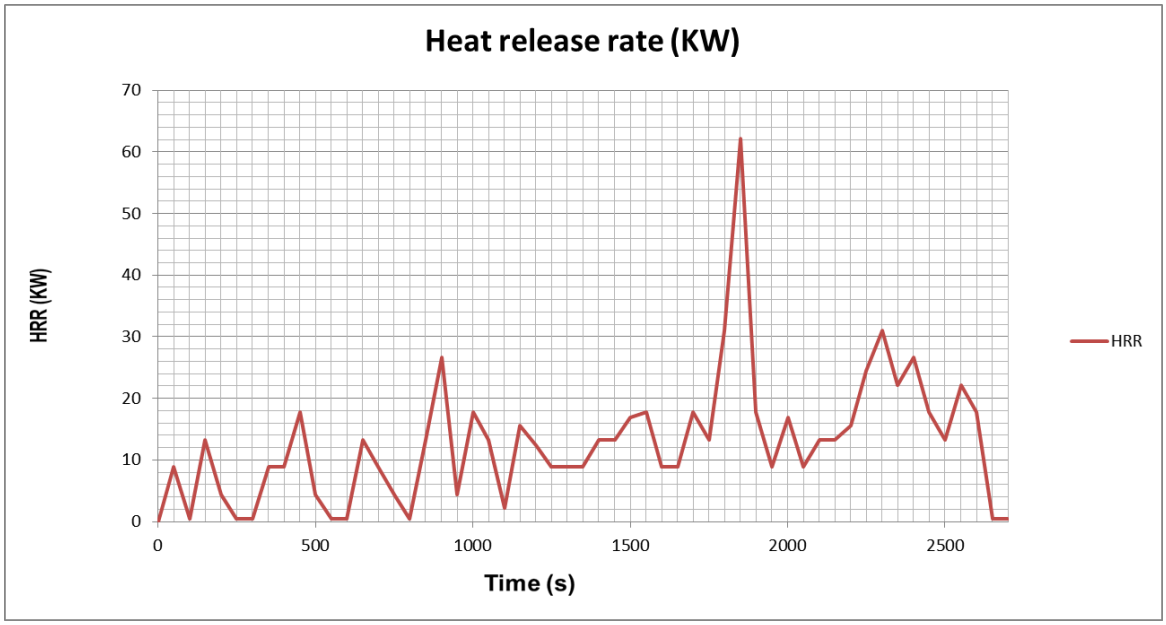


Fig 7-44 Actual heat release rate of fourth test

**Theoretical heat release rate**

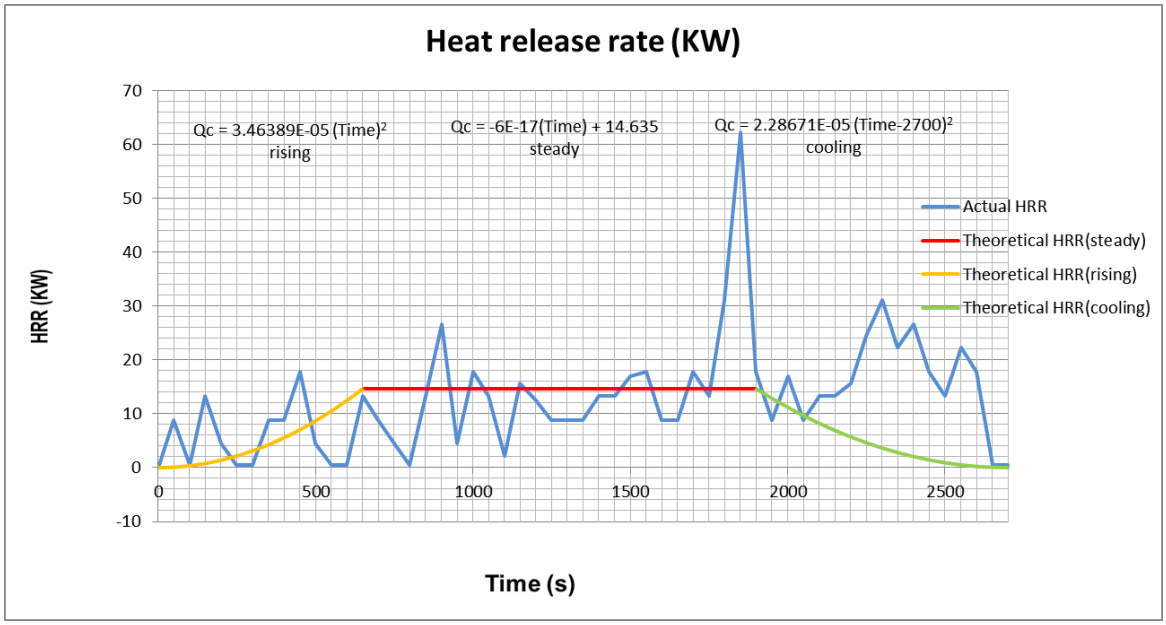


Fig 7-45 Theoretical heat release rate of fourth test

**Temperature distribution (Actual $Q_c$):**

All temperature distribution change with time are monitored by the program and shown in the following figure (Fig 7-46):

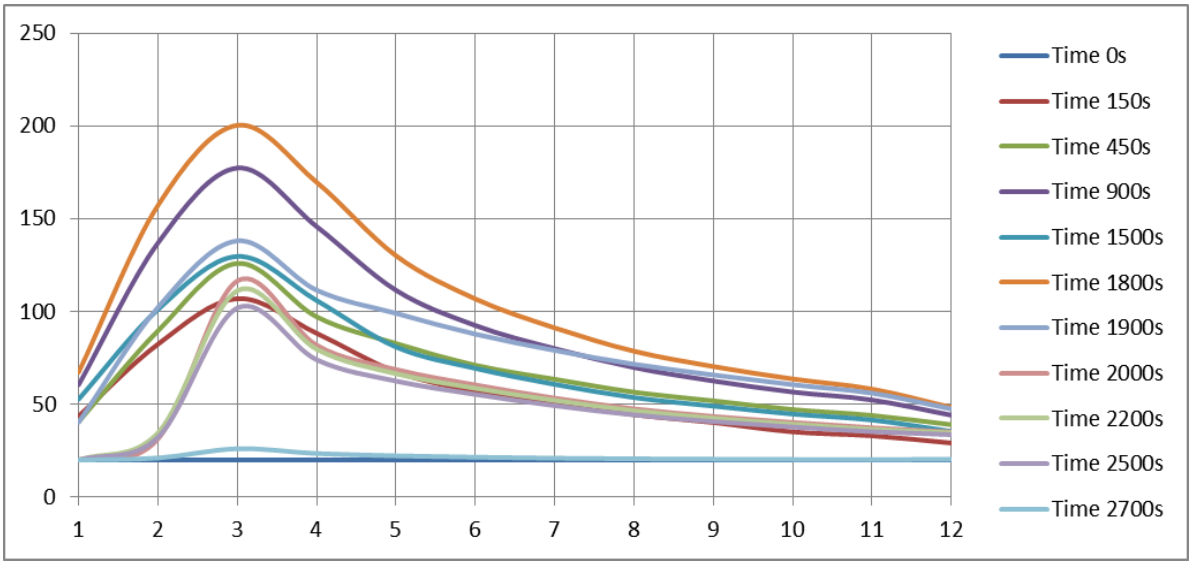


Fig 7-46 Temperature (℃) changes with tube length(m) during the fourth modeled stages

Temperature monitoring in each segment separately shows in following figure (Fig 7-47)

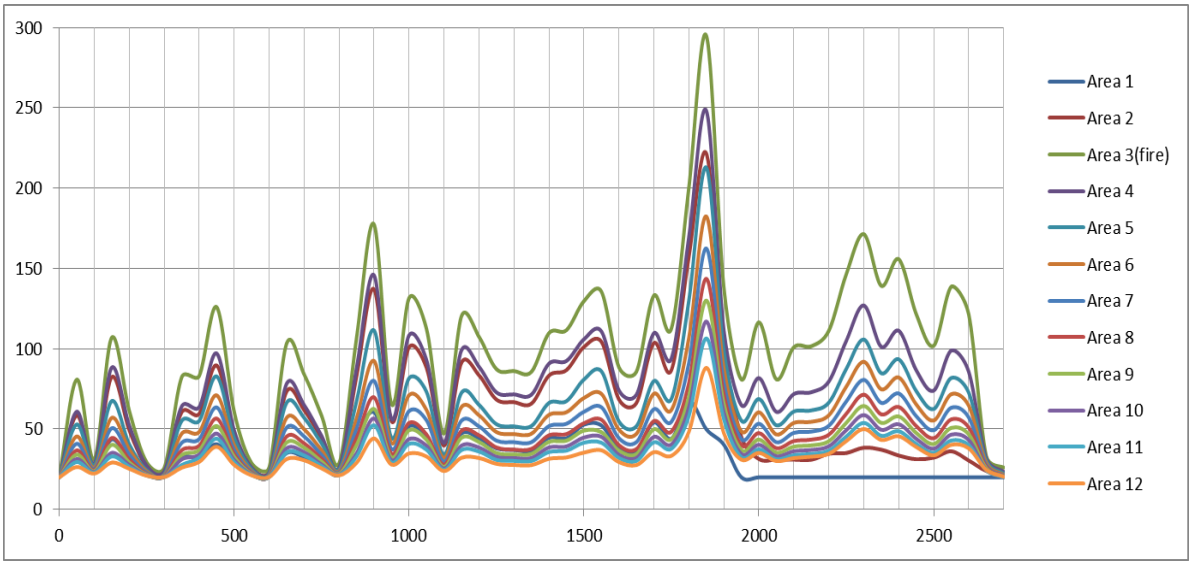


Fig 7-47 Temperature(℃) monitoring in each segment separately during different time(s)

Regarding the temperature distribution along change of levels, they are monitored by trees in different stations in tube and shown in the next figures (**Actual $Q_c$**): (Fig 7-48 – Fig 7-50):

**Tree at segment 5**

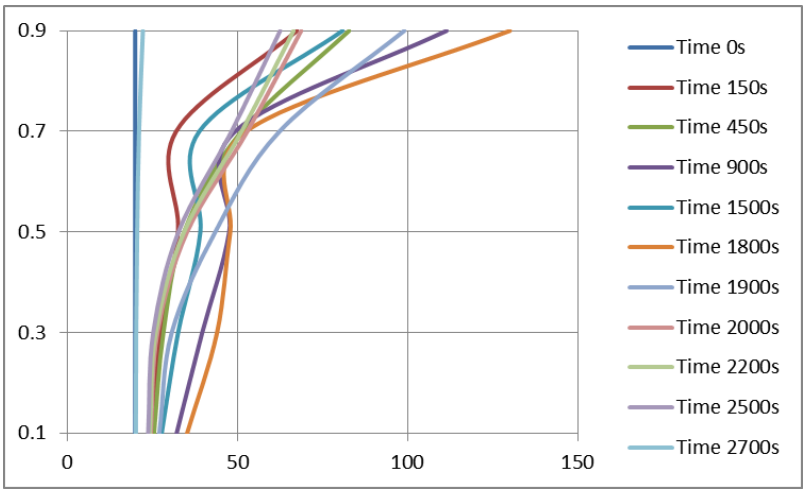


Fig 7-48 Temperature (℃) changes with tube level (m) according to different time stages in segment 5

**Tree at segment 7**

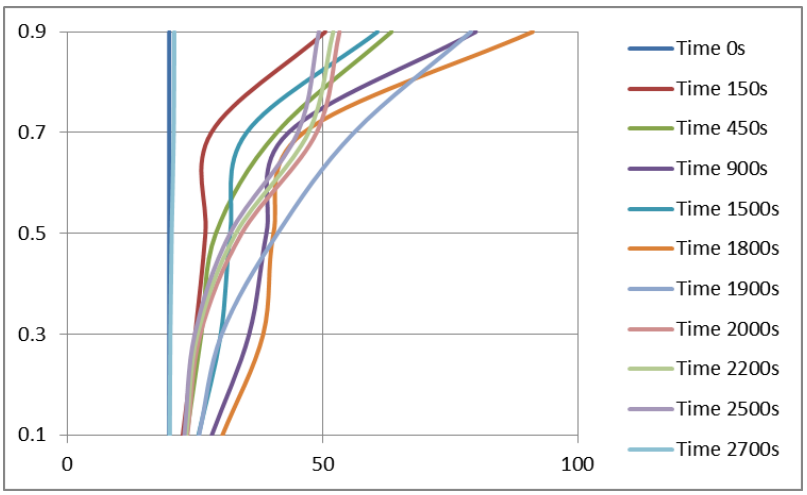


Fig 7-49 Temperature (℃) changes with tube level (m) according to different time stages in segment 7

**Tree at segment 11**

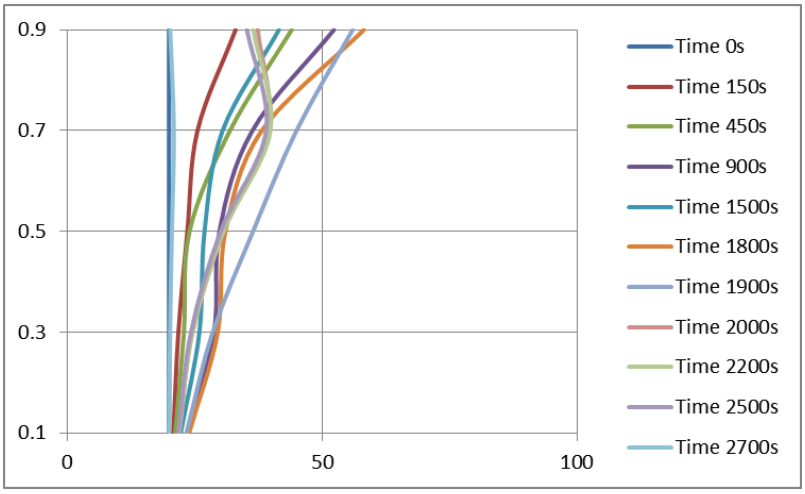


Fig 7-50 Temperature (℃) changes with tube level (m) according to different time stages in segment 11

**Temperature distribution (Theoretical $Q_c$):**

All temperature distribution change with time are monitored by the program and shown in the following figure (Fig 7-51):

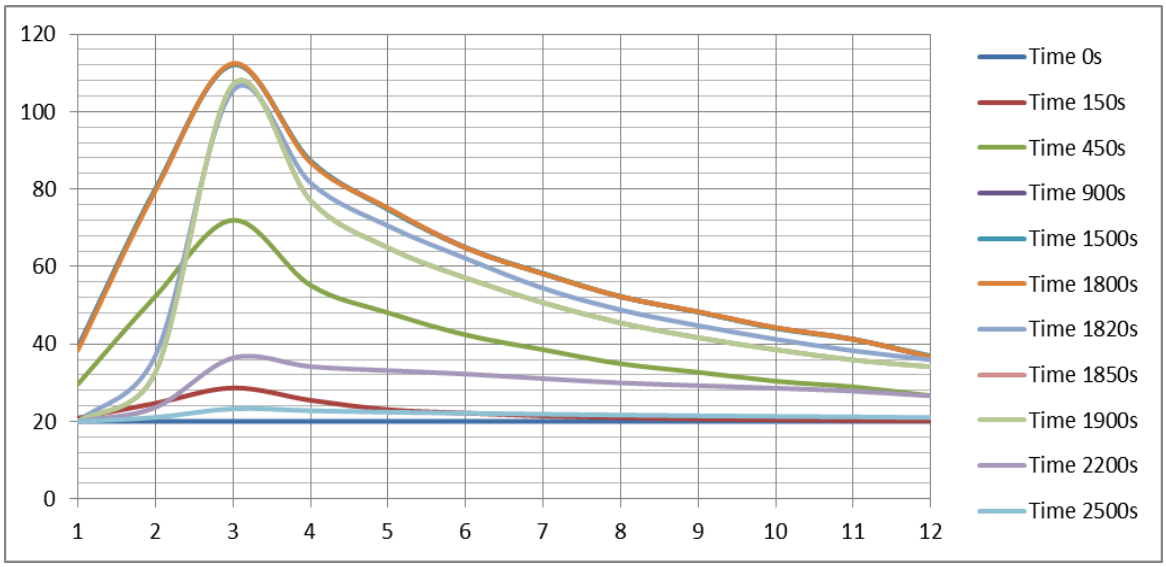


Fig 7-51 Temperature (℃) changes with tube length (m) during the fourth modeled stages

Temperature monitoring in each segment separately shows in following figure (Fig 7-52)

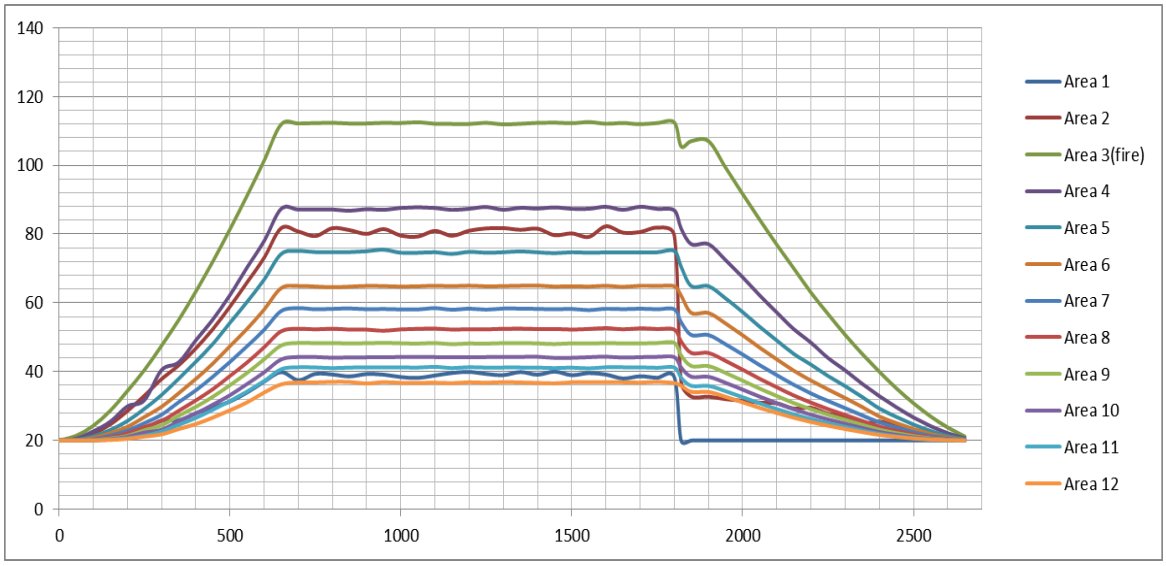


Fig 7-52 Temperature(℃) monitoring in each segment separately during different time(s)

Regarding the temperature distribution along change of levels, they are monitored by trees in different stations in tube and shown in the next figures (**Theoretical $Q_c$**): (Fig 7-53– Fig 7-55):

**Tree at segment 5**

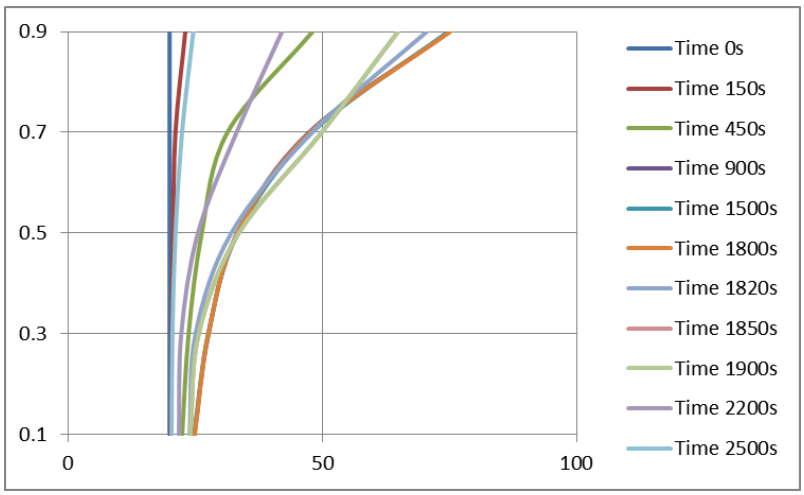


Fig 7-53 Temperature (℃) changes with tube level (m) according to different time stages in segment 5

**Tree at segment 7**

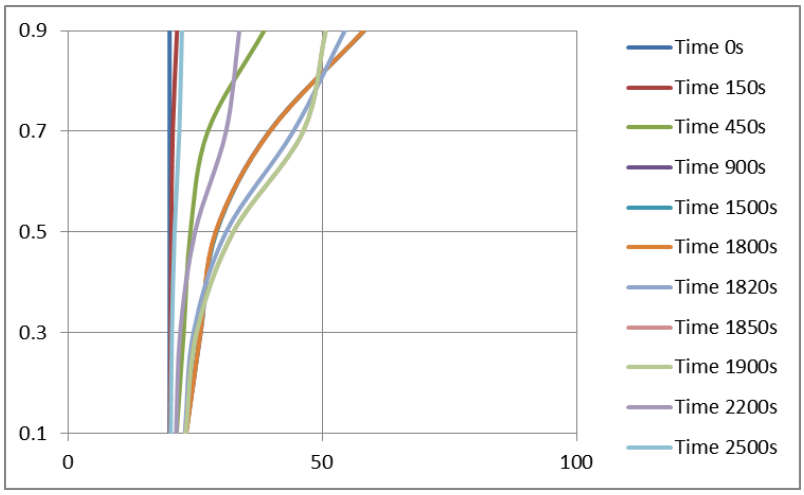


Fig 7-54 Temperature (℃) changes with tube level (m) according to different time stages in segment 7

**Tree at segment 11**

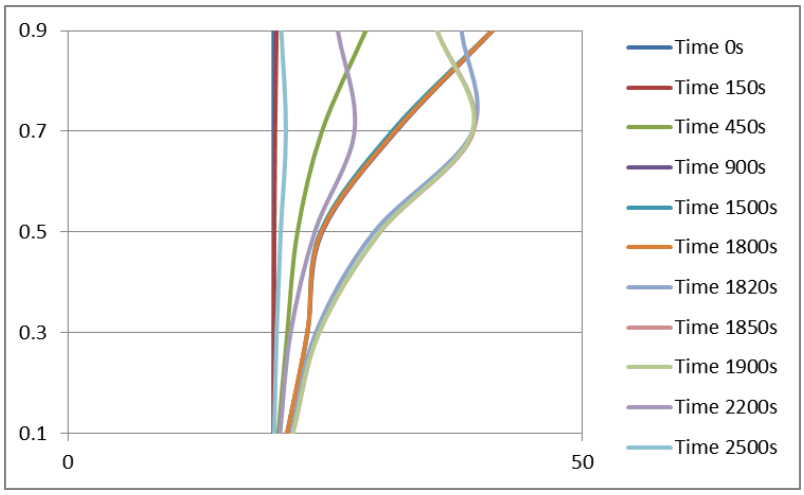


Fig 7-55 Temperature (℃) changes with tube level (m) according to different time stages in segment 11

# 8. Results of the analyses

## 8.1 Comparison between small scale experiment and numerical modeling

The aim of this chapter is to collect all main results followed by a comparison between experimental and numerical model, at the same time, the numerical model can be divided to two parts: Actual Heat Release Rate modeling and Theoretical Heat Release Rate modeling.

Table 8-1 First test result analysis

| **Test** | | **Experiment** | **Numerical modeling** | |
|---|---|---|---|---|
| **1** | | **Small Scale Experiment** | **Modeling With Actual HRR** | **Modeling With Theoretical HRR** |
| **Fuel Condition** | | Using a 26 cm diameter stainless steel pan filled with a quantity of diesel fuel (1400 gram) | | |
| **Ventilation condition** | | Non-Ventilation | | |
| **Ceiling Temperature At The Area With Fire (Area 3)** | | Rising to 180℃ at 500s, then steady around the temperature 180℃ until 2100s then cooling down | Rising to 200℃ at 200s, then very fluctuation around the average temperature 150℃ until 2000s then cooling down, the highest temperature is up to 450℃ | Rising to 170℃ at 450s, then steady around the temperature 170℃ until 2000s then cooling down |
| **Temperature Description In The Whole tunnel** | **Horizontal Direction** | The highest temperature is in the area with fire(area 3), and lower with the distance from area 3 increased | | |
| | **Vertical Direction** | The highest temperature is in the ceiling which have a highest position, and lower with the position decreased | | |
| **Ventilation Effect** | | Non-Ventilation | | |
| **Comments** | | Due to the high fluctuation in experimental HRR values, the actual HRR modeling have a big difference in temperature behavior while the theoretical HRR results in temperature have the same behavior compare to the experiment results | | |

Table 8-2 Second test result analysis

| **Test** | | **Experiment** | **Numerical modeling** | |
|---|---|---|---|---|
| **2** | | **Small Scale Experiment** | **Modeling With Actual HRR** | **Modeling With Theoretical HRR** |
| **Fuel Condition** | | Using a 26 cm diameter stainless steel pan filled with a quantity of diesel fuel (700 gram) | | |
| **Ventilation condition** | | Non-Ventilation | | |
| **Ceiling Temperature At The Area With Fire (Area 3)** | | Rising to 170℃ at 180s, then steady around the temperature 170℃ until 800s then cooling down | Rising to 200℃ at 100s, then very fluctuation around the average temperature 120℃ until 1150s then cooling down, the highest temperature is up to 330℃ | Rising to 170℃ at 200s, then steady around the temperature 170℃ until 850s then cooling down |
| **Temperature Description In The Whole tunnel** | **Horizontal Direction** | The highest temperature is in the area with fire(area 3), and lower with the distance from area 3 increased | | |
| | **Vertical Direction** | The highest temperature is in the ceiling which have a highest position, and lower with the position decreased | | |
| **Ventilation Effect** | | Non-Ventilation | | |
| **Comments** | | Due to the high fluctuation in experimental HRR values, the actual HRR modeling have a big difference in temperature behavior while the theoretical HRR results in temperature have the same behavior compare to the experiment results | | |

Table 8-3 Third test result analysis

| Test | | Experiment | Numerical modeling | |
|---|---|---|---|---|
| 3 | | Small Scale Experiment | Modeling With Actual HRR | Modeling With Theoretical HRR |
| Fuel Condition | | Using a 26 cm diameter stainless steel pan filled with a quantity of diesel fuel (900 gram) | | |
| Ventilation condition | | Started at the 2 minute of testing time with a value of 2.5m/s | | |
| Ceiling Temperature At The Area With Fire (Area 3) | | Rising to 80℃ at 100s, then decrease to 70℃ at 120s because of the ventilation, then continue increase to110 ℃ at 150s, then steady around the temperature 70℃ until 800s then cooling down | Rising to 250℃ at 180s, and in 120s the ventilation effect is small, then very fluctuation around the average temperature 270℃ until 700s, then cooling down because of the decrease of the HRR | Rising to 220℃ at 120s, then decrease to 200℃ at 125s because of the ventilation, then continue increase to248 ℃ at 150s, then steady around the temperature 248℃ until 800s then cooling down |
| Temperature Description In The Whole tunnel | Horizontal Direction | The highest temperature is in the area with fire(area 3), and lower with the distance from area 3 increased | | |
| | Vertical Direction | The highest temperature is in the ceiling which have a highest position, and lower with the position decreased | | |
| Ventilation Effect | | When ventilation start, temperature in the tunnel begin decrease, the decrease velocity faster when close to the ventilation fans, then during a short time, temperature increase again because of the HRR increase | | |
| Comments | | Due to the high fluctuation in experimental HRR values, the actual HRR modeling have a big difference in temperature behavior and the theoretical HRR results in temperature also have a big difference in the highest temperature when compare to the experiment results because under ventilation, the imprecise measurement of the HRR data | | |

Table 8-4 Fourth test result analysis

| **Test** | | **Experiment** | **Numerical modeling** | |
|---|---|---|---|---|
| **4** | | **Small Scale Experiment** | **Modeling With Actual HRR** | **Modeling With Theoretical HRR** |
| **Fuel Condition** | | Using a 18 cm diameter stainless steel pan filled with a quantity of diesel fuel (790 gram) | | |
| **Ventilation condition** | | Started at the 30 minute of testing time with a value of 2.5m/s | | |
| **Ceiling Temperature At The Area With Fire (Area 3)** | | Rising to 120℃ at 500s, then very fluctuation around the average temperature 120℃ until 1800s then the temperature decrease due to the ventilation effect, finally cooling down | Rising to 115℃ at 150s, then very fluctuation around the average temperature 120℃ until 1800s, the highest temperature is 300℃, then decrease to 100℃ at 1900s because of the ventilation start, finally cooling down with a very fluctuation velocity | Rising to 112℃ at 650s, then steady around the temperature 115℃ until 1800s then decrease to 105℃ between 1820s and 1900s because of the ventilation start, finally cooling down |
| **Temperature Description In The Whole tunnel** | **Horizontal Direction** | The highest temperature is in the area with fire(area 3), and lower with the distance from area 3 increased | | |
| | **Vertical Direction** | The highest temperature is in the ceiling which have a highest position, and lower with the position decreased | | |
| **Ventilation Effect** | | When ventilation start, temperature in the tunnel begin decrease, the decrease velocity faster when close to the ventilation fans | | |
| **Comments** | | Due to the high fluctuation in experimental HRR values, the actual HRR modeling have a big difference in temperature behavior while the theoretical HRR results in temperature have a roughly consistence with the experiment results | | |

## 8.2 Ventilation effects analysis in theoretical modeling

Test 3 theoretical numerical modeling was chosen to test the temperature affected by ventilation. There were two different conditions: 1. No ventilation during the whole process. 2. Ventilation started at 120s with the velocity 2.5m/s.

Temperature monitoring in each segment separately show in the following figures: no-ventilation condition (Fig 8-1); ventilation condition (Fig 8-2).

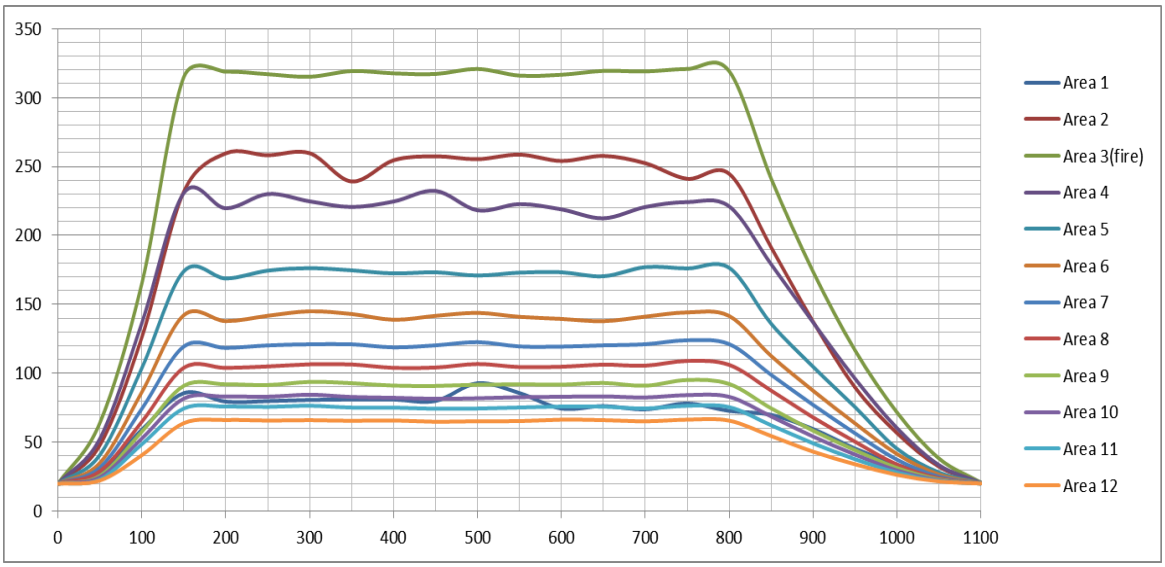


Fig 8-1 Temperature(℃) in each segment in no ventilation condition during different time (s)

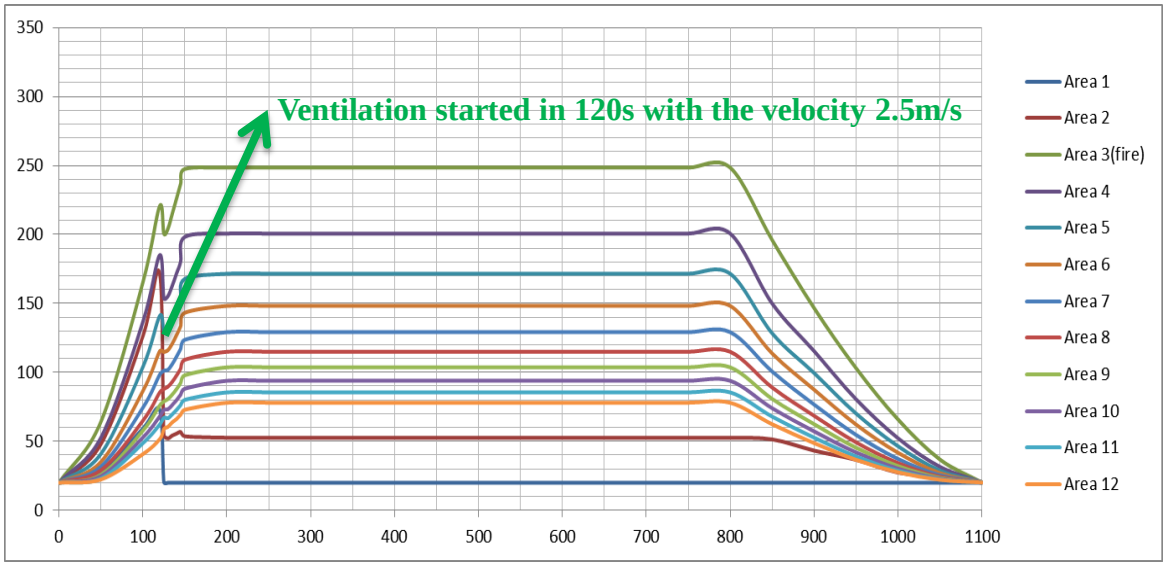


Fig 8-2 Temperature (℃) in each segment separately while ventilation started in 120s (2.5m/s)

The differences between the two figures show the temperature reduction effect under ventilation, the temperature had an instantaneous drop when ventilation started. At the same time, the reduction magnitude is different in each area, and the reduction magnitude is higher when close to the ventilation fans, this phenomenon can also be seen in temperature changes with tube length figures: no-ventilation condition (Fig 8-3); ventilation condition (Fig 8-4).

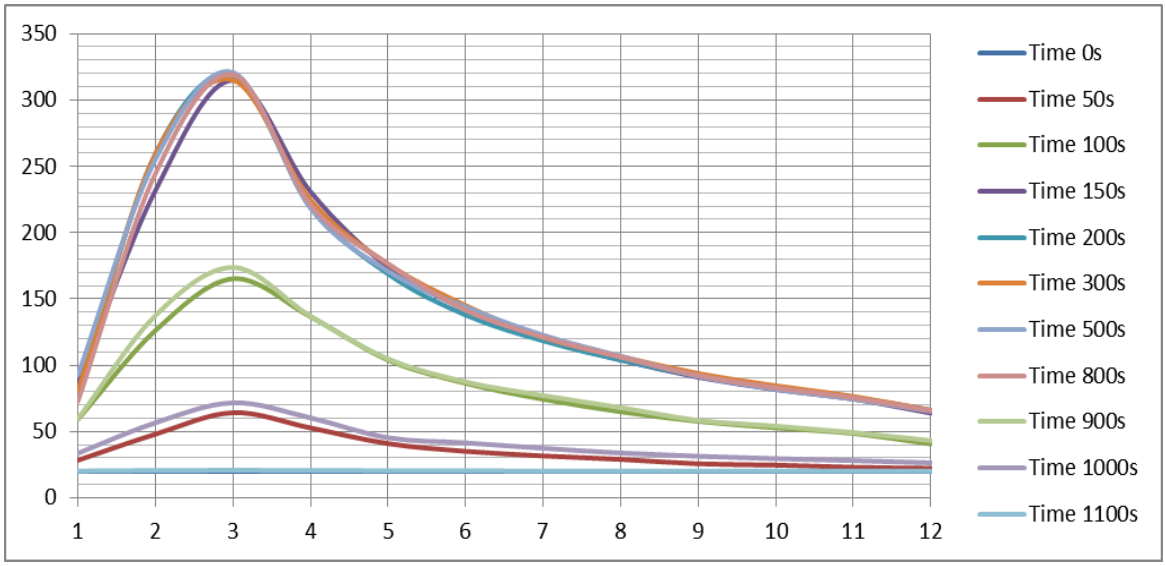


Fig 8-3 Temperature (℃) changes with tube length (m) in no ventilation condition

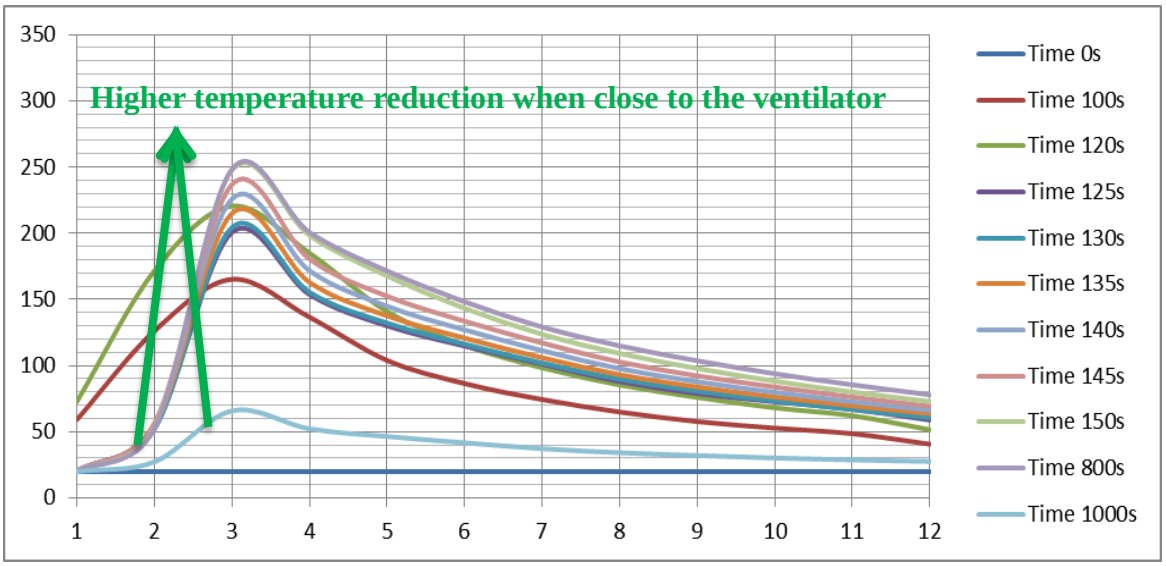


Fig 8-4 Temperature (℃) changes with tube length(m) while ventilation started in 120s (2.5m/s)

## 8.3 Temperature changed by the propagation of smoke in different areas

Test 1 actual HRR numerical modeling (0s~250s, Fig 8-5) was chosen to test the phenomenon of the smoke propagation affects the temperature in different areas.

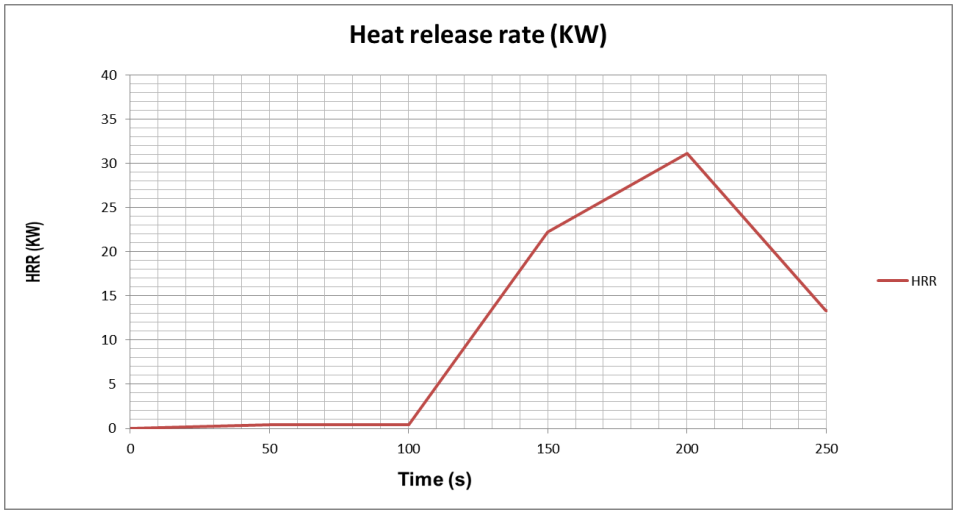


Fig 8-5 Heat release rate for running the analysis of the smoke propagation effect

Then the temperature monitoring in each segment separately (Fig 8-6)

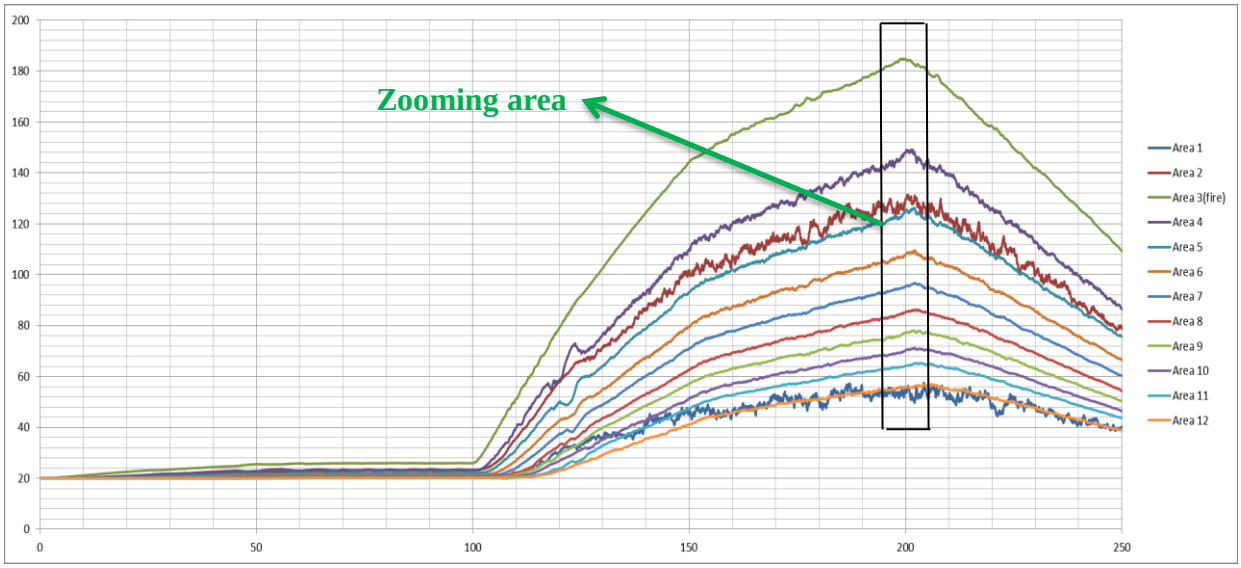


Fig 8-6 Temperature (℃) in each segment alone the test time (s)

The box shows in the figure denote a time period which contain the peak temperature in each segment. To analyze the smoke propagation effect, a paned figure will show in follows, a different temperature peak time in each area is also accommodating in the figure (Fig 8-7). A table (Table 8-5) followed to descript the peak temperature time in each segment and the computational average boundary velocities.

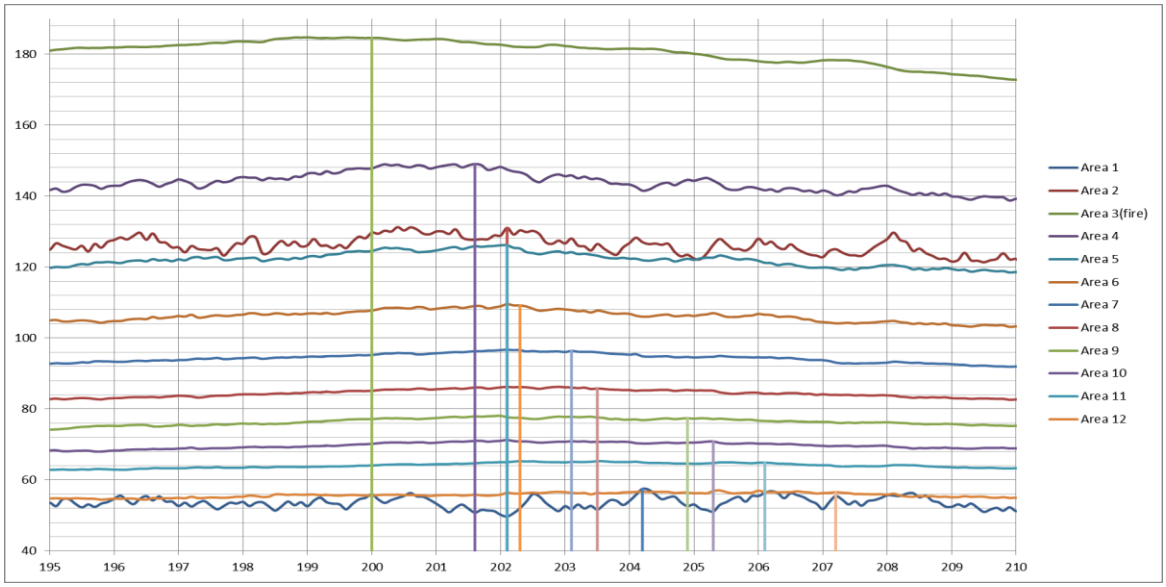


Fig 8-7 Different temperature (℃) peak time in each area alone the test time (s)

Table 8-5 Description of the peak temperature and the average boundary velocities

| Area | 1 | 2 | 3(Fire) | 4 | 5 | 6 | 7 | 8 | 9 | 10 | 11 | 12 |
|---|---|---|---|---|---|---|---|---|---|---|---|---|
| temperature(C) | 57.4831 | 131.0456 | 184.6 | 149 | 126.15 | 109.2 | 96.37 | 85.77 | 77.4 | 70.8 | 64.87 | 56.57 |
| peak time(s) | 204.2 | 202.1 | 200 | 201.6 | 202.5 | 203.1 | 203.8 | 204.4 | 205.1 | 206 | 206.5 | 207.2 |
| Area width (m) | 1 | 1 | 1 | 1 | 1 | 1 | 1 | 1 | 1 | 1 | 1 | 1 |

| computational average boundary velocities(m/s) | | -0.476 | -0.476 | 0.625 | 1.111 | 1.667 | 1.429 | 1.667 | 1.429 | 1.67 | 1.25 | 1.429 | |
|---|---|---|---|---|---|---|---|---|---|---|---|---|---|

Following table (Table 8-6) shows the average boundary velocity come from the MATLAB simulation result.

Table 8-6 Average velocity computed by the MATLAB program

| Area | 1 | 2 | 3 | 4 | 5 | 6 | 7 | 8 | 9 | 10 | 11 | 12 |
|---|---|---|---|---|---|---|---|---|---|---|---|---|

| time period for smoke travelling(s) | | 202.1 ~204.2 | 200~ 202.1 | 200~ 201.6 | 201.6 ~202.5 | 202.5 ~203.1 | 203.1 ~203.8 | 203.8 ~204.4 | 204.4 ~205.1 | 205.1 ~206 | 206~ 206.5 | 206.5 ~207 | |
|---|---|---|---|---|---|---|---|---|---|---|---|---|---|
| Average velocity in MATLAB(m/s) | | -0.78 | 0.082 | 0.169 | 0.757 | 0.855 | 0.935 | 0.931 | 1.028 | 1.07 | 1.11 | 1.155 | |

The velocity computed by the propagation of the smoke (Table 8-5) just a little different with the velocity coming from the MATLAB simulation result (Table 8-5), the phenomenon of the smoke propagation affects the temperature in different areas can be proved by these two results.

A 3D (Fig 8-8) colored map presented below show the temperature distribution in the longitudinal cross-section at some significant time-steps (0~250s) in test 1 actual HRR numerical modeling result.

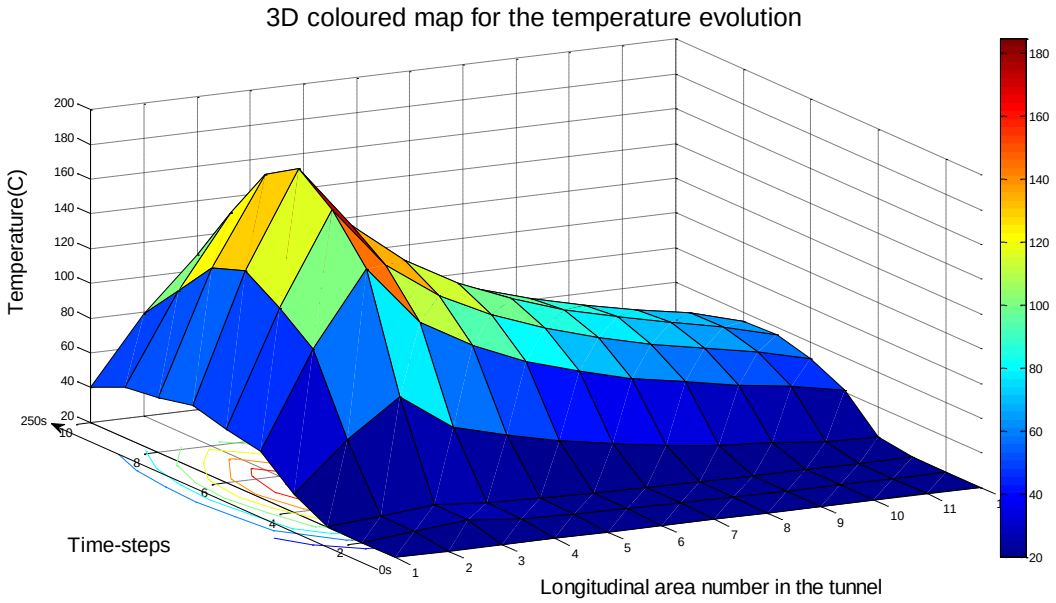


Fig 8-8 3D colored map for the temperature evolution (0~250s), test 1 actual HRR

Following 2D colored figures show the development of the temperature in the tunnel in some special fire time (100s, 150s, 200s, and 250s)

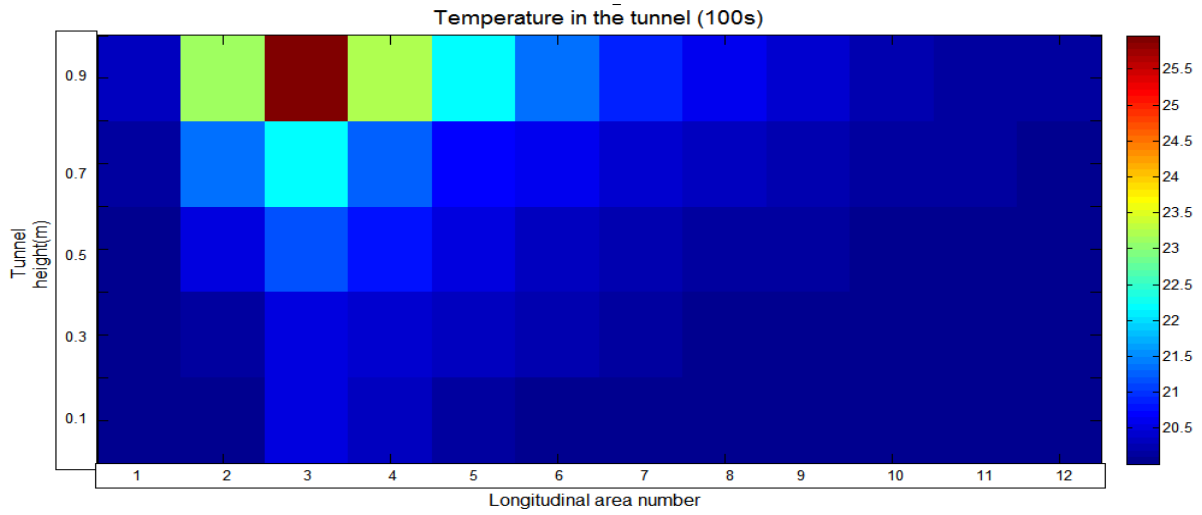


Fig 8-9 2D colored map for the temperature (℃) distribution (100s), test 1 actual HRR

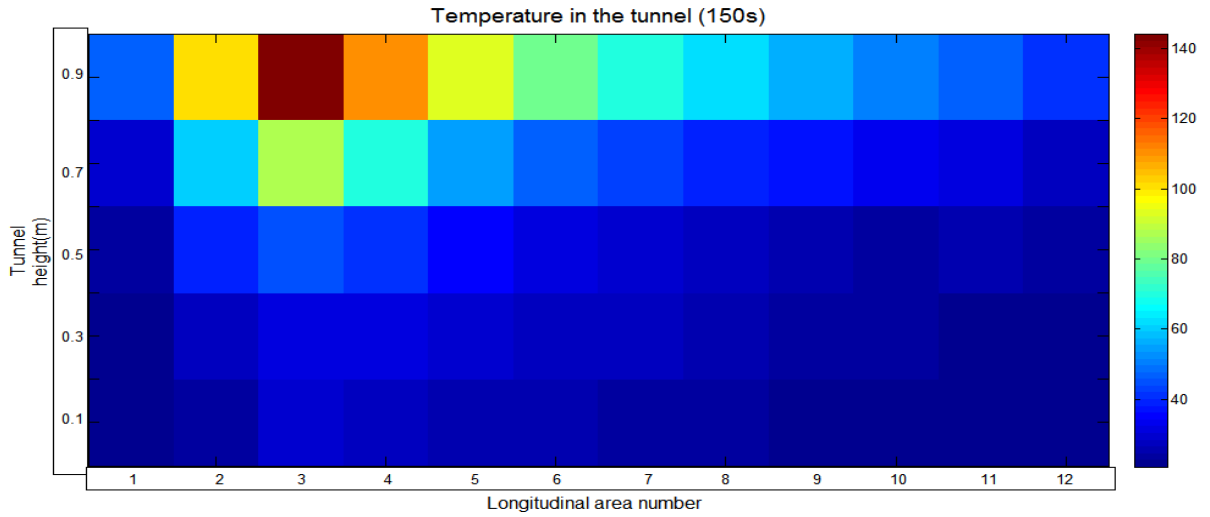


Fig 8-10 2D colored map for the temperature (℃) distribution (150s), test 1 actual HRR

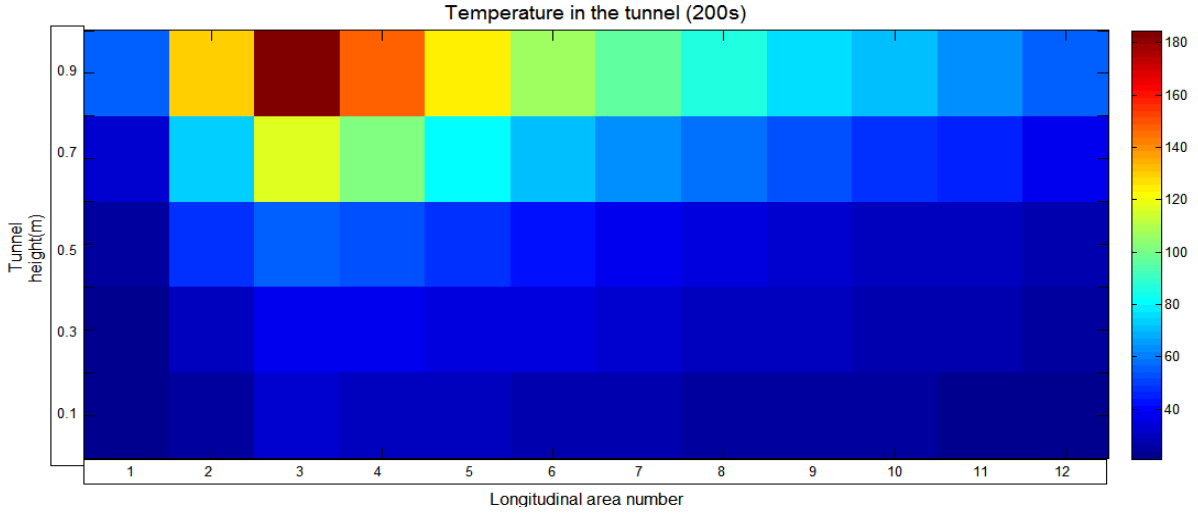


Fig 8-11 2D colored map for the temperature (℃) distribution (200s), test 1 actual HRR

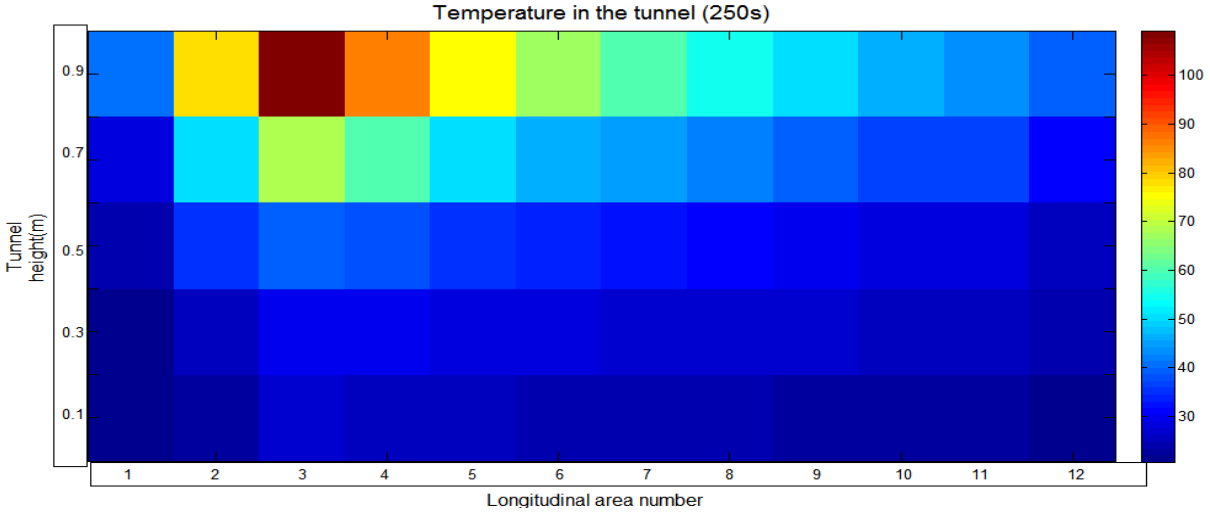


Fig 8-12 2D colored map for the temperature (℃) distribution (250s), test 1 actual HRR

## 8.4 Comments

### 8.4.1 Fuel

For the weight of the fuel, Test 1 and Test 2 are compared to check the influence of the weight of the fuel in the tunnel fire, in which Test 1 (1400 gram diesel) and Test 2 (700 gram diesel), the difference of these two test is the time of the fire stage, for Test 1, the fire rising stage ended in 500s, then steady state until 2000s, and cooling down until 2500s, for Test 2, the fire rising stage ended in 200s, then steady state until 850s, and cooling down until 1550s. But for other properties such as the highest temperature in the tunnel and the distribution of the temperature, these properties are almost the same in Test 1 and Test2. So when the weight of the fuel changed, the only influence of this parameter is the fire time stage, more fuel can keep a long fire time. And other properties such as the highest temperature and the temperature distribution in the tunnel are not changed by this parameter (weight of the fuel).

For the surface of burning area, which already known before, the peak of the HRR is determined by multiply the parameters: Mass burning rate ($kg/m^2/sec$), Effective heat of combustion (kJ/kg) and the burning area ($m^2$), in which the first two parameters are constant values under the diesel fuel, so the only influence parameter in the peak HRR is the surface of burning area, when the surface is lager, the peak HRR value is higher, so the temperature in the tunnel is higher, this conclusion is easily identified while compare the Test2 (26 cm diameter fuel pan) with Test4 (18 cm diameter fuel pan) during the time before ventilation.

### 8.4.2 Ventilation

Both experiment and numerical modeling results shows that ventilation has a great effect on temperature distribution, the effect is the reduction of temperature, and the reduction velocity is faster when close to the ventilation fans (Test 3 and Test 4). At the same time the ventilation also accelerates the mass burning rate compared to the case of no ventilation, this effect can be easily seen in the actual HRR value of Test 3 (120 s) and Test 4 (1800 s), but this is really a problem for numerical modeling because of the imprecise of the weight loss measurement, some inconsistency happens between the numerical modeling and the experiment, so the precisely of the weight loss measurement should be enhanced, this will be introduced in the future research.

### 8.4.3 Numerical modeling result

There are two different kind of numerical modeling scheme, one is modeling under the Actual HRR values and another is modeling under the Theoretical HRR.

In the first case (Actual HRR), the temperature distribution results have some non-realistic fluctuations, so the results are quite imprecise; this evidence raises some uncertainty about the reliability of the fuel weight measurements, this probably because of the aerodynamic effect of the gas against the bottom of the fuel pan during the gas movement.

In the second case (Theoretical HRR), three different time period was adopt during the analysis (rising, steady and cooling), while in the steady period, an average of the actual HRR was adopted, the other two stage, rising and cooling stage, a model of $t^2$ fire was adopted. The results of the Theoretical HRR modeling have a more effective fitting with the experimental temperatures in the fire region. But what is still not very satisfactory is that some results (Test3) have bad consistency with the experimental results, because the Theoretical HRR values are also depends on the Actual ones, if the Actual HRR values are bad, the Theoretical value are bad too.

So there have a conclusion that both the Actual HRR and the Theoretical HRR are highly depends on the fuel weight loss measurements, but the aerodynamic effect of the gas against the bottom of the fuel pan during the gas movement really affect the result, so there should have some improvement of the precisely of the weight loss measurement, this will be introduced in the future research.

## 8.5 Future research

### 8.5.1 Aerodynamic effect

The aerodynamic effect influence the weight loss measurement shows below (Fig 8-13)

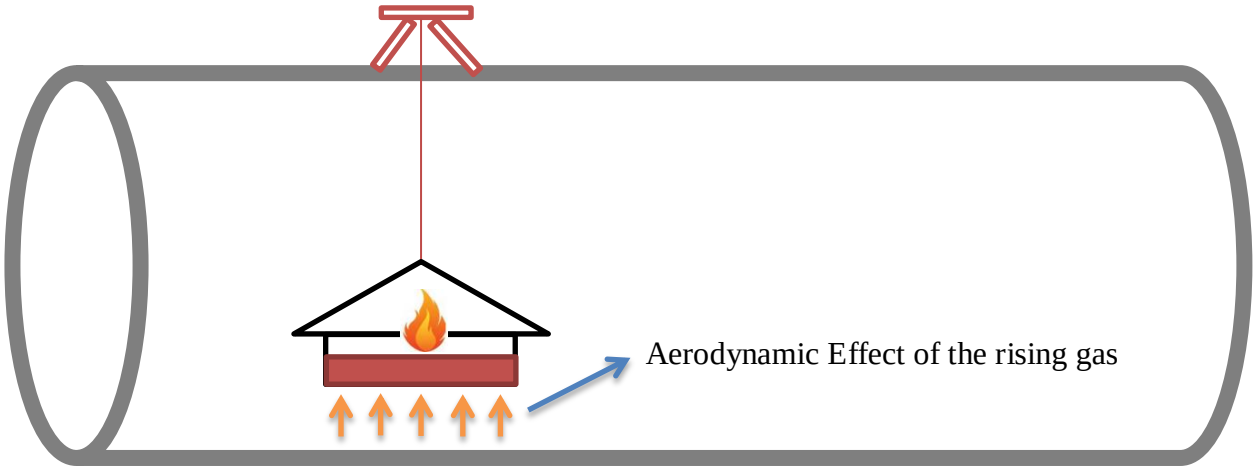


Fig 8-13 Aerodynamic Effect of the rising gas to the fuel pan

In order to reduce the aerodynamic effect of the gas against the bottom of the fuel pan during the gas movement, a box deposed on the bottom of the fuel pan during the experiment (Fig 8-14), so with the reduction of the aerodynamic effect, the weight loss rate are more accurate, as same as the HRR values, so the high fluctuation of the temperature in the theoretical modeling can be eliminated.

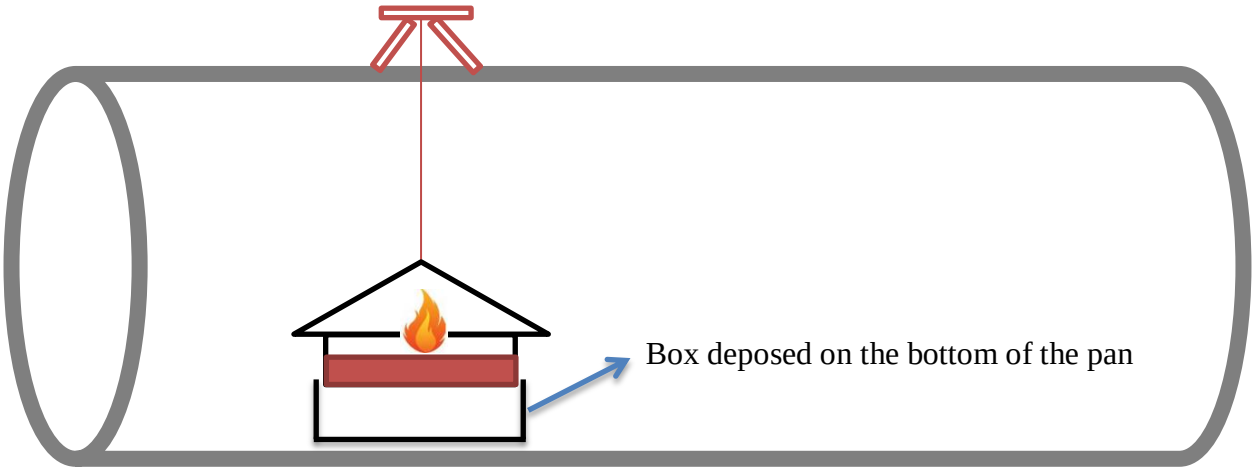


Fig 8-14 A box deposed on the bottom of the pan to eliminate the Aerodynamic Effect

### 8.5.2 Ventilation scheme

A different ventilation scheme needs to be applied on the tube, since the ventilation in the current research applied on full area of tube. On contrary, it needs to be more realistic to be projected on only the upper part of the tube.

Following figure (Fig 8-15) shows the scheme of installation the old ventilation fans during the experiment.

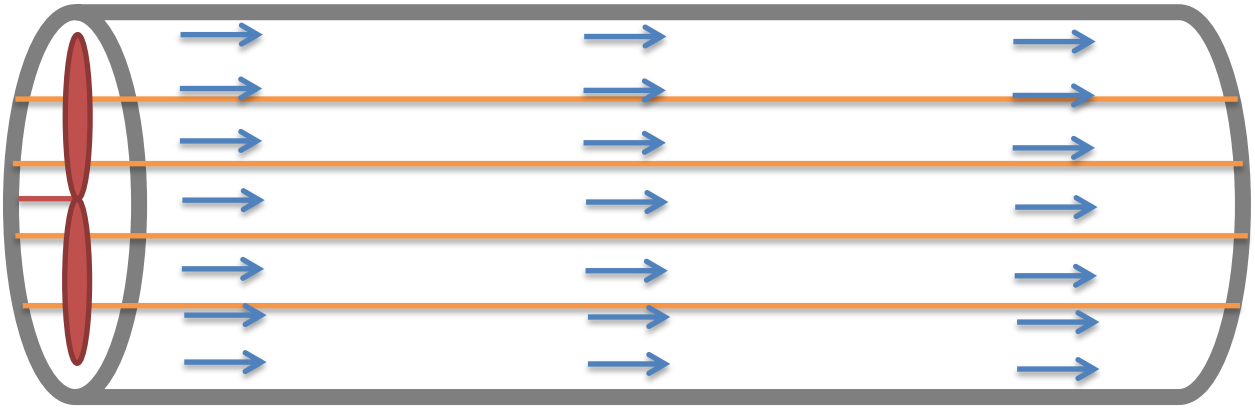

Fig 8-15 The scheme of installation the old ventilation fans

Following figure (Fig 8-16) shows the scheme of installation the new ventilation fans during the experiment.

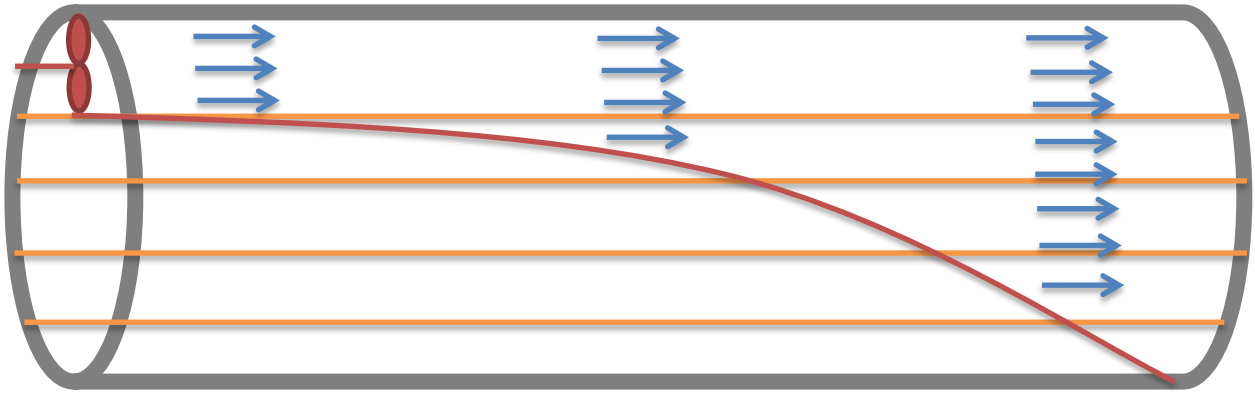

Fig 8-16 The scheme of installation the new ventilation fans

For the numerical modeling, the old ventilation scheme is add a velocity in all layers in the 1st area during the ventilation time.

While applying the new ventilation scheme is quite easy, just need to add a velocity in the top layer in the 1st area during the ventilation time.

### 8.5.3 Adding a rate term of Radiation ($Q_r$) to the numerical modeling

During the whole analysis of this research, the governing equations (Equation 7-7 and Equation 7-8) don't consider the radiation heat transfer term. But radiation heat transfer is a very important mechanism, the radiation heat flux is assumed to consist of three directional components between layers or layer and wall (the upward, the downward and the horizontal one from each layer) as shown by arrows in Fig 8-5. In the fire room, radiation heat transfer from the flame (a point at the mean flame height, assumed jm-th) to the wall segments is considered, as shown by broken lines in Fig 8-17.

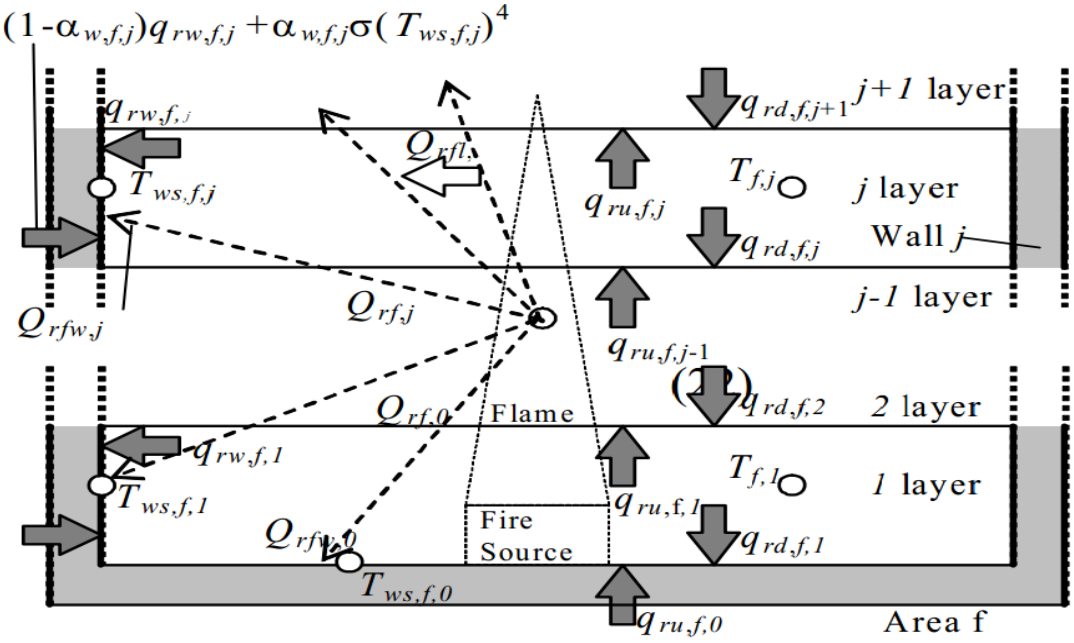


Fig 8-17 Radiation heat transfer with fire

The upward, downward and horizontal heat fluxes, $q_{ru,i,j}$, $q_{rd,i,j}$ and $q_{rw,i,j}$ are calculated as follows;

$$q_{ru,i,j}=(1-\alpha_{r,i,j})F_{LL,i,j}q_{ru,i,j-1}+\alpha_{r,i,j}\sigma T_{i,j}{}^4+(1-\alpha_{r,i,j})F_{WL,i,j}\{(1-\alpha_{rw,i,j})q_{rw,i,j}+\alpha_{rw,i,j}\sigma T_{w,i,j,1}{}^4\}(8-1)$$

$$q_{rd,i,j}=(1-\alpha_{r,i,j})F_{LL,i,j}q_{rd,i+1,j}+\alpha_{r,i,j}\sigma T_{i,j}{}^4+(1-\alpha_{r,i,j})F_{WL,i,j}\{(1-\alpha_{rw,i,j})q_{rw,i,j}+\alpha_{rw,i,j}\sigma T_{w,i,j,1}{}^4\}(8-2)$$

$$q_{rw,i,j}=(1-\alpha_{r,i,j})F_{LW,i,j}q_{ru,i,j-1}+(1-\alpha_{r,i,j})F_{LW,i,j}q_{rd,i,j+1}+\alpha_{r,i,j}\sigma T_{w,i,j,1}{}^4+Q_{radw,j}/A_{w,i,j}(8-3)$$

Where $\alpha_{r,i,j}$ the radiation absorptivity, changes according to the gas temperature and mass fractions, and $F$ is the view factor. Hence the net radiation heat gain of the layer $Q_{r,i,j}$, is

$$Q_{r,i,j}=A_{f,i}(q_{ru,i,j-1}-q_{ru,i,j}+q_{rd,i,j+1}-q_{rd,i,j})$$
$$-A_{w,i,j}\{q_{rw,i,j-1}-[(1-\alpha_{rw,i,j})q_{rw,i,j}+\alpha_{rw,i,j}\sigma T_{w,i,j,1}{}^4]\}+Q_{radl,i,j}\ (i\neq f, Q_{radl,i,j}=0)(8-4)$$

### 8.5.4 Slenderness effect

The effect of slenderness ratio between length and depth of tunnel has an effect on temperature and smoke distribution. Therefore, there should be performed some new tests in a longer tube to check the effect of slenderness ratio on the obtained results, but construct a new tube is not economical, so cover a part of the outlet of the concrete tube is an alternative method.

Following figure (Fig 8-18) shows the smoke behavior in the old tunnel (smaller slenderness)

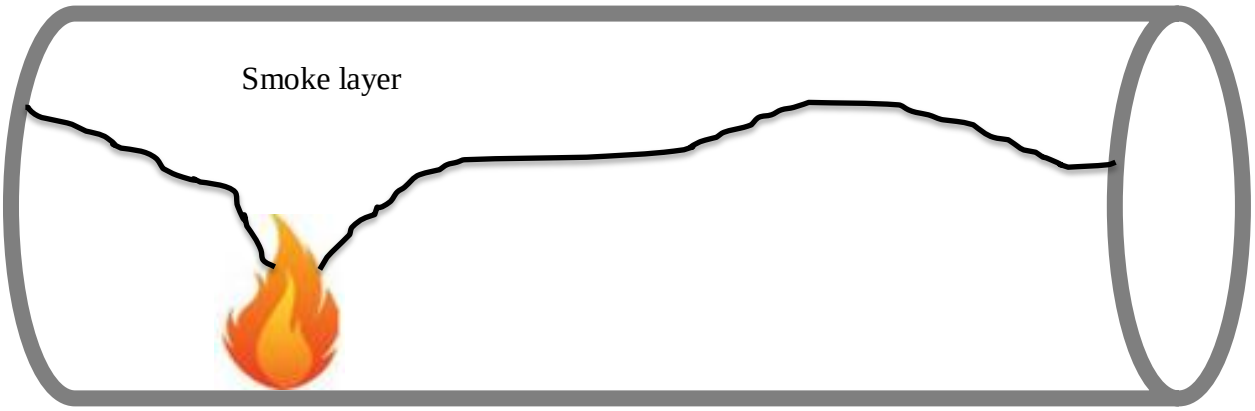


Fig 8-18 Smoke behavior in the old tunnel (smaller slenderness)

Following figure (Fig 8-19) shows the smoke behavior in the new tunnel (larger slenderness).

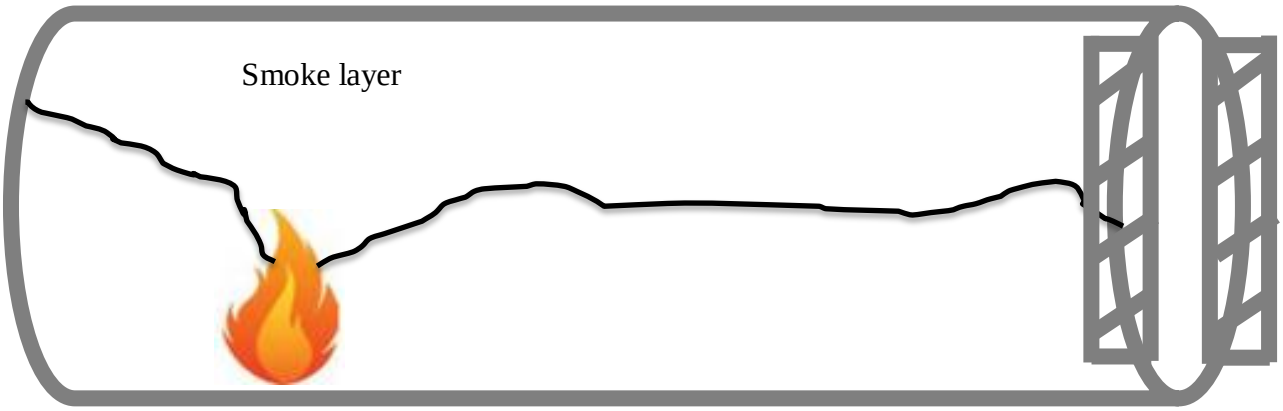


Fig 8-19 Smoke behavior in the new tunnel (larger slenderness)

For the numerical modeling, when applying a larger slenderness in the new tunnel, the method is just lengthening the tunnel by changing the boundary values.

# 9. Conclusions

The most important scope of this research is to describe the behavior and distribution of temperature resulting from fires in a scaled tunnel model under the effect of ventilation and non-ventilation conditions. It is important to monitor and study the behavior of fire in scaled models, then identify the results coming from the experimental test of concrete tube by numerical modeling by using MATLAB (Multi-Zone concept), then doing the evaluation of consistence between achieved experimental and numerical results and compare themselves, the work was focused on numerical modeling of the fire scenario.

The main conclusions that can be drawn from this research are shown in the following:

## 9.1 Multi-Layer Zone model

The model that has been developed is based on the partition of the tunnel in zones and layers. This means that all the model variables (temperature, pressure, gas velocity) are provided in each control volume, this allows to work out a more effective description of the fire scenario compared to the original (two-zone) models (Ozone, Cfast6, etc.). On the other hand, this brings in a remarkable simplification of the mathematical framework of the physical problem compared to a field model based on computational fluid dynamics (CFD) applied to fire-development simulation. The Multi-Layer zone model provides a simpler description of the fire scenario, but it is adequate for the engineering design requirements. Moreover, most drawbacks in the description of the role of the main parameters are avoided and a sizable reduction of CPU time is allowed. So, this type of approach (Multi-Layer Zone Model) looks the best compromise for cost effective engineering applications.

## 9.2 Comments on fitting the experimental results

Numerical modeling results (Time-Temperature plots) obtained from the model while using the theoretical HRR input is fitting the experimental results well. The difference is just in the range of 5-10℃, partly due to the measurement errors during the experiment. But when using the raw (actual) HRR input, the difference is big and more fluctuation is observed. This difference is

due to the noisy HRR data taken from the experiment, because of the aerodynamic effect of the moving gas on the fuel container. Hence, dividing the raw HRR in different stages depicted by different models (rising stage: $t^2$ model, steady stage: average steady line model, cooling stage: $t^2$ model) is the crucial step for better approaching the real situation.

## 9.3 Computation time-step

The model requires a limited set of input data (geometry, ventilation and HRR data), after determination of these inputs, a computation time step is decisive to the whole computation time, and following figure (Fig 9-1) shows different computation time step result in different whole computation time (Numerical Modeling 1 hour).

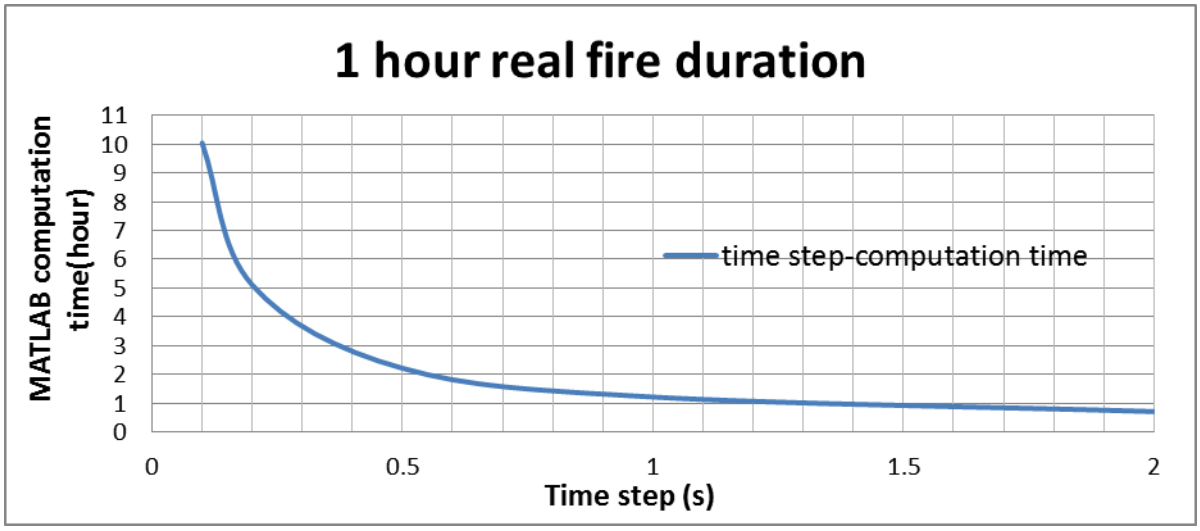


Fig 9-1 Different computation time step result in different whole computation time

In order to analyze the temperature result influenced by different computation time-step (0.1s, 0.2s, 0.5s, and 0.6s), two ceiling point A and B in the tunnel (Fig 9-2) were chosen under a special Heat Release Rate condition (Fig 9-3), finally the modeling result was shown in the next figure (Fig9-4).

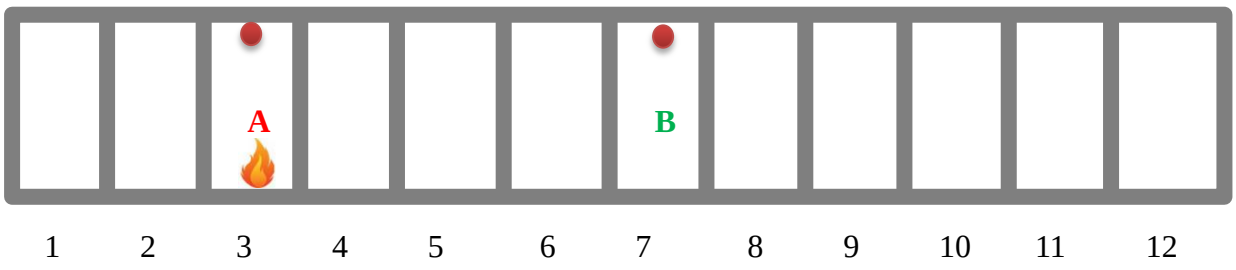


Fig 9-2 Two ceiling point A and B in the tunnel

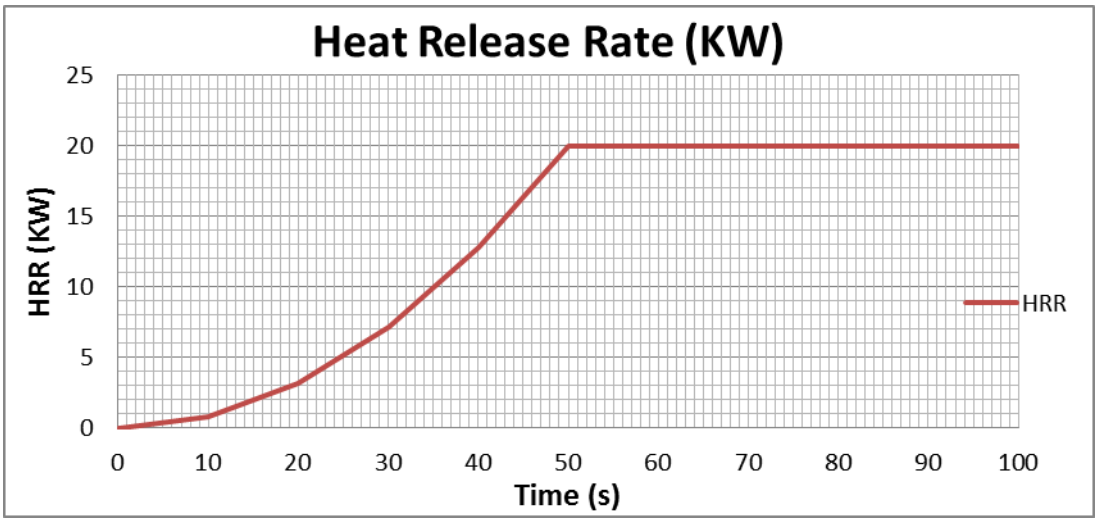


Fig 9-3 A special Heat Release Rate condition

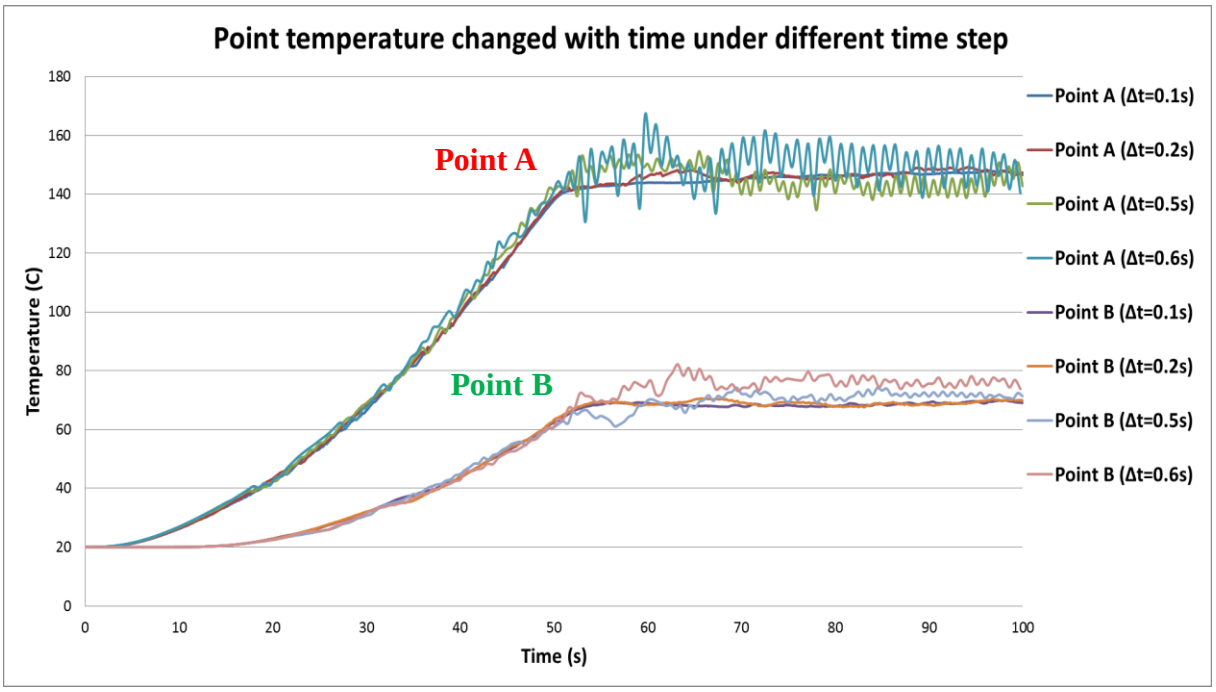


Fig 9-4 Point temperature changed with time under different time step

According to the modeling result, gas temperature in the tunnel behaved steady when computation time step between 0.1-0.2s, then some significant fluctuation happened when the time step is larger than 0.5s, as a matter of fact, the time step in the range of 0.1~0.5s have the highest accuracy in this research.

## 9.4 Possible improvements to the software

Reasonable explanations for the lack of better fitting relationship between numerical and experimental result are due to following reasons.

1. Boundary conditions: the temperature considered in the boundary is ambient condition (20℃) and the gas velocity in the boundary is also in the ambient condition (0m/s), but in the real situation, boundary gas also have relative high temperature and velocity due to the development of the fire.

2. Radiation heat transfer does not consider in this model, but in the real situation, the radiation heat flux is assumed to consist of three directional components between layers or layer and wall (the upward, the downward and the horizontal one from each layer). In the fire room, radiation heat transfer from the flame (a point at the mean flame height) to the wall segments is considered.

3. Convective heat release rate: in Suzuki's model [4] it is assumed that all the heat released by the fire rises to the top layer. In this work, it has been assumed as default that 70% (fuel dependent) rises to the top layer and other 30% is transferred to each layer by radiation. In fact, this rate is not accurate enough and may even change during different fire stage.

Numerical results (Time-Temperature plots) obtained from the present model are fitting the experimental results fairly well. The difference is just in the range of 5-10℃, so the above discussed simplifying assumptions in this model look reasonable and well fitted to the engineering requirements.

## 9.5 Comments on future research

Beyond the mentioned improvements, a new series of tests and numerical analyses should be performed in order to solve the following problems: Reduce the aerodynamic effect of the gas against the bottom of the fuel pan during the gas movement. A different ventilation scheme needs to be more realistic to be projected on only the upper part of the tube. Add a rate term (radiation heat transfer) to the numerical model. The effect of slenderness ratio between length and depth of tunnel has an effect on temperature and smoke distribution.

More details in the new experimental and numerical modeling method on future research can be found in chapter 8.5.

# Appendix-MATLAB SCRIPT

```
      % FIRE SAFETY IN TUNNEL: NUMERICAL MODELING OF SMALL SCALE TESTS
clc;
clear all;
            %1.information
% input data
N=12;     %area number
M=5;      %layer number
f=3;       %area with fire
Ventilation=0; %ventilation velocity at left boundary (m/s)
VTime=0;    %ventilation starting time (s)

Rpan=0.26;  %diameter of pan (m)
i=1:N;     %area number
j=1:M;      %layer number
x=1:N+1;     %horizontal bondary number
y=1:M;      %vertical bondary number
Cp=1.04; %specific heat KJ/kg/K
Tamb(i,j)=293;  %ambient temperature K
rowamb(i,j)=1.205; %ambient gas density kg/m^3
roww=2400; %density of wall kg/m^3
g=9.8;
beta=0.539;
Kw=0.0011; % kw/m/K
Cw=0.88; %KJ/kg/K
B=0.338;
Uw=exp(-beta*(Kw*roww*Cw)^B);
alfaC=0.035; %KW/m^2/K
P00(i,j)=1.013*10^5; % initial pressure Pa
lambda=0.001;
d=1/4;
deltat=0.1;    % Time step (s)
T(i,j)=293;   % assume initial temperature distribution at time=0  K
deltax(i,j)=12/N; % m
deltaz(i,j)=1/M;
```

```
u(x,y)=0;
for n=1:N
for m=1:(M-1)/2
V(n,m)=(0.5*2*acos((0.5-m/M)/0.5)*0.5^2-sqrt(0.5^2-(0.5-m/M)^2)*(0.5-m/M)-(0
.5*2*acos((0.5-(m-1)/M)/0.5)*0.5^2-sqrt(0.5^2-(0.5-(m-1)/M)^2)*(0.5-(m-1)/M)
))*(12/N);
end
for m=(M+1)/2
V(n,m)=(2*(0.5*2*asin((0.5-(m-1)/M)/0.5)*0.5^2+(0.5-(m-1)/M)*sqrt(0.5^2-(0.5
-(m-1)/M)^2)))*(12/N);
end
for m=((M+3)/2):M
    V(n,m)=V(n,M+1-m);
end
end

rowsum0(:,1)=0.5*rowamb(:,1);
for n=2:M
   rowsum0(:,n)=rowsum0(:,n-1)+rowamb(:,n);
end
   P0=P00-g*rowsum0.*deltaz;

 for m=1:M
 for n=1:N
 P__o(n,m)=P0(n,m);
end
end
P__o1= P__o;
P__o2= P__o;

for Time=0:deltat:2500
 % input Qc (Theoretical HRR data of test 1)
for n=1:N
for m=1:M
    if Time>=0 & Time<=450
        if n==f
            if m==M
                Qc(n,m)=0.7*(0.000132240741*Time^2);
            elseif m<=(M-1)/2
                Qc(n,m)=(2/(3*M-3))*0.3*(0.000132240741*Time^2);
            else
```

```
            Qc(n,m)=(4/(3*M-3))*0.3*(0.000132240741*Time^2);
        end
    else
        Qc(n,m)=0;
    end
end
if Time>450 & Time<=2000
    if n==f
        if m==M
            Qc(n,m)=0.7*(1e-16*Time+26.77875);
        elseif m<=(M-1)/2
            Qc(n,m)=(2/(3*M-3))*0.3*(1e-16*Time+26.77875);
        else
            Qc(n,m)=(4/(3*M-3))*0.3*(1e-16*Time+26.77875);
        end
    else
        Qc(n,m)=0;
    end
end
if Time>2000 & Time<=2500
    if n==f
        if m==M
            Qc(n,m)=0.7*(0.000107115*(Time-2500)^2);
        elseif m<=(M-1)/2
            Qc(n,m)=(2/(3*M-3))*0.3*(0.000107115*(Time-2500)^2);
        else
            Qc(n,m)=(4/(3*M-3))*0.3*(0.000107115*(Time-2500)^2);
        end
    else
        Qc(n,m)=0;
    end
end
end
end

      %2.convection to wall
row=1.205*293./T;
for n=1:N
for m=1:(M-1)/2
Aw(n,m)=(0.5*2*acos((0.5-m/M)/0.5)-0.5*2*acos((0.5-(m-1)/M)/0.5))*(12/N);
end
```

```
for m=(M+1)/2
Aw(n,m)=2*0.5*2*asin((0.5-(m-1)/M)/0.5)*(12/N);
end
for m=((M+3)/2):M
    Aw(n,m)=Aw(n,M+1-m);
end
end
Tw=Tamb+Uw*(T-Tamb);
Qw=alfaC*(T-Tw).*Aw;

           %3.fire plume flow
for n=1:N
for m=1:M;
    if m<=M-1
    if n==f

Mfp(n,m)=0.21*(1.205^2*g/Cp/293)^(1/3)*(sum(Qc(n,:)))^(1/3)*((m/M)^(5/3)-((m
-1)/M)^(5/3));
    else
        Mfp(n,m)=0;
    end
    end
    if m==M
        if n==f

Mfp(n,m)=-0.21*(1.205^2*g/Cp/293)^(1/3)*(sum(Qc(n,:)))^(1/3)*((m-1)/M)^(5/3)
;
        else
          Mfp(n,m)=0;
        end
    end
end
end

           %4.horizontal flow

for X=1:3
for U=1:inf
for J=1:inf
for I=1:inf
```

```
for n=1:N;
for m=1:M;
    if n==1
        if u(n,m)>=0
            Mh(n,m)=(V(n,m)/(12/N))*u(n,m).*rowamb(n,m);
        else
            Mh(n,m)=(V(n,m)/(12/N))*u(n,m).*row(n,m);
        end
        if u(n+1,m)>=0
            Mh(n+1,m)=(V(n,m)/(12/N))*u(n+1,m).*row(n,m);
        else
            Mh(n+1,m)=(V(n,m)/(12/N))*u(n+1,m).*row(n+1,m);
        end
    elseif n==N
        if u(n,m)>=0
            Mh(n,m)=(V(n,m)/(12/N))*u(n,m).*row(n-1,m);
        else
            Mh(n,m)=(V(n,m)/(12/N))*u(n,m).*row(n,m);
        end
        if u(n+1,m)>=0
            Mh(n+1,m)=(V(n,m)/(12/N))*u(n+1,m).*row(n,m);
        else
            Mh(n+1,m)=(V(n,m)/(12/N))*u(n+1,m).*rowamb(n,m);
        end
    else
         if u(n,m)>=0
            Mh(n,m)=(V(n,m)/(12/N))*u(n,m).*row(n-1,m);
        else
            Mh(n,m)=(V(n,m)/(12/N))*u(n,m).*row(n,m);
        end
        if u(n+1,m)>=0
            Mh(n+1,m)=(V(n,m)/(12/N))*u(n+1,m).*row(n,m);
        else
            Mh(n+1,m)=(V(n,m)/(12/N))*u(n+1,m).*row(n+1,m);
        end
    end
end
end
```

```
for n=1:N
for m=1:M
    if n==1
    A(n,m)=Cp*(1/2)*(Mh(n,m)+abs(Mh(n,m)))*Tamb(n,m);
    B(n,m)=Cp*(1/2)*(abs(Mh(n+1,m))-Mh(n+1,1)).*T(n+1,m);
    C(n,m)=-(Cp*(1/2)*(abs(Mh(n,m))-Mh(n,m)).*T(n,m));
    D(n,m)=-(Cp*(1/2)*(Mh(n+1,m)+abs(Mh(n+1,m))).*T(n,m));
    elseif n==N
    A(n,m)=(Cp*(1/2)*(Mh(n,m)+abs(Mh(n,m))).*T(n-1,m));
    B(n,m)=(Cp*(1/2)*(abs(Mh(n+1,m))-Mh(n+1,m)).*Tamb(n,m));
    C(n,m)=-(Cp*(1/2)*(abs(Mh(n,m))-Mh(n,m)).*T(n,m));
    D(n,m)=-(Cp*(1/2)*(Mh(n+1,m)+abs(Mh(n+1,m))).*T(n,m));
    else
    A(n,m)=(Cp*(1/2)*(Mh(n,m)+abs(Mh(n,m))).*T(n-1,m));
    B(n,m)=(Cp*(1/2)*(abs(Mh(n+1,m))-Mh(n+1,m)).*T(n+1,m));
    C(n,m)=-(Cp*(1/2)*(abs(Mh(n,m))-Mh(n,m)).*T(n,m));
    D(n,m)=-(Cp*(1/2)*(Mh(n+1,m)+abs(Mh(n+1,m))).*T(n,m));
    end
end
end

for n=1:N

maxerr(n)=sum(A(n,:))+sum(B(n,:))+sum(C(n,:))+sum(D(n,:))-sum(Qw(n,:))+sum(Q
c(n,:));
end
maxerr;


for m=1:M
    for n=1
    if maxerr(n)>=0
    u__n(n,m)=u(n,m)-(1/M)*0.49*maxerr(n)/Cp/T(n,m);
    else
    u__n(n,m)=u(n,m)-(1/M)*0.49*maxerr(n)/Cp/Tamb(n,m);
    end
    end
    for n=2:N
    if maxerr(n)>=0
        if maxerr(n-1)>=0
```

```
u__n(n,m)=u(n,m)+(1/M)*0.49*maxerr(n-1)/Cp/T(n-1,m)-(1/M)*0.49*maxerr(n)/Cp/
T(n,m);
        else

u__n(n,m)=u(n,m)+(1/M)*0.49*maxerr(n-1)/Cp/T(n,m)-(1/M)*0.49*maxerr(n)/Cp/T(
n,m);
        end
    elseif maxerr(n)<0
        if maxerr(n-1)>=0

u__n(n,m)=u(n,m)+(1/M)*0.49*maxerr(n-1)/Cp/T(n-1,m)-(1/M)*0.49*maxerr(n)/Cp/
T(n-1,m);
        else

u__n(n,m)=u(n,m)+(1/M)*0.49*maxerr(n-1)/Cp/T(n,m)-(1/M)*0.49*maxerr(n)/Cp/T(
n-1,m);
        end
    end
    end
    for n=N+1
    if maxerr(n-1)>=0
    u__n(n,m)=u(n,m)+(1/M)*0.49*maxerr(n-1)/Cp/T(n-1,m);
    else
    u__n(n,m)=u(n,m)+(1/M)*0.49*maxerr(n-1)/Cp/Tamb(n-1,m);
    end
    end
end
if max(abs(u-u__n))<=10^(-8)
    break
end
u=u__n;
end
u__n1=u__n;
u__n2=u__n;

for m=1:M
    for n=1
        if u__n(n,m)>=0
            if abs(max(0,0))>=abs(min(u__n(n+1,m),0))
                pv(n,m)=0.5*rowamb(n,m)*0^2;
```

```
                Ff(n,m)=0;
            else
                pv(n,m)=0.5*row(n,m)*u__n(n+1,m)^2;

Ff(n,m)=lambda/(2*d)*deltax(n,m).*row(n,m).*u__n(n+1,m)*abs(u__n(n+1,m)).*Aw
(n,m)./(pi*(12/N));
            end
            P__11(n,m)=P0(n,m)+pv(n,m)-Ff(n,m)-0.5*row(n,m)*u__n(n,m)^2;
        elseif u__n(n,m)<0
            if abs(max(0,0))>=abs(min(u__n(n+1),0))
                pv(n,m)=0.5*rowamb(n,m)*0^2;
                Ff(n,m)=0;
            else
                pv(n,m)=0.5*row(n,m)*u__n(n+1)^2;

Ff(n,m)=lambda/(2*d)*deltax(n,m).*row(n,m).*u__n(n+1,m)*abs(u__n(n+1,m)).*Aw
(n,m)./(pi*(12/N));
            end
            P__11(n,m)=P0(n,m)+pv(n,m)-Ff(n,m)+0.5*rowamb(n,m)*u__n(n,m)^2;
        end
    end
    for n=2:N
        if u__n(n,m)>=0
            if abs(max(u__n(n-1,m),0))>=abs(min(u__n(n+1,m),0))
                pv(n,m)=0.5*row(n-1,m)*u__n(n-1,m)^2;

Ff(n,m)=lambda/(2*d)*deltax(n-1,m).*row(n-1,m).*u__n(n-1,m)*abs(u__n(n-1,m))
.*Aw(n-1,m)./(pi*(12/N));
            else
                pv(n,m)=0.5*row(n,m)*u__n(n+1,m)^2;

Ff(n,m)=lambda/(2*d)*deltax(n,m).*row(n,m).*u__n(n+1,m)*abs(u__n(n+1,m)).*Aw
(n,m)./(pi*(12/N));
            end
            P__11(n,m)=P__11(n-1,m)+pv(n,m)-Ff(n,m)-0.5*row(n,m)*u__n(n,m)^2;
        elseif u__n(n,m)<0
            if abs(max(u__n(n-1,m),0))>=abs(min(u__n(n+1,m),0))
                pv(n,m)=0.5*row(n-1,m)*u__n(n-1,m)^2;

Ff(n,m)=lambda/(2*d)*deltax(n-1,m).*row(n-1,m).*u__n(n-1,m)*abs(u__n(n-1,m))
.*Aw(n-1,m)./(pi*(12/N));
```

```
            else
                pv(n,m)=0.5*row(n,m)*u__n(n+1,m)^2;

Ff(n,m)=lambda/(2*d)*deltax(n,m).*row(n,m).*u__n(n+1,m)*abs(u__n(n+1,m)).*Aw
(n,m)./(pi*(12/N));
            end

P__11(n,m)=P__11(n-1,m)+pv(n,m)-Ff(n,m)+0.5*row(n-1,m)*u__n(n,m)^2;
        end
    end
end
if max(max(abs(P__11-P__o1)))<=1e-06
    break
end
P__o1=P__11;
end

for m=1:M
    for n=N
        if u__n(n+1,m)>=0
            if abs(max(u__n(n,m),0))>=abs(min(0,0))
                pv(n,m)=0.5*row(n,m)*u__n(n,m)^2;

Ff(n,m)=lambda/(2*d)*deltax(n,m).*row(n,m).*u__n(n,m)*abs(u__n(n,m)).*Aw(n,m
)./(pi*(12/N));
            else
                pv(n,m)=0;
                Ff(n,m)=0;
            end
            P__22(n,m)=P0(n,m)-pv(n,m)+Ff(n,m)+0.5*rowamb(n,m)*u__n(n+1,m)^2;
        elseif u__n(n+1,m)<0
            if abs(max(u__n(n,m),0))>=abs(min(0,0))
                pv(n,m)=0.5*row(n,m)*u__n(n,m)^2;

Ff(n,m)=lambda/(2*d)*deltax(n,m).*row(n,m).*u__n(n,m)*abs(u__n(n,m)).*Aw(n,m
)./(pi*(12/N));
            else
                pv(n,m)=0;
                Ff(n,m)=0;
            end
            P__22(n,m)=P0(n,m)-pv(n,m)+Ff(n,m)-0.5*row(n,m)*u__n(n+1,m)^2;
```

```
        end
    end
    for n=1:N-1
        if u__n(n+1,m)>=0
            if abs(max(u__n(n,m),0))>=abs(min(u__n(n+2,m),0))
                pv(n,m)=0.5*row(n,m)*u__n(n,m)^2;

Ff(n,m)=lambda/(2*d)*deltax(n,m).*row(n,m).*u__n(n,m)*abs(u__n(n,m)).*Aw(n,m
).*(pi*(12/N));
            else
                pv(n,m)=0.5*row(n+1,m)*u__n(n+2,m)^2;

Ff(n,m)=lambda/(2*d)*deltax(n+1,m).*row(n+1,m).*u__n(n+2,m)*abs(u__n(n+2,m))
.*Aw(n+1,m).*(pi*(12/N));
            end

P__22(n,m)=P__22(n+1,m)-pv(n,m)+Ff(n,m)+0.5*row(n+1,m)*u__n(n+1,m)^2;
        elseif u__n(n+1,m)<0
            if abs(max(u__n(n,m),0))>=abs(min(u__n(n+2,m),0))
                pv(n,m)=0.5*row(n,m)*u__n(n,m)^2;

Ff(n,m)=lambda/(2*d)*deltax(n,m).*row(n,m).*u__n(n,m)*abs(u__n(n,m)).*Aw(n,m
).*(pi*(12/N));
            else
                pv(n,m)=0.5*row(n+1,m)*u__n(n+2,m)^2;

Ff(n,m)=lambda/(2*d)*deltax(n+1,m).*row(n+1,m).*u__n(n+2,m)*abs(u__n(n+2,m))
.*Aw(n+1,m).*(pi*(12/N));
            end

P__22(n,m)=P__22(n+1,m)-pv(n,m)+Ff(n,m)-0.5*row(n,m)*u__n(n+1,m)^2;
        end
    end
end
if max(max(abs(P__22-P__o2)))<=1e-06
    break
end
P__o2=P__22;
end
P__o=0.5*(P__11+P__22);
P=0.5*(P__11+P__22);
```

```
for Q=1:100
for G=1:100
for n=1:N
for m=1:M
   P_n0(n,m)=P(n,1);
end
end
rowsum_n(:,1)=0*row(:,1);
for n=2:M
 rowsum_n(:,n)=rowsum_n(:,n-1)+0.5*(row(:,n-1)+row(:,n));
end
P__n=P_n0-g*rowsum_n.*deltaz;

for n=1:N
for m=1:M
   P_n00(n,m)=P(n,5);
end
end
rowsum_n1(:,M)=0*row(:,M);
for n=1:M-1
rowsum_n1(:,n)=rowsum_n1(:,n+1)+0.5*(row(:,n)+row(:,n+1));
end
P__n1=P_n00+g*rowsum_n1.*deltaz;
P_n=0.5*(P__n1+P__n);

for m=1:M
    for n=1
        if abs(max(0,0))>=abs(min(u__n1(n+1,m),0))
            pv(n,m)=0;
            Ff(n,m)=0;
        else
            pv(n,m)=0.5*row(n,m)*u__n1(n+1,m)^2;

Ff(n,m)=lambda/(2*d)*deltax(n,m).*row(n,m).*u__n1(n+1,m).*abs(u__n1(n+1,m)).
*Aw(n,m)./(pi*(12/N));
        end
        if P0(n,m)-P_n(n,m)+pv(n,m)-Ff(n,m)>=0
            u___n1(n,m)=sqrt(2*(P0(n,m)-P_n(n,m)+pv(n,m)-Ff(n,m))/row(n,m));
        else
```

```
u___n1(n,m)=-sqrt(-2*(P0(n,m)-P_n(n,m)+pv(n,m)-Ff(n,m))/rowamb(n,m));
        end
    end
    for n=2:N
        if abs(max(u___n1(n-1,m),0))>=abs(min(u__n1(n+1,m),0))
            pv(n,m)=0.5*row(n-1,m)*u___n1(n-1,m)^2;

Ff(n,m)=lambda/(2*d)*deltax(n-1,m).*row(n-1,m).*u___n1(n-1,m).*abs(u___n1(n-
1,m)).*Aw(n-1,m)./(pi*(12/N));
        else
            pv(n,m)=0.5*row(n,m)*u__n1(n+1,m)^2;

Ff(n,m)=lambda/(2*d)*deltax(n,m).*row(n,m).*u__n1(n+1,m).*abs(u__n1(n+1,m)).
*Aw(n,m)./(pi*(12/N));
        end
        if P_n(n-1,m)-P_n(n,m)+pv(n,m)-Ff(n,m)>=0

u___n1(n,m)=sqrt(2*(P_n(n-1,m)-P_n(n,m)+pv(n,m)-Ff(n,m))/row(n,m));
        else

u___n1(n,m)=-sqrt(-2*(P_n(n-1,m)-P_n(n,m)+pv(n,m)-Ff(n,m))/row(n-1,m));
        end
    end
    for n=N+1
         if abs(max(u___n1(n-1,m),0))>=abs(min(0,0))
            pv(n,m)=0.5*row(n-1,m)*u___n1(n-1,m)^2;

Ff(n,m)=lambda/(2*d)*deltax(n-1,m).*row(n-1,m).*u___n1(n-1,m).*abs(u___n1(n-
1,m)).*Aw(n-1,m)./(pi*(12/N));
        else
            pv(n,m)=0.5*rowamb(n-1,m)*0^2;
            Ff(n,m)=0;
        end
        if P_n(n-1,m)-P0(n-1,m)+pv(n,m)-Ff(n,m)>=0

u___n1(n,m)=sqrt(2*(P_n(n-1,m)-P0(n-1,m)+pv(n,m)-Ff(n,m))/rowamb(n-1,m));
        else

u___n1(n,m)=-sqrt(-2*(P_n(n-1,m)-P0(n-1,m)+pv(n,m)-Ff(n,m))/row(n-1,m));
        end
```

```
    end
end
P=P_n;
u__n1=u___n1;
end

for m=1:M
    for n=N+1
        if abs(max(u__n2(n-1,m),0))>=abs(min(0,0))
            pv(n,m)=0.5*row(n-1,m)*u__n2(n-1,m)^2;

Ff(n,m)=lambda/(2*d)*deltax(n-1,m).*row(n-1,m).*u__n2(n-1,m).*abs(u__n2(n-1,
m)).*Aw(n-1,m)./(pi*(12/N));
        else
            pv(n,m)=0;
            Ff(n,m)=0;
        end
        if P_n(n-1,m)-P0(n-1,m)+pv(n,m)-Ff(n,m)>=0

u___n2(n,m)=sqrt(2*(P_n(n-1,m)-P0(n-1,m)+pv(n,m)-Ff(n,m))/rowamb(n-1,m));
        else

u___n2(n,m)=-sqrt(-2*(P_n(n-1,m)-P0(n-1,m)+pv(n,m)-Ff(n,m))/row(n-1,m));
        end
    end
    for n=2:N
        if abs(max(u__n2(n-1,m),0))>=abs(min(u___n2(n+1,m),0))
            pv(n,m)=0.5*row(n-1,m)*u__n2(n-1,m)^2;

Ff(n,m)=lambda/(2*d)*deltax(n-1,m).*row(n-1,m).*u__n2(n-1,m).*abs(u__n2(n-1,
m)).*Aw(n-1,m)./(pi*(12/N));
        else
            pv(n,m)=0.5*row(n,m)*u___n2(n+1,m)^2;

Ff(n,m)=lambda/(2*d)*deltax(n,m).*row(n,m).*u___n2(n+1,m).*abs(u___n2(n+1,m)
).*Aw(n,m)./(pi*(12/N));
        end
        if P_n(n-1,m)-P_n(n,m)+pv(n,m)-Ff(n,m)>=0

u___n2(n,m)=sqrt(2*(P_n(n-1,m)-P_n(n,m)+pv(n,m)-Ff(n,m))/row(n,m));
        else
```

```
u___n2(n,m)=-sqrt(-2*(P_n(n-1,m)-P_n(n,m)+pv(n,m)-Ff(n,m))/row(n-1,m));
        end
    end
    for n=1
        if abs(max(0,0))>=abs(min(u___n2(n+1,m),0))
            pv(n,m)=0;
            Ff(n,m)=0;
        else
            pv(n,m)=0.5*row(n,m)*u___n2(n+1,m)^2;

Ff(n,m)=lambda/(2*d)*deltax(n,m).*row(n,m).*u___n2(n+1,m).*abs(u___n2(n+1,m)
).*Aw(n,m)./(pi*(12/N));
        end
        if P0(n,m)-P_n(n,m)+pv(n,m)-Ff(n,m)>=0
            u___n2(n,m)=sqrt(2*(P0(n,m)-P_n(n,m)+pv(n,m)-Ff(n,m))/row(n,m));
        else

u___n2(n,m)=-sqrt(-2*(P0(n,m)-P_n(n,m)+pv(n,m)-Ff(n,m))/rowamb(n,m));
        end
    end
end
P=P_n;
u__n2=u___n2;
end

p__o=P_n;
u=0.5*(u___n1+u___n2);
end
p__o=P_n;

for m=1:M
for n=1
    if Time<VTime
        u(n,m)=0.5*(u___n1(n,m)+u___n2(n,m));
    elseif Time>=VTime
        u(n,m)=0.5*(u___n1(n,m)+u___n2(n,m))+Ventilation;
    end
for n=2:N
        u(n,m)=0.5*(u___n1(n,m)+u___n2(n,m));
    end
```

```
end
end

for n=1:N;
for m=1:M;
    if n==1
        if Mh(n,m)>=0
            Hh(n,m)=Cp*Mh(n,m).*Tamb(n,m);
        else
            Hh(n,m)=Cp*Mh(n,m).*T(n,m);
        end
        if Mh(n+1,m)>=0
           Hh(n+1,m)=Cp*Mh(n+1,m).*T(n,m);
        else
           Hh(n+1,m)=Cp*Mh(n+1,m).*T(n+1,m);
        end
    elseif n==N
        if Mh(n,m)>=0
            Hh(n,m)=Cp*Mh(n,m).*T(n-1,m);
        else
            Hh(n,m)=Cp*Mh(n,m).*T(n,m)  ;
        end
        if Mh(n+1,m)>=0
           Hh(n+1,m)=Cp*Mh(n+1,m).*T(n,m);
        else
           Hh(n+1,m)=Cp*Mh(n+1,m).*Tamb(n,m);
        end
    else
        if Mh(n,m)>=0
            Hh(n,m)=Cp*Mh(n,m).*T(n-1,m);
        else
            Hh(n,m)=Cp*Mh(n,m).*T(n,m)  ;
        end
        if Mh(n+1,m)>=0
           Hh(n+1,m)=Cp*Mh(n+1,m).*T(n,m);
        else
           Hh(n+1,m)=Cp*Mh(n+1,m).*T(n+1,m);
        end
    end
end
end
```

```
            %5.vetical flow

for n=1:N
  if n==f
      for m=M

Hv(n,m)=-Cp*Mfp(n,m)*T(n,m)+(1/2)*(Hh(n,m)+abs(Hh(n,m)))+(1/2)*(abs(Hh(n+1,m
))-Hh(n+1,m))-(1/2)*(abs(Hh(n,m))-Hh(n,m))-(1/2)*(abs(Hh(n+1,m))+Hh(n+1,m))-
Qw(n,m)+Qc(n,m);
      end
      for m=2:M-1

Hv(n,m)=-Cp*Mfp(n,m)*T(n,m)+(1/2)*(Hh(n,m)+abs(Hh(n,m)))+(1/2)*(abs(Hh(n+1,m
))-Hh(n+1,m))-(1/2)*(abs(Hh(n,m))-Hh(n,m))-(1/2)*(abs(Hh(n+1,m))+Hh(n+1,m))-
Qw(n,m)+Qc(n,m)+Hv(n,m+1);
      end
      for m=1
        Hv(n,m)=0;
      end
  else
      for m=M

Hv(n,m)=(1/2)*(Hh(n,m)+abs(Hh(n,m)))+(1/2)*(abs(Hh(n+1,m))-Hh(n+1,m))-(1/2)*
(abs(Hh(n,m))-Hh(n,m))-(1/2)*(abs(Hh(n+1,m))+Hh(n+1,m))-Qw(n,m)+Qc(n,m);
      end
      for m=2:M-1

Hv(n,m)=(1/2)*(Hh(n,m)+abs(Hh(n,m)))+(1/2)*(abs(Hh(n+1,m))-Hh(n+1,m))-(1/2)*
(abs(Hh(n,m))-Hh(n,m))-(1/2)*(abs(Hh(n+1,m))+Hh(n+1,m))-Qw(n,m)+Qc(n,m)+Hv(n
,m+1);
      end
      for m=1
        Hv(n,m)=0;
      end
  end
end

for n=1:N
for m=1:M
    if m==1
```

```
        Mv(n,m)=Hv(n,m)./(Cp*T(n,m));
        if Hv(n,m+1)>=0
            Mv(n,m+1)=Hv(n,m+1)./(Cp*T(n,m+1));
        else
            Mv(n,m+1)=Hv(n,m+1)./(Cp*T(n,m));
        end
    elseif m==M
        if Hv(n,m)>=0
        Mv(n,m)=Hv(n,m)./(Cp*T(n,m));
        else
        Mv(n,m)=Hv(n,m)./(Cp*T(n,m-1));
        end
    else
        if Hv(n,m)>=0
        Mv(n,m)=Hv(n,m)./(Cp*T(n,m));
        else
        Mv(n,m)=Hv(n,m)./(Cp*T(n,m-1));
        end
        if Hv(n,m+1)>=0
        Mv(n,m+1)=Hv(n,m+1)./(Cp*T(n,m+1));
        else
        Mv(n,m+1)=Hv(n,m+1)./(Cp*T(n,m));
        end
    end
end
end

          %6.temperature
for n=f
for m=1:M
    Y(n,m)=Mfp(n,m)*T(n,m);
end
end

for n=1:N
for m=1:M
  if n==f
    if m==1

deltaT(n,m)=deltat*(1./(Cp*row(n,m).*V(n,m)))*((Hv(n,m+1)-Cp*Mv(n,m+1)*T(n,m
))+(Hh(n,m)-Cp*Mh(n,m)*T(n,m))-(Hh(n+1,m)-Cp*Mh(n+1,m)*T(n,m))-Qw(n,m)+Qc(n,
```

```
m));
    elseif m==M

deltaT(n,m)=deltat*(1./(Cp*row(n,m).*V(n,m)))*(Cp*sum(sum(Y))-(Hv(n,m)-Cp*Mv
(n,m)*T(n,m))+(Hh(n,m)-Cp*Mh(n,m)*T(n,m))-(Hh(n+1,m)-Cp*Mh(n+1,m)*T(n,m))-Qw
(n,m)+Qc(n,m));
    else

deltaT(n,m)=deltat*(1./(Cp*row(n,m).*V(n,m)))*((Hv(n,m+1)-Cp*Mv(n,m+1)*T(n,m
))-(Hv(n,m)-Cp*Mv(n,m)*T(n,m))+(Hh(n,m)-Cp*Mh(n,m)*T(n,m))-(Hh(n+1,m)-Cp*Mh(
n+1,m)*T(n,m))-Qw(n,m)+Qc(n,m));
    end
 else
      if m==1

deltaT(n,m)=deltat*(1./(Cp*row(n,m).*V(n,m)))*((Hv(n,m+1)-Cp*Mv(n,m+1)*T(n,m
))+(Hh(n,m)-Cp*Mh(n,m)*T(n,m))-(Hh(n+1,m)-Cp*Mh(n+1,m)*T(n,m))-Qw(n,m)+Qc(n,
m));
    elseif m==M

deltaT(n,m)=deltat*(1./(Cp*row(n,m).*V(n,m)))*(-(Hv(n,m)-Cp*Mv(n,m)*T(n,m))+
(Hh(n,m)-Cp*Mh(n,m)*T(n,m))-(Hh(n+1,m)-Cp*Mh(n+1,m)*T(n,m))-Qw(n,m)+Qc(n,m))
;
    else

deltaT(n,m)=deltat*(1./(Cp*row(n,m).*V(n,m)))*((Hv(n,m+1)-Cp*Mv(n,m+1)*T(n,m
))-(Hv(n,m)-Cp*Mv(n,m)*T(n,m))+(Hh(n,m)-Cp*Mh(n,m)*T(n,m))-(Hh(n+1,m)-Cp*Mh(
n+1,m)*T(n,m))-Qw(n,m)+Qc(n,m));
      end
end
end
end
deltaT(i,j);
Time                              % real Time (s)
T(i,j)=T(i,j)+deltaT(i,j)         % Temperature in each time step (K)
K=round(10*Time+1);
Ttime(:,:,K)=T(:,:);
end
```

# References

[1] Beard A., Carvel R. (eds.), "The handbook of Tunnel Fire Safety", Thomas Telford, London, 2nd Edition.

[2] Drysdale D., "An Introduction to Fire Dynamics", John Wiley & Sons, 2nd Edition 1999

[3] Philip J. DiNenno (eds.), "SFPE Handbook of Fire Protection Engineering", 3rd Edition, 2002

[4] Suzuki, Keichi, Tanaka, Takeyoshi, et al., 2004. "An application of a multi-layer zone model to a tunnel fire". In: Proceedings of the Sixth Asia Oceania Symposium on Fire Science and Technology, Daegu, Korea, 17–20 March.

[5] Suzuki, K., Harada K., and Tanaka, T., "A Multi-Layer Zone Model for Predicting Fire Behavior in a Single room", the 6-th Symposium of IAFSS, Jun. 2001.

[6] Xiaojun, C. (2008). "Simulation of temperature and smoke distribution of a tunnel fire based on modifications of multi-layer zone model". Tunneling and Underground Space Technology, 23, 75–79

[7] Xiaojun C., Lizhong Y., Zhihua D., Weicheng F. "A Multi - Layer Zone Model for Predicting Fire Behavior in a Fire Room", Fire Safety Journal, Vol. 40, 2005, pp. 267- 281.

[8] Chow, W.K., 1996. Simulation of tunnel fires using a zone model. Tunneling and Underground Space Technology 11, 221–236.

[9] ] A. N. Beard, D. D. Drysdale. "A non-linear model of major fire spread in a tunnel". Fire Safety Journal, 1995, 24: 337−357.

[10] Peacock. R. D, Jones W. W., Reneke P. A., et al. "CFAST-consolidated model of fire growth and smoke transport (version 6) user's guide". NIST Special Publication1041, Gaithersburg, USA, 2005.

[11] Ingason, H. and ZhenLi, Y., "Model Scale Tunnel Fire Tests with Longitudinal ventilation", Fire Safety Journal, 2010.

[12] BAMONTE P., FELICETTI R., GAMBAROVA P.G. and NAFARIEH A, "On the Fire Scenario in Road Tunnels: a Comparison between Zone and Field Models", Department of Structural Engineering, Politecnico di Milano, Applied Mechanics and Materials Vol. 82 (2011) pp. 764-769.

[13] Jain S., Kumar S., Kumar S., Sharma T., "Numerical simulation of fire in a tunnel: Comparative study of CFAST and CFX predictions", Tunneling and Underground Space Technology 23 (2008) 160–170.

[14] Bettis, R.J., Jagger, S.F. and Moodie, K. Reduced scale simulations of fires in partially blocked tunnels. Proc. of the International Conference on Fires in Tunnels, October 10-11, 1994, Borås (Sweden), pp.162-186.

[15] Carvel R.O., A.N. Beard, P.W. Jowitt and D.D. Drysdale (2004) "The influence of tunnel geometry and ventilation on the Heat Release Rate of a fire". Fire Technol., 40, 5-26.

[16] Lönnermark A, "On the Characteristics of Fires in Tunnels", Department of Fire Safety Engineering, Lund University, Sweden, 2005

[17] Mahmoud Mohamed Kamal Ahmed, "Fire safety in concrete tunnels-First results on small scale tests", Chapter 4, 2012.

[18] Ingason H. and A. Lönnermark (2005) Heat Release Rates from heavy goods vehicle trailers in tunnels. Fire Safety J., 40, 646-668.